FACULTY OF SCIENCE AND TECHNOLOGY

MASTER'S THESIS

Study programme / specialisation: Environmental Technology/ Water Science and Technology	Spring 2023 Open / ~~Confidential~~
Author: Julia Susanne Cassandra Vestvik Halvorsen	
Supervisor at UiS: Roald Kommedal Co-supervisor: External supervisor(s): Ole Magne Homestad (GE HealthCare Lindesnes)	
Thesis title: Degradation of iodinated contrast media in biological treatment plant at GE HealthCare Lindesnes.	
Credits (ECTS): 30	
Keywords: Iodinated contrast media (ICM) Biotransformation, dehalogenation, Transformation products (TPs), Mass-spectrometry (MS)	Pages: 75 + 2 Front pages + appendixes 61 pages 14/6-23 Stavanger Sustna Vestvik

Degradation of iodinated contrast media in biological treatment plant at GE HealthCare Lindesnes.

Master`s Thesis

Julia Susanne Cassandra Vestvik Halvorsen

Environmental Technology Study Program
Water Science and Technology
Department of Mathematics and Natural Science
University of Stavanger

2023

Summary

Iodinated contrast media (ICM) are used all over the world.

Side streams form production ICM containing acetate (90 %), solvents (methanol, acetone, 2-Methoxy ethanol, and isopropanol) and ICM are treated by a biological treatment plant combining anaerobic extended granule sludge bed (EGSB) technology with an aerobic moving bed bioreactor (MBBR) as polish step.

Samples from the three anaerobic EGSBs and aerobic CFIC reactor was analyzed by ion - chromatography and HPLC with UV-detector coupled with a single-quadrupole mass-specter (MS). Reduction of iohexol in EGSBs were 96-98 % and 100% for iodixanol and intermediates. ICM was not detected in samples after aerobic MBBR reactor.

25 TPs was detected from EGSB 1 and 2, whereas 15 TPs was detected in samples form EGSB 3 using full scan-mode with mass range 150-1600 m/z. Differences in biological community between EGSB 1 and 2 compared to EGSB 3 was observed, may be the reason for differences in TPs. In samples form aerobic reactor (CFIC) 8 TPs was detected.

Free iodide increased from 16 mg/L to 85 mg/L (EGSB 1), 80 mg/L (EGSB 2) and 55 mg/L (EGSB 3). Free iodide did not increase after CFIC. Indication that reductive dehalogenation only occurred in the anerobic reactors. TP 694, TP 451, and TP 366 related to deiodinated ICM was detected in all EGSBs. Only TP 451 was detected in CFIC. Four known iohexol TPs (TP 833, TP 775, TP 657 and TP366) from literature was detected using single-ion mass (SIM) scan-mode.

New TPs (TP 459, TP 711, TP 342, and TP 585) of iohexol was detected in the EGSBs. Suggestive structure for four of the TPs was drawn. Deiodination by addition of hydroxyl group was suspected. TPs detected in CFIC was not detectable by the UV-detector, indicating possible breaking of the aromatic-ring structure of the ICM.

The study showed that the efficiency of the biological treatment plant at GE HealthCare has changed drastically since 2020. The complexity of observed TPs is a result of the presence of other impurities from production that form TPs in addition to those formed from intermediates, iohexol and iodixanol.

Dehalogenation and subsequent degradation by oxidative aerobic processes was confirmed. Treatment with activated carbon was shown to be an effective way to remove TPs from CFIC effluent, while treatment with Ion-exchange resin was less efficient.

Acknowledgements

I would like to thank my employer GE HealthCare Lindesnes for the opportunity to work with a very important topic for us as a main producer of iodinated contrast media. A special thanks to my dear colleague and super chemist O.M Homestad for help with MS-specter interpretations and general discussions. Thanks to process engineer Eivind Nordin for help with sampling from the WWTP and for providing, data and pictures. Thanks to Roald Kommedal for being my supervisor on this project. Finally, I must thank my colleague and husband Sigbjørn for discussions on environmental issues, support and stepping in as full-time maid the last weeks of this work.

Julia Susanne Cassandra Vestvik Halvorsen

June 2023

Table of Contents

List of Abbreviations

EGSB	**Extended granular sludge bed**
CFIC	**Continuous flow intermittent cleaning aerobic reactor**
K_{ow}	**Octanol /water partition coefficient**
TPs	**Transformation products**
ICM	**Iodinated contrast media**
WWTP	**Wastewater treatment plant**
SIM	**Single ion monitoring**
HESI	**Heated electron spray ionization**
MBBR	**Moving bed bioreactor**
PNEC	**Predicted no effect concentration**
IC	**Ion-Chromatography**
MS	**Mass-Spectrometry**
pSig	**Pounds per square in gauge (14,5 pSig = 1 bar)**
HPLC	**High pressure liquid chromatography**
540	**First iodinated intermediate for synthesis of iohexol and iodixanol.**
541	**Second iodinated intermediate (acetylated 540)**
BAT	**Best available technology**
IED	**Industrial Emission Directive**

Keywords: Iodinated contrast media (ICM) degradation, Biotransformation, dehalogenation, Transformation products (TPs), Mass-spectrometry (MS)

1. Introduction

The iodinated contrast media (ICM) Iohexol was first listed in Norway and Sweden in 1982 [1]. Today iohexol is extensively used in over 100 countries and is listed on WHOs essential drug list [2].

ICM are used to detect problems in the brain, heart, blood vessels, stomach, joints, pancreas, bladder, reproductive tract, and other parts of the body. [1, 2] This makes Iohexol a critical important pharmaceutical for diagnostics. Increased availability of professional healthcare in development countries in Asia and Africa as well as the development of new areas of application has ensured a drastic increase in production volume of Iohexol.

Iohexol and ICM in general is excreted unmetabolized from the body through the urine [3] Iohexol enters the wastewater system and wastewater treatment plants (WWTPs). The designed inertness and solubility of the ICM makes it elusive, resulting in iohexol and other ICM being found in groundwater, rivers, and sediments all over the world.

Every year tons of ICM enter the natural water systems. The fate and ecological consequence of these emissions have not been of primary concern because of the low toxicity of the compound itself. [4] However, partial degradation give rise to transformation products (TPs) which in some cases exert higher toxicity. Study by NIVA in 2006 argued that the limited degradation of iohexol in seawater reduced the risk of the observed toxicity of TPs formed by microbial degradation [5]. Structure of TPs depends on parent compound, abiotic chemical properties like pH, temperature, presence of natural organic compounds, radicals involved and bacterial activity. The diversity of TPs and the difficulty of evaluating their ecological effects poses a problem [6]

In later years the focus on xenobiotics in the environment has increased. The recovery of pharmaceuticals and personal care products in surface waters, groundwaters and drinking water in the ug/L range, has raised concern of the public.

Studies of natural waters, WWTS and hospitals effluents has shown variable results in terms of degradation of ICM [7] However, mineralization is rarely observed [4]. Mineralization refers to the complete biodegradation to form an inorganic substance and CO_2.

Bio transformed or biodegraded is a process where organic substrates molecule is broken down by microorganisms and results in a reduction of the molecular mass [8]. The term degraded also includes degradation by abiotic processes. In this thesis, degradation will be used to describe biotransformation.

GE HealthCare produces the non-ionic ICM, iohexol and iodixanol. Producing about 50 % of the ICM in the world. Every second 3 patients receive a dose of ICM produced at Lindesnes. Iohexol from GE HealthCare is sold under commercial name Omnipaque [9] The volume is expected to grow with > 10% per year, is response to increased marked shares and increase in global demand. Application to the directorate of the environment in Norway gave an estimate of production volume of 19500 tons in 2030 [10]

At Lindesnes site iohexol is released into the environment through waste streams emitted to the sea.

The industrial emission directive (IED) was implemented in EØS in 2015. In 2016 it was incorporated into the law of pollution in Norway. Requirements for the industry to reduce its emissions significantly increased [11]. For ICM producer GE HealthCare the Zero-emission project established BAT-conclusions (best available technology) in compliance with the concession of emission. Emissions of ICM to the recipient (sea) was 45 tons I 2022, with an upper limit of 75 tons p.a.

Iohexol is the biggest product in volume at GE-Lindesnes. [10] The user dose is relatively high (200 g/ examination) [12] The emission of ICM at GE Health Care Lindesnes, exceeds 375 000 user doses per year.

The polluters pay principle puts the economic burden on the industry. As primary producers of pharmaceuticals, GE HealthCare strives to achieve knowledge and take responsibility of the full life cycle of the products.

1.2 Aims and objectives.

In 2022 over 26 tons of ICM and its derivates entered the WWTP at Lindesnes site. The concentrations in the wastewater treatment plant (WWTP) are in the mg/L range. Data of degradation of ICM and its intermediates in adapted anaerobic combined with aerobic bioreactors a lacking. As primary producer of ICM GE HealthCare objective is evaluate the fate of ICM within this WWTP and generate more knowledge about possible treatments for ICM emissions.

The aim of this study is divided into 3 sub-objectives.

Firstly, to validate a method for detection of ICM and their intermediates in wastewater from the biological treatment plant. Combining HPLC separation utilizing UV-detection with single-quad MS-spectrometry for determination of TPs generated in the system.

Secondly to evaluate the generation of TPs, by multiple sample points form anaerobic and aerobic bioreactor, comparing the results with analysis from start-up of the WWTP in 2020 with focus on dehalogenation and possible cleavage of the aromatic-ring structure.
Third objective is to evaluate if generated TPs ca be removed by use of activated carbon or ion-exchange resins.

2 Literature review and theoretical background.

2.1 X-ray contrast structure.

ICM produced at GE HealthCare are non-ionic derivatives of 2,4,6-triiodobenzoic acids with polar carboxyl and hydroxyl moieties.
(5-[N-(2,3-dihydroxypropyl) acetamido]-2,4,6-triiodo-N, N0-bis(2,3dihydroxypropyl) isophthalamide or iohexol is synthesized from a **5**-amino-N-N-bis (2,3) dihydroxypropylphtalamid acid base compound. This compound is a benzene ring structure with 2 side chains in addition to an amide group at the 5 positions [6]. The X-ray property is achieved by nucleophile substitution reaction of hydrogen by iodine ions in the ortho-orto-para position of the aromatic ring structure to give 5-amino-N, N'-bis(2,3-dihydroxypropyl)-2,4,6-triiodo-1,3-benzenedicarboxamide (540).

The three iodine atoms are near one another on the benzene ring back-bone. This serves the purpose of stabilizing the molecule, by restricting deiodination and subsequent toxic effect by free iodide in the patient [4, 6].
Iohexol is produces by modification of the amide group by acetylation (541- intermediate) followed by alkylation reaction. Iodixanol is synthesized by a dimerization reaction of two 541 (intermediates). Figure 2.1 shows the structures of the ICM mentioned here.

The added alkylating group contributes to high water solubility, low toxicity and inertness that is critical for its safe administration. The octanol/water partition coefficient ($K_{OW)}$ of iohexol, iodixanol, and intermediates 540 and 541 are -3,05, -3,37. -1,82 and < -2 respectively [4] and SDS). Bioaccumulation potential is expected to be low. Molecular weights of ICM are

relatively large with iodixanol being the largest (1550 g/mol), iohexol (821g/mol) and intermediates 540 (705 g/mol) and 541 (747 g/mol) having smaller mass.

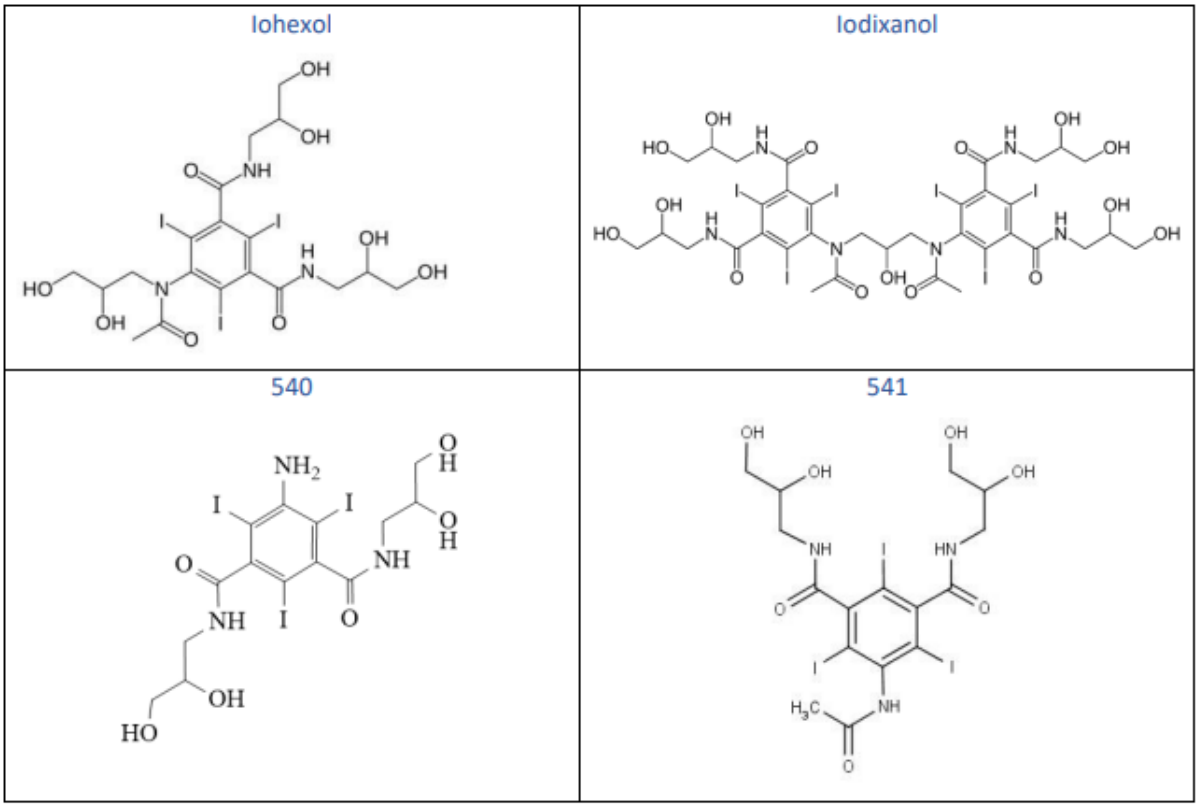

Figure 2.1: Structure of Iohexol (821,2 m/z), iodixanol (1550 m/z) and the intermediates 540 (705 m/z) and 541 (747 m/z). [Own data]

2.2 Fate of X-ray contrast media in the environment.

2.2.1 ICM abundance

ICM are administered at high doses (up to 200 g/dose). Iodine accounts for close to 50 % of the molecular weight [4]. The stability of the molecule in the human body results in 100% non-metabolized ICM being excreted by the kidneys. Half-life of ICM is 2 hours, with 75 % removal after 4 h, and nearly 100 % within 24 h [4]. The wide application of the ICM as a diagnostic tool is evident in the observation of ICM in effluents form sewage treatment plants (STPs) and rivers in Germany [7] and in rivers, surface water in Spain [13], United States and

China [14, 15]. In China ICM concentration of 160 ng/L and 97,4 ng/L was detected in Huangpu River and Tahu Lake [15]. Iohexol has been detected in hospital wastewater (0,07-3810 ug/L), surface waters (0,01-1,326 ug/L), ground water (0,003-0,187 ug/L) and drinking water (0,001—0,034 ug/L) [4]. Water solubility water and inertness and volume used is the main reason why ICM like iohexol is found in the wastewater systems, effluent form WWTP and natural water systems like rivers, lakes, and groundwater [4, 16].

Adsorption of ICM in sludge systems have also been found to be low [17].

2.2.2 Ecotoxicity and formation of transformation products.

Short term toxicity tests with iohexol (10 g/L high-level) showed no toxic effect on bacteria Pseudomonas. Putida, algae (Scenedesmus.*Subspicatus*), Crustaceans (Daphnia.*magna)* and fish (Dario.*Rerio*) [18]. Use of photolytic or oxidative processes in WWTPs or photolytic reactions in natural surface waters, however, have been linked to increased toxicity [4, 16, 18] The toxicity is connected to dehalogenation with subsequent formation of halo nitriles, trihalomethane, halo acetamide and halo acetonitrile's [20]

In china a study observed a trihalomethane concentration of 430 ug/L following WWTP [4, 15]. Predicted no effect concentration (PNEC) of 146 ug/L for Trihalomethanes in aqueous environments have been determined [21]

12 biotransformation products (TPs) of iopromide in aerobic water-soil systems using semi-preparative HPLC, mass fragmentation experiments. The purposed route of transformation was modifications to the hydroxylated side chains. The tri-iodinated aromatic ring remained intact in the study [22].
In another study reductive deiodination of precursor,5-amino-2,4,6-triiodophthalic acid was observed [23]. 11 transformation products from iohexol (TP 863, TP849, TP835, TP833, TP775, TP745, TP687A, TP687B, TP657, TP629 and TP599) was observed in aerobic tests in soil-sediment water interactions. 100 % biotransformation of parent compound was observed [13]. In another study by same author, 46 TPs was detected for iohexol, iomeprol, iopamidol and iopromide in drinking water, surface water and groundwater. Mainly through biological treatment [24]. Ecotoxicity of transformation products have not been performed in accordance with established protocols for Ecotox-testing. However, effluent after biological treatment showed lower toxicity than in the influent [6]. Study from NIVA 2006 however, registered higher toxicity, suggesting release of free iodide to be the reason for the observed effects [5]. Achieving full mineralization may be necessary to avoid the formation of toxic TPs post emission.

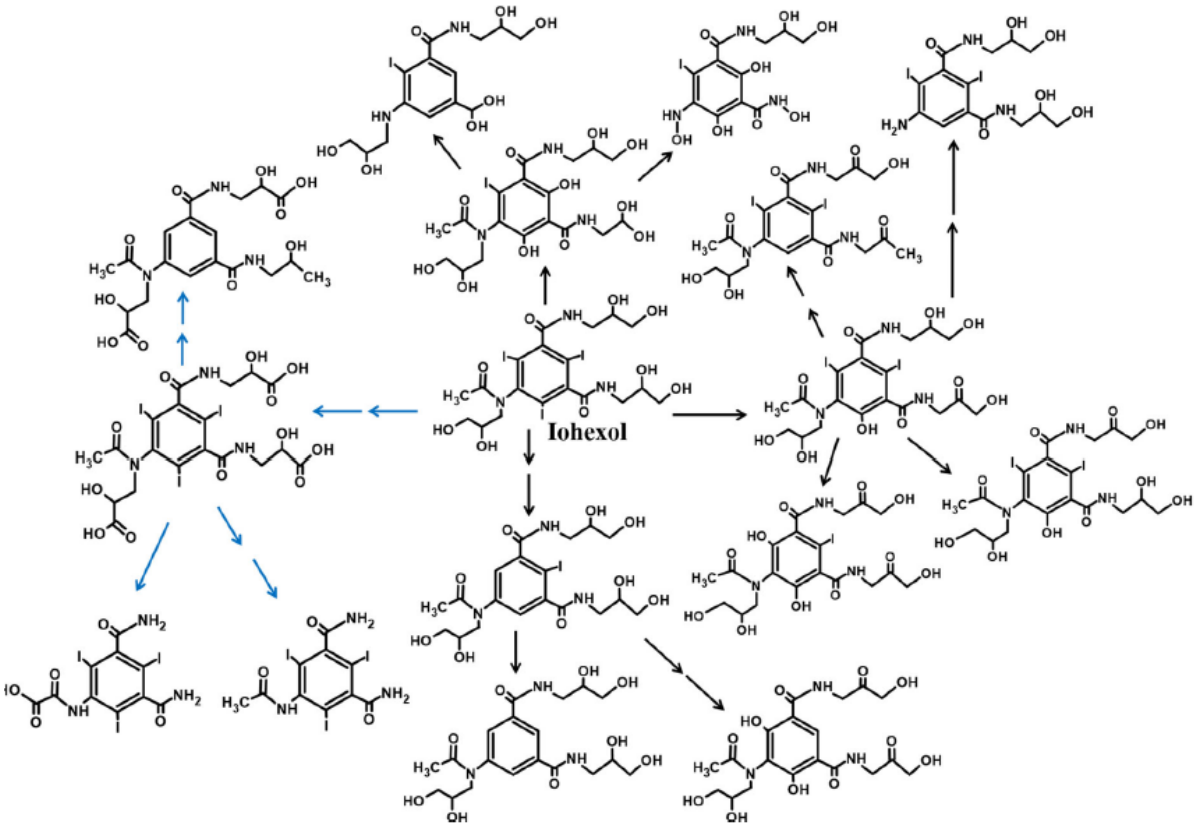

Figure 2.2: TP identified for iohexol by use of advanced oxidative procedures (black arrows) and from biodegradation (blue arrows) [6]

2.2.3 Challenges in reaching total mineralization of X-ray media.

General factors biodegradation are biotic and abiotic factors affect the biotransformation and mineralization of xenobiotics. The structure of the molecule is often used to assess if the molecule is expected to be degraded in nature [25, 26]

The presence of microorganisms with unspecific enzymatic activity followed by a product that can be utilized by other microorganisms are necessary to achieve full mineralization. However, intermediates are often generated that accumulate in the environment [26]. Abiotic factors like pH, presence of organic substrate, electron donors and acceptors, water availability, temperature and concentration of the target chemical are important [27]

Many chemicals are degraded through Co-metabolism. Studies show that addition of organic compounds like acetate and methanol can increase Co-metabolism of aromatic compounds [28]

The chemical might be below a threshold value for degradation. Low initial concentration of microbes able to degrade the chemical or no such community present [29]. Iohexol has three iodides attached to the aromatic ring in addition to two heavily branched sidechains and an amide group at the 5 positions [6]. The presence of halogens branched side groups and number of aromatic rings are of great importance. The proximity of the iodide atoms that makes iohexol safe for administration through restriction of formation of free iodide, in turn also prevents its degradation after excretion from the body. It is suggested that the cleavage of C-halogen bonds can strongly enhance the biodegradation of ICM [4]. Deiodination is therefor the first step in making the aromatic structure susceptible to attack.

2.3 Dehalogenation

Two methods of dehalogenation of aromatic compounds under anerobic conditions have been identified. The first is reductive dehalogenation and the second is a hydrolysis reaction [30]

Reductive dehalogenation is defined as the removal of a halogen substituent from a molecule with a concurrent addition of electrons to the molecule [27].
Dehalogenation of non-aromatic compounds include several mechanisms, but for aromatic compounds the reductive dehalogenation and hydrolysis the mechanisms described so far [27, 30]
For homocyclic aromatic compounds (only C-C bonds in the ring structure) reductive dehalogenation is the main observed mechanism [30] The initial time where dehalogenation is undetectable time or lag phase is called acclimatation period [27]. It has been shown in tests with microbial dehalogenation that this phase can vary from less than a month, to over 6 months [27, 30] Dehalogenation of aromatic amines occurs mainly in the Otho and Para position. It has also been shown that removal of chloride and bromine from aromatic compounds are easier when a destabilizing group like carboxyl of hydroxyl are present. A study suggested that methanogenic environments where the typical redox potential are – 0,3 V and the preferred carbon acceptor is carbon dioxide and methane is produced was the optimal environment for this kind of biotransformation [27].
Deiodination was shown to be coupled to microbial growth in a study of precursor molecule of ICM 5-amino-2,4,6-triiodophthalic acid. The study was done in a mixed culture sludge

system under anaerobic conditions. Three deiodinated compounds was detected. However, deiodination was only observed when ethanol was added as a carbon source [23].
The same author showed that the same ICM precursor molecule was mineralized in an anaerobic-aerobic fixed bed reactor. In this study the deiodination step was seen during the anaerobic step followed by carbon removal in the aerobic step. This suggest that deiodination may enable more efficient degradation in an aerobic polish step and even mineralize the compound completely [31]. Using inoculum of biofilm from pipes close to emission point at GE Health Care I 2006, a lab scale test showed a 22 % mineralization of iohexol after 39 days. Free iodide was detected, supporting the importance of deiodination to achieve this [5].

2.4 Cleavage of benzene-ring

Mineralization of ICM require the breaking of the benzene ring. Under anaerobic conditions monocyclic aromatic can undergo reduction of one or more double bonds of the rings structure, ring cleavage and carboxylation [32].

The adaptation period in one study under anaerobic conditions was 100-120 days for Benzene and 200-250 days for Xylene. The effect of degradation decreased if preferred substrates like methanol and acetate was present [33].

It has been shown that monoaromatic hydrocarbons can like benzene, toluene and xylene can be degraded. Biodegradation of benzene can be achieved under both aerobic and anaerobic conditions. Peripheral enzymes that convert different aromatic compounds play an important role in anaerobic degradation. The peripheral pathways under such reactions converge to benzoyl-CoA. In aerobic degradation formation of catechol with the addition of two hydroxyl groups to the benzene ring ending in ring-cleavage by ring hydroxylation pathway or alkyl substituent oxidation pathway. Enzymatic activity by Toluene dioxygenases attacks the aromatic ring and generated dehydroxylated compounds. Toluene-Monooxygenases on the other hand attack the ring structure and generates arene oxides that due to low stability form phenols. Dihydroxy-compounds undergo fission. The products from can be metabolized in the Krebs cycle [28].

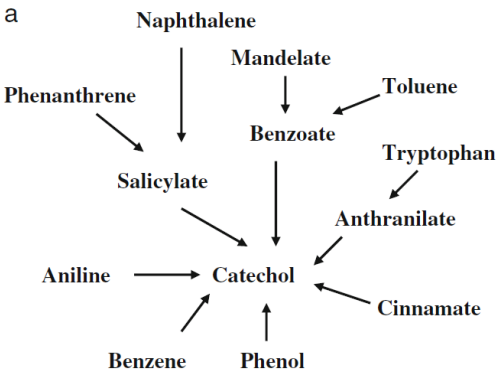

Figure 2.3: Degradation of aromatic compounds to catechol.

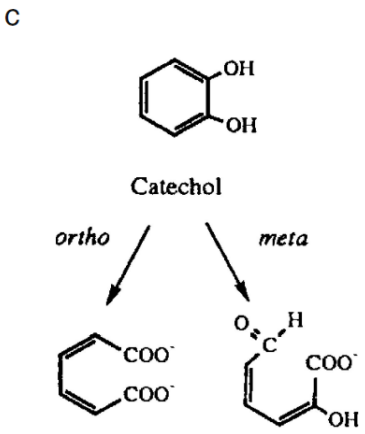

Figure 2.4: Fission of catechol (Orto and meta)

2.5 Biological treatment of production side streams containing high concentration of iohexol, iodixanol and its intermediates.

2.5.1 Biological treatment plant GE Health Care Lindesnes.

Biological treatment is a cost-effective technology for treatment of a variety of chemical side streams [4]. The technology was considered BAT for treatment of acetate and solvent side streams that contributed most of the annual emission to the sea [10]. Concentration of ICM in the reactor is in the mg/L range (table 2.1) ICM was then evaluated as a non-biodegradable COD. The feed is comprised 95 % acetate, with the residual organics being methanol, isopropanol and 2-methoxyethanol. The biological treatment plant is made up of an anerobic main treatment (98 % COD reduction). 3 extended granular sludge bed (EGSB) reactors, each 400 m ^{3} operating with a constant flowrate of 30 m^3/h. The EGSB 1 and 2 was commissioned in 2020 and EGSB 3 was commissioned in April 2023. Conversion of acetate and solvents produces 50 000 N/m^3 of biogas each week. With 98 % of the acetate converted to methane gas during the anaerobic step. The biogas consists of 75-80 % methane, CO_2 and < 100 ppm H_2S. After anaerobic treatment an aerobic polish-step (CFIC) is applied. The aerobic step is a MBBR using polyethylene biocarriers to facilitate a biofilm

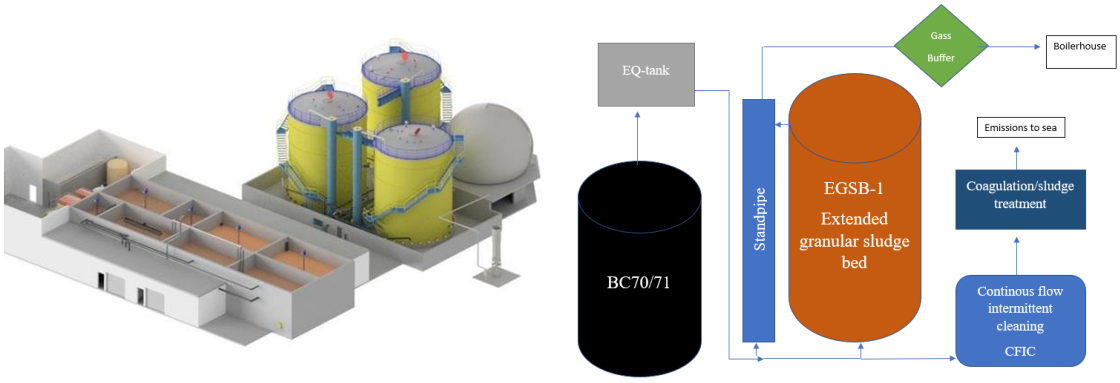

Figure 2.5: Model of biological treatment plant by Econvert in collaboration with Biowater solutions. Commissioned November 2020. [34]

Table 2.1: Concentration of ICM and derivates measured by quantitative HPLC. Sample from EQ-tank BC70/71 which functions as feed tanks for the EGSB (anaerobic bioreactor).

Contrast media constitute	**Concentration in feed**
Dijod-540 (contaminant in intermediate 540)	*3,50 mg/L*
541 (2nd intermediate)	*25,56 mg/L*
540 (1st intermediate)	*22,26 mg/L*
Iohexol	*37,21 mg/L*
Iodixanol	*23,29 mg/L*
Total ICM	*111,8 mg /l*
Total ICM	*80,5 kg/day* *29,3 tons/year*

The concentrations vary due to batch production in the respective production areas. The sample value in table 2.1 is based on a pooled weekly sample form the EQ-tank that feeds the EGSBs. About 50% of the ICM weight is iodine. The loss of iodine in the reactor is there for estimated to be half of the value of total ICM from table 2.1.

2.5.2 Biological community in EGSB 1, 2 and 3

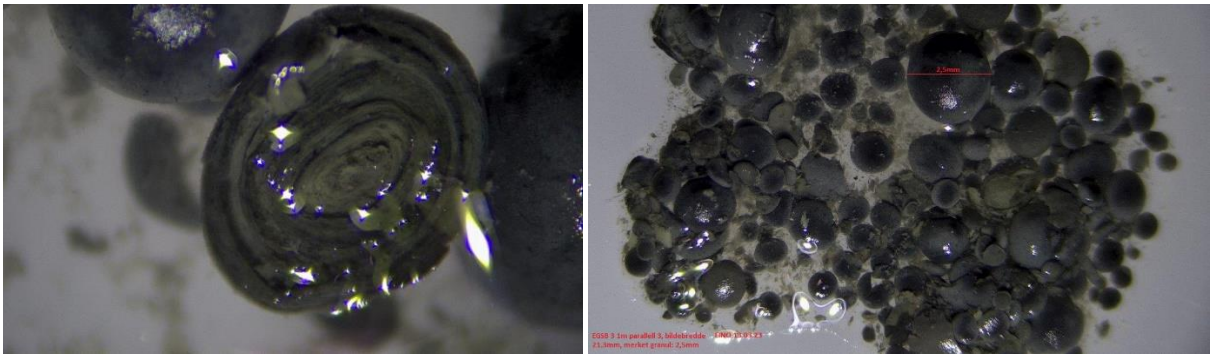

Figure 2.6: a) Cross section of anaerobic granule b) Granule distribution, largest granules was 2 mm. Pictures was taken using light-microscope by process engineer Eivind Norin at P-16.

In March 2023 studies was of the microbial community was performed by using extraction DNA form granules from EGSBs and the biofilm from the CFIC. The results showed that EGSB 1 and 2 was nearly identical. EGSB 3 distinguished itself from the other reactors. Microbial diversity investigation showed that that EGSB 1 and 2 showed a higher abundance of Geobacter, Sphaerocheta, Tenufilum and Sulfospirillum.

Pelobacter, *Bacillus*, *Synthophobacter* was present in all rectors, but with higher abundance in EGSB 3. Geobacter and Sphaerocheta abundance in EGSB 3 was hardly detectable. EGSB 1 and 2 shows comparable results with EGSB 1 having slightly more reads in the investigation than EGSB 2 [35].

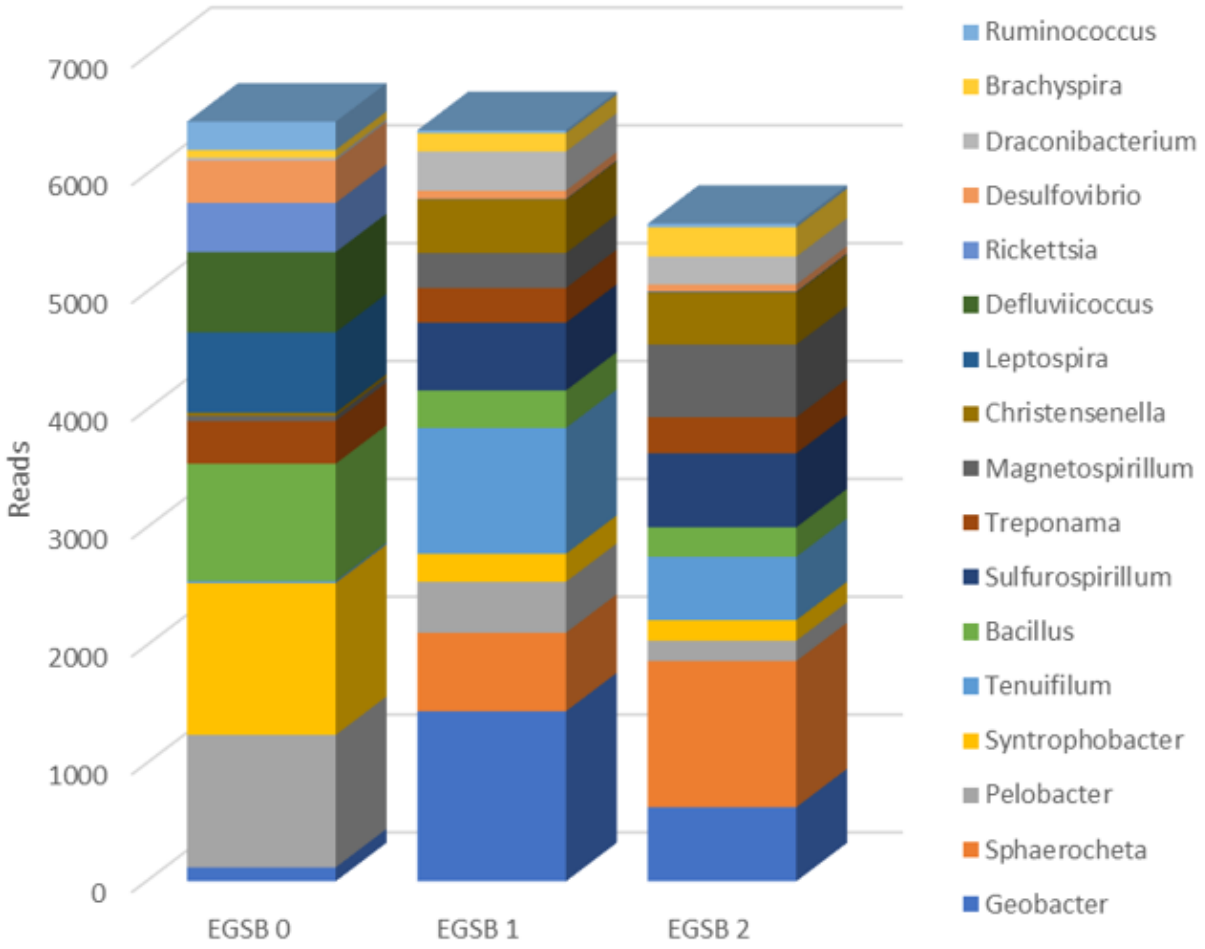

Figure 2.7: 16S rRNA analysis of bacterial community in EGSB 1, 2 and 3 (April 2023). EGSB 0 = EGSB 3. Analysis was done under commissioning of EGSB 3 to evaluate the change in the microbial community over time [35].

2.5.3 HPLC results after commissioning of EGSB 1 and 2 (December 2020)

Tests was performed 4 months after commissioning of the biological treatment plant. Samples was taken from feed tank, EGSBs and CFIC to evaluate the fate of ICM from the feed. Results showed that all ICM was present after treatment. Comparison between the feed solution (figure 2.8), and EGSB (figure 2.9) and CFIC (figure 2.10) illustrates the limited change in ICM levels through the WWTP.

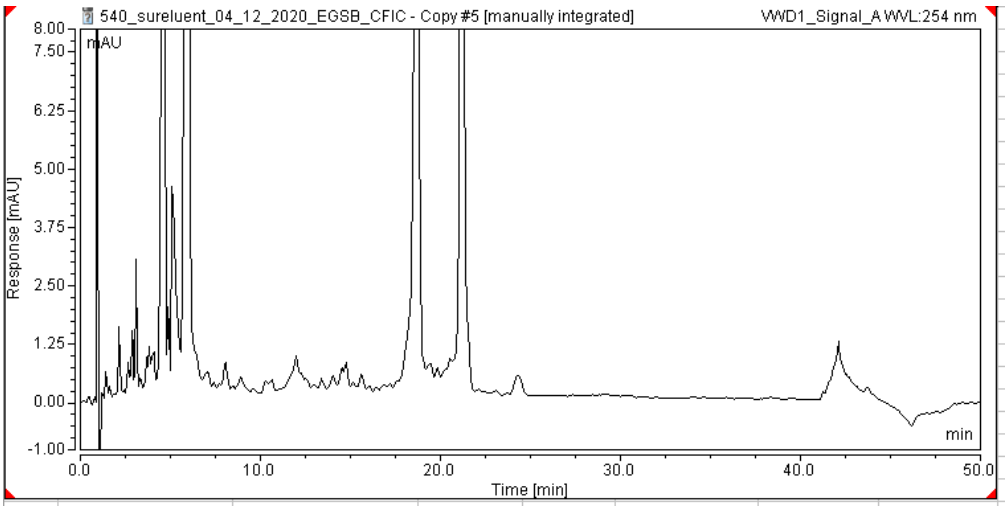

Figure 2.8: HPLC results from feed (SP3) in 2020 4 months after commissioning. (Own analytical data)

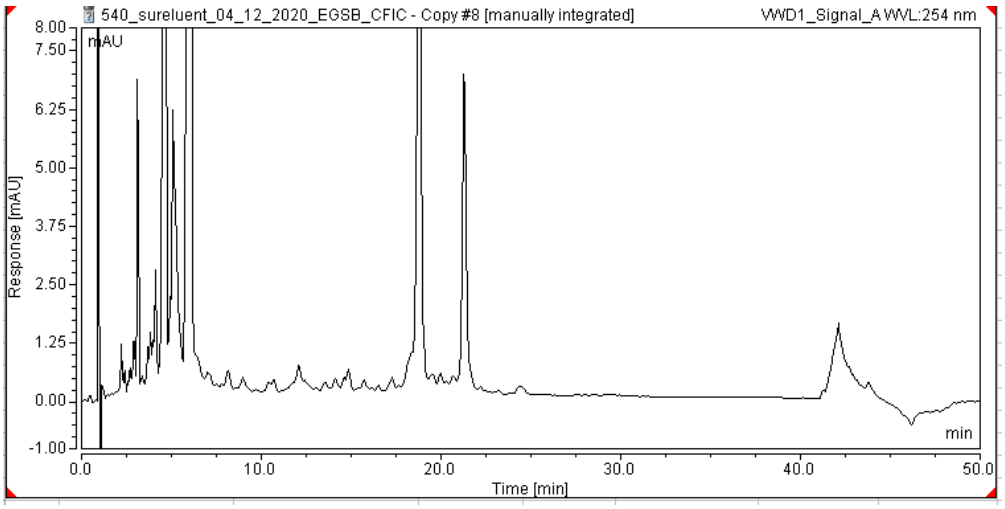

Figure 2.9: HPLC analysis results from EGSB 2 (SP10) in 2020, 4 months after commissioning. (Own analytical data)

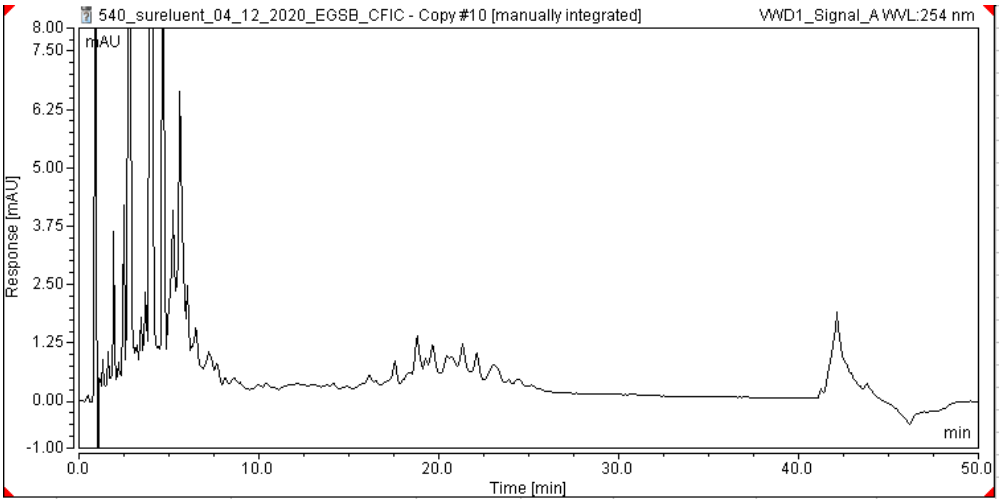

Figure 2.10: HPLC-analysis from CFIC (SP29) Dec 2020, 4 months after commissioning.

(Own analytical data)

2.5.4 Detection of ICM and potential TPs in wastewater.

LC-MS is a powerful analytical instrument, with high sensitivity and low detection limit. The advantage with using MS combined with HPLC-separation and UV-detector is the ability to combine the data from retention time and the m/z for evaluation of the analytes. Detection of parent ICM and TPs have been detected at ng/L range, using HPLC-ESI_MS-MS [17]. ICM was detected in German sewer-systems with concentration of 1 ug/L, using LC-ESI tandem MS [36]. Full elucidation of the chemical structure of the TPs has been shown by combining LC hybrid triple quadrupole linear ion trap mass spectrometer and nuclear magnetic resonance [17]. The MS-detector increases sensitivity, add certainty and selectivity [37].

2.5 Single -quadrupole mass-spectrometry (SQ-MS)

This technology can provide sensitive and selective detection of organic molecules.
Interfacing High Performance Liquid Chromatography (HPLC or LC) with MS provides one of the most powerful analytical tools available.
Mass spectrometry is a very powerful analytical technique used for identification of unknown compounds, quantification of known compounds, determination of mass and chemical structure.

The basic function of an MS detector is to measure the mass-to-charge ratio of ions. The unit of mass used is the Dalton (Da). The MS detector gives the mass (m) to charge (z) of the molecule. The m/z can only be referred to the mass of the ion if the charge of the ion Is one.

Single Quadrupole Good scan function sensitivity good selectivity/sensitivity via SIM scanning High duty cycle with SIM. However, SIM functionality are subject to matrix interferences and thereby limit detection limits [37, 38]

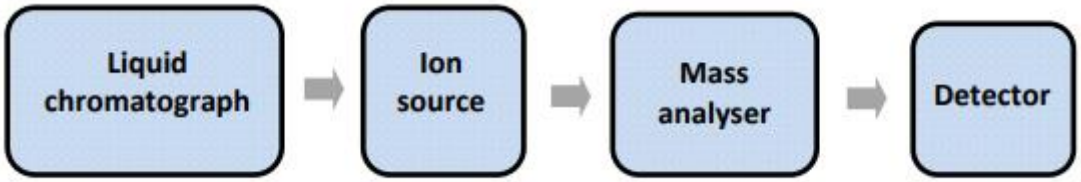

Figure 2.11 Simple schematic of the basic components in A LC-MS system [37].

Separation is performed in LC-column and compounds enter the MS. The compound is ionized in the and dried by nitrogen, removing the mobile phase. The ionized compounds are passed to the mass analyzer and separated based on the stability on the stability of trajectories they have in the oscillating electric field in the quadrupole rod structures. Behind the quadrupoles a charged plate (positive or negative) attracts the ions to the detector. Results are presented in a total ion current (TIC). TIC is the relative abundance of all the ions in the mass specter. The TIC is plotted against time giving ions-abundance relative to time. The exact mass under each peak is extracted as MS-specters. In MS-specter all masses are relative to the peak with highest intensity (base peak).

3. Materials and methods

Analytical methods of chromatography were used in this study. Standards and methods for determination of anions by ion-chromatography was performed in accordance with internal methods used in environmental emission monitoring program. The HPLC method and MS-method was created as a part of this thesis.

3.1 Sampling and sample preparations

Samples was taken from several sample points at in the period March-May 2023. Sampling form WWTP was done by the site process engineer. Table 2 shows the sample point identity and description. Each sample was 1 liter in volume collected in 1 liter plastic bottle. The sample contained no trace of biomass form the WWTP. The samples were filtered through a 0,45 µm filter by using a funnel and a flask attached to a vacuum. Filtrate was kept at 4 ℃ until analysis. Samples for HPLC/LC-MS and IC was filtered through a 0,22 µm syringe prior to analysis.

Table 3.1: Overview of sample points selected from the WWTP.

Sample points	Posision
SP3	**EQ-tank EGSB 1 feed**
SP4	**EQ-tank EGSB 2 Feed**
SP 33	**EQ-tank EGSB 3 Feed**
SP9	**Effluent EGSB 1**
Sp10	**Effluent EGSB 2**
SP29	**Prior to coagulation tank.**
SP36	**Effluent EGSB 3**
SP39	**Effluent from hydrocyclon between EGSB and CFIC**

3.2 HPLC-MS

3.2.1 Separation and quantitative analysis of ICM.

HPLC analysis was performed on a Vanquish Flex system from Thermo Scientific. The system was purchased in 2022 and was validated as a part of the preparation for this study. The system is a modular system equipped with a quad-pump with degasser, auto-sampler, variable wavelength UV-detector, column department, switch-valve, CAD-detector, and a single-Quad mass spectrometer (MS). Separation of the ICM was performed on a Luna, 3 µm C18, 150 x 2 mm column (Phenomenex). The mobile phase was MilliQ-water with 0,1 % formic acid and Acetonitrile (superlco, LC-MS grade). The HPLC was performed using gradient elution (see table 3) with flowrate 0,250 ml/min. UV-detector wavelength was 254 nm. Samples was filtered through a 0,22 µm syringe filter directly into HPLC-vials. Quantification of ICM in the samples was done using calibration standard. Stock solution (ICM) was made by weighing in 1g/L of each component iodixanol, iohexol, 540 (intermediate 1), 541 (intermediate 2) and ABA-HCl (raw-material) in MilliQ-water. A calibration standard was made by diluting stock solution 1:100.

Testing with neutral pH was done by using pure MilliQ-water without formic acid.
Chromeleon 7.3 workstation chromatography data handling software was used to process the data from the analysis.

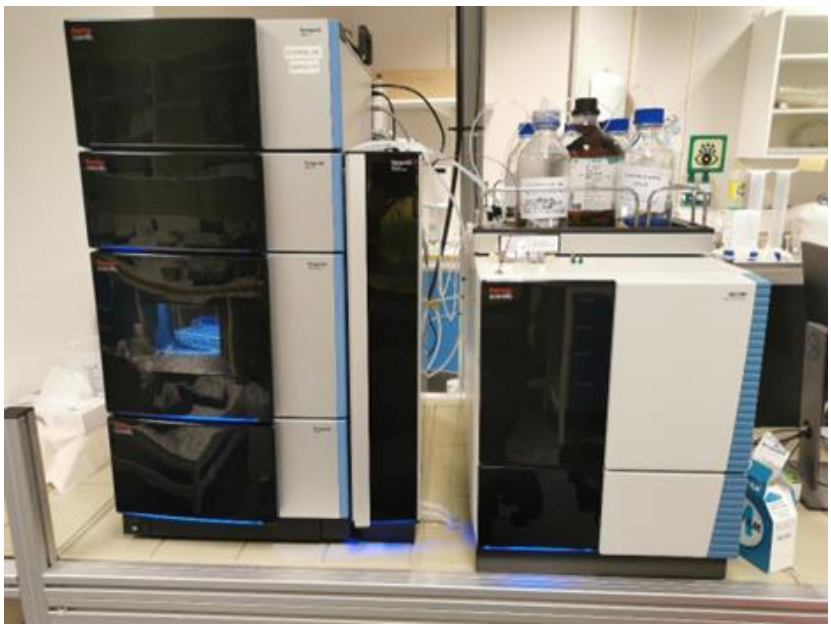

Figure 3.1: Overview of the HPLC-MS (Vanquish Flex, Thermo Scientific)

Table 3.2: Gradient elution program for the HPLC and HPLC-MS analysis.

Time	Mobile phase composition	
	Acetonitrile	MilliQ-water + 0,1 % formic acid
0	3 %	97 %
30	10 %	90 %
40	20,3 %	79,7 %
40	50 %	50 %
41	3 %	97 %
48	3 %	97 %

The gradient ensures separation of all ICM parent molecules, intermediates and selected known impurities that enters the WWTP. Equilibration of 8 min was applied to ensure stabile constituents starting the next sample. Table 3.2 shows the composition of the mobile phase during elution.

3.2.2 Full scan- MS

Following pre-separation on the HPLC-column, the analytes was further analyzed using the MS, giving the mass to charge (*m/z*) of the analytes. Using the column switch, the transfer from the HPLC-column to the MS for specter acquisition was set to 2 min. The first 2 min, the flow was derived to waste. Salts and smaller hydrophilic molecules that elutes early from the HPLC-column, increases the noise in the specter. Acquisition after 1 and 2 minutes were tested. Mass-range during full-scan was Acquisition was performed using full-scan was 150-1600 m/z using comparative mode and positive ion polarity. Specter acquisition was between 2-40 min of the 48 min run. Several methods were tested to give optimal conditions (table 3.3). The Chromeleon wizard easy viewer was used to generate methods based on three parameters. Sensitivity vs Robustness, Volatility of mobile phase (high vs less), Thermal stability of analyte (stabile vs labile). Sensitivity is adjusted by decreasing the sweep-gas, while robustness is decreased. ICM are thermostable and a method with high temperature in ion-transfer tube increases the ionization of these compounds. However, if the TPs are more thermos labile, a lower temperature would be necessary to stop fragmentation.

In total 6 methods were tested.

Threshold for registration for peaks in the MS-specter was set to filter out all peak's lower that 10 % of peak with highest intensity.

Table 3.3: Overview of the methods tested for optimization of the analysis using the mass-spectrometers.

Parameters	Unit	Method 1	Method 2	Method 3	Method 4	Method 5	Method 6
Vaporization temperature	℃	144	144	144	144	317	144
Ion-transfer tube temperature	℃	300	400	400	150	400	150
Sheat-gas	pSIG	32,3	32,3	32,3	32,3	58,8	32,3
Aux-gas	pSIG	3,6	3,6	3,6	3,6	5,2	3,6
Sweep-gas	pSIG	0,5	2,0	0,0	0,0	0,5	0,5
Source voltage Positive ions	Volt	3000	3000	3000	3000	3000	3000

3.2.3 Testing and validation of LC-MS method

Standard validations parameters were performed before testing of wastewater form biological treatment plant. Linearity, specificity, accuracy, and precision was tested using 4 levels of calibrations standards (Level 1: 0,1, Level 2: 0,01, Level 3: 0,001 and Level 4: 0,0001 g/L). Standards was made using stock solution (chapter 3.2.1). Standard level 1 was used to evaluate accuracy and precision. Specificity was performed by verifying the m/z of known ICM and intermediates was performed on mass-spectrometer using standard solution level 1. Mass of compounds in the calibration standard was iohexol (821 m/z), iodixanol (1550 m/z), 541 (747 m/z), 540 (705 m/z) and ABA-HCl (362 m/z).

3.3 Ion chromatography (IC)

Samples for analysis by IC was prepared by filtering samples from SP3, SP9, SP10, SP36 and SP29 through 0,22 µm syringe filter. The filtered sample was diluted 1:25 in fresh MilliQ-water and transferred to HPLC-vials. Calibration standard stock-solution was made by using sodium iodide (I^- 1,423 g/L, VWR), and Sodium Chloride (Cl^- 2,50 g/L VWR). Working standard was made by diluting stock solution 1:100 in MilliQ-water.

Samples was analyzed on a Dionex integrion HPIC system (Thermo Scientific). Separation was done using an Ion-Pac AS18 analytical (2mm x 250 mm) column and Ion-Pac AG18 Guard (2 mm x 250 mm) pre-column (Thermo Scientific). MilliQ-water and Potassium hydroxide (Eluent Generator Cartridge) was used as mobile phase. The method detects anions present in the solution using a conductometer. Chloride was added to the calibration standard as it is expected to remain unchanged through the biological treatment plant.

Table 3.4: Instrument parameters IC.

Parameters	
Column temperature	40 ℃
Cell temperature (detector)	35 ℃
Flow	0,250 ml/min
Suppressor current	38 mA (milliampere)
Injection volume	10 µl

KOH (Cartridge KOH (Thermo Scientific) was automatically mixed according to the method input (Chromeleon). MilliQ water and potassium hydroxide (KOH) were used to make eluent with the described concentration in table 3.5

Table 3.5: Overview of gradient elution IC.

Time	Concentration (KOH) mM
0 – 5,5	12
5,5 - 11	12-60
11 - 24	60
24 – 24,1	60-12
24,1 - 27	12

3.4 Single ion monitoring (SIM) targeting deiodinated compounds and selected TPs of iohexol from literature.

Single ion-monitoring (SIM) was used to detect the presence of specific ions in the sample. This was done to achieve higher sensitivity and reduce noise. Scan time was set to the same time frame as the full scan (2-40 min of the 48 min run). The dwell time used on the target ion increases and in turn increases the sensitivity of the method. Besides the MS-detector change from full scan to SIM, all other parameters were as described in chapter 3.2.1 and 3.2.2. MS method 1 (table 4) was selected. Default values in method 1, is suitable for mist compounds, recommended by the CM wizard. The masses presented in table 3.6, was used to look for proof of deiodination in the biological treatment plant as well as look for TPs already described for iohexol in nature [17]

Table 3.6: Overview of the method for SIM analysis targeting deiodated variations of iohexol and intermediates 540 and 541. Iohexol TP_1 to 10 are masses of known TPs of iohexol found in soil and aquatic environments [17] *The table was imported from Chromeleon 7.2 chromatography data processing software.*

	Name	Start Time (min)	End Time (min)	Mass	Ion Polarity	Source CID Voltage	Tube Lens Voltage
▶	IOH_TP_1	2	40	694,3	Positive	0	Last Tune
	IOH_TP_2	2	40	567	Positive	0	Last Tune
	IOH_TP_3	2	40	440,5	Positive	0	Last Tune
	540_TP_1	2	40	578,35	Positive	0	Last Tune
	540_TP_2	2	40	451,4	Positive	0	Last Tune
	540_TP_3	2	40	324,5	Positive	0	Last Tune
	541_TP_1	2	40	620,1	Positive	0	Last Tune
	541_TP_2	2	40	493,2	Positive	0	Last Tune
	541_TP_3	2	40	366,3	Positive	0	Last Tune
	IOhexol TP_1	2	40	863	Positive	0	Last Tune
	Iohexol TP_2	2	40	849	Positive	0	Last Tune
	Iohexol TP_3	2	40	835	Positive	0	Last Tune
	Uohexol TP_4	2	40	833	Positive	0	Last Tune
	Iohexol TP_5	2	40	775	Positive	0	Last Tune
	Iohexol TP_6	2	40	745	Positive	0	Last Tune
	Iohexol TP_7	2	40	687	Positive	0	Last Tune
	IOhexol TP_8	2	40	657	Positive	0	Last Tune
	Iohexol_TP_9	2	40	629	Positive	0	Last Tune
	IOhexol TP_10	2	40	599	Positive	0	Last Tune
*							Last Tune

3.5 Treatment of TPs with activated carbon (MCN)

Samples from SP 29 (CFIC), SP3 and SP 36 (EGSB 3) was treated with MCN activated carbon prior to analysis with LC-MS as described in chapter 3.3. MCN carbon is a high performance, high purity carbon with a broad adsorption range. The microporosity is especially good [49].

400 ml of each sample was added 1,0 grams of MCN activated carbon powder (Carlson ltd) in an 800 ml beaker. A magnetic stirrer was used to insure sufficient mixing. The sample was mixed in 1 hour, filtered by use of a 15 µm filter paper to remove the MCN carbon. The treated sample was then filtered through a 0,22 µm syringe-filter, and analyzed by LC-MS.

3.6 Treatment of TPs with ion-exchange resins.

Ion-exchange treatment was performed on samples from SP29 and SP36.
400 ml of each sample was added acidic ion-exchange and caustic ion-exchange resins (DOW chemicals) in according to instructions of the supplier. The ion-exchange was performed as a mixed-bed in an 800 ml glass beaker at room temperature. The sample was stirred in 1 hour followed by separation of the ion-exchange resin. The pH before and after the treatment was measured using pH-indicator paper.

4. Results

4.1 Results HPLC and Mass-specter for calibration standard solution.

The method was validated to ensure that the quantification of ICM was accurate, with good linearity for the expected range of ICM. Qualitative MS-detection of m/z for known components was confirmed. All tests were accepted, and the method was evaluated as “fit for purpose”.

4.1.1 Precision

4.1: Precision results based on 4 parallels of standard solution injected. Areal % of all compounds was used as parameters.

Standard	541 (areal %)	Iohexol (areal %)	Iodixanol (areal %)	540 (areal %)
Average	25,8667	16,8133	21,6133	17,22
Standard deviation (SD)	0,04041	0,44636	0,33561	0,33867
Confidence interval ±	0,14479	1,59914	1,20237	1,21335
Relative standard deviation (RSD) %	0,15624	2,65477	1,55279	1,96675

Precision observed in the HPLC method was good, with an RSD < 5 %

4.1.2 Accuracy

Accuracy was calculated according to formula:

Accuracy (%) = $\frac{Measured\ consentration\ g/L}{Theoretical\ concentration\ g/L}$ * 100 %

The accuracy for each compound was within ± 2% of the theoretical concentration represented by the value of the standard solution.

Iohexol = 99,0 %

Iodixanol = 98,3 %

540 = 99,0 %

541 = 99,0 %

Since ABA-HCl is not an ICM, but a raw-material, it is not included here.

4.1.3 Specificity

Resolution was good for all components in the calibration standard. Both on HPLC and TIC. The of m/z observed for was in accordance with the known mass of the compound. Isomers was observed for iohexol. Table 4.2 shows the retention time and m/z for the detected peaks. However, the resolution in the UV-specter was higher than that observed for the TIC.

Reduced ionization of ICM compounds compared t the strong chromophore of the benzene ring structure. ABA-HCl visible in as peak 1 in figure 4.1 and 4.2 showed opposite result and

increased intensity, as the compound is easily ionized with high ion abundance in the TIC-chromatogram.

4.1.4 Linearity

Using 4 levels of calibration standards with 2 parallels at each level, a standard curve was constructed.

The results showed very good linearity in the selected range.

Data with calibration curves for each component is listed in Appendix I.

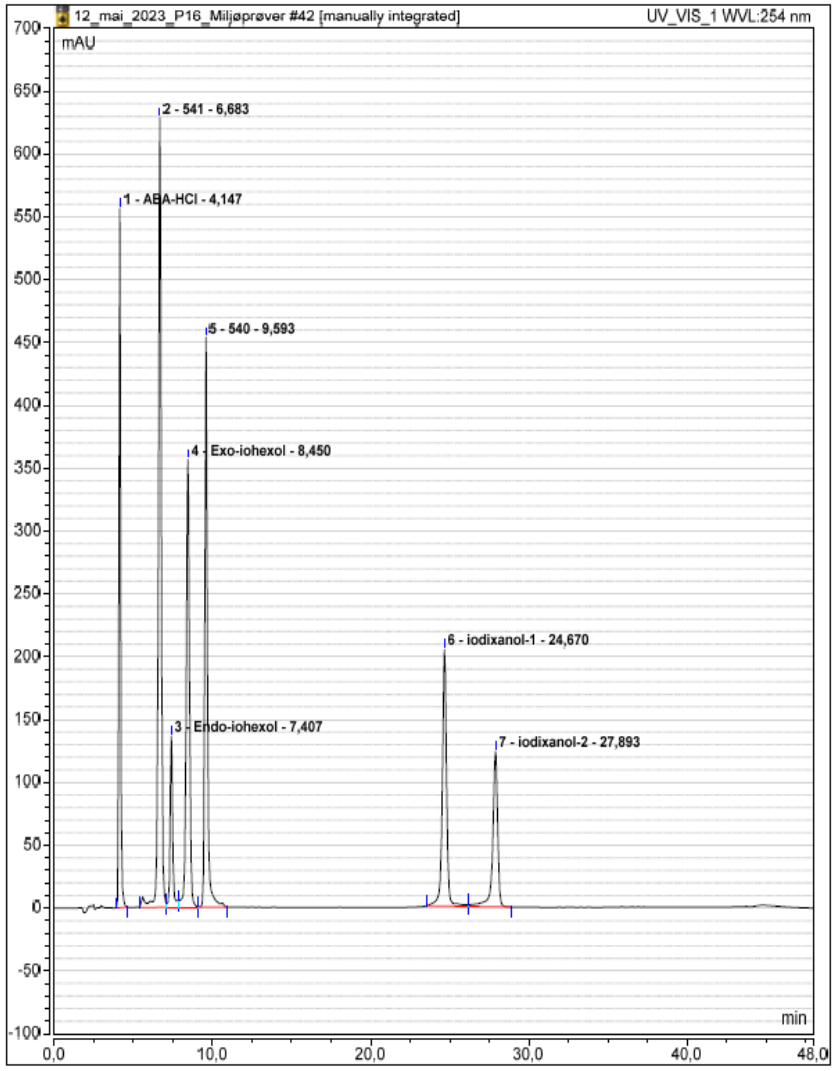

Figure 4.1: HPLC analysis of standard solution using UV-detectror at 254 nm.

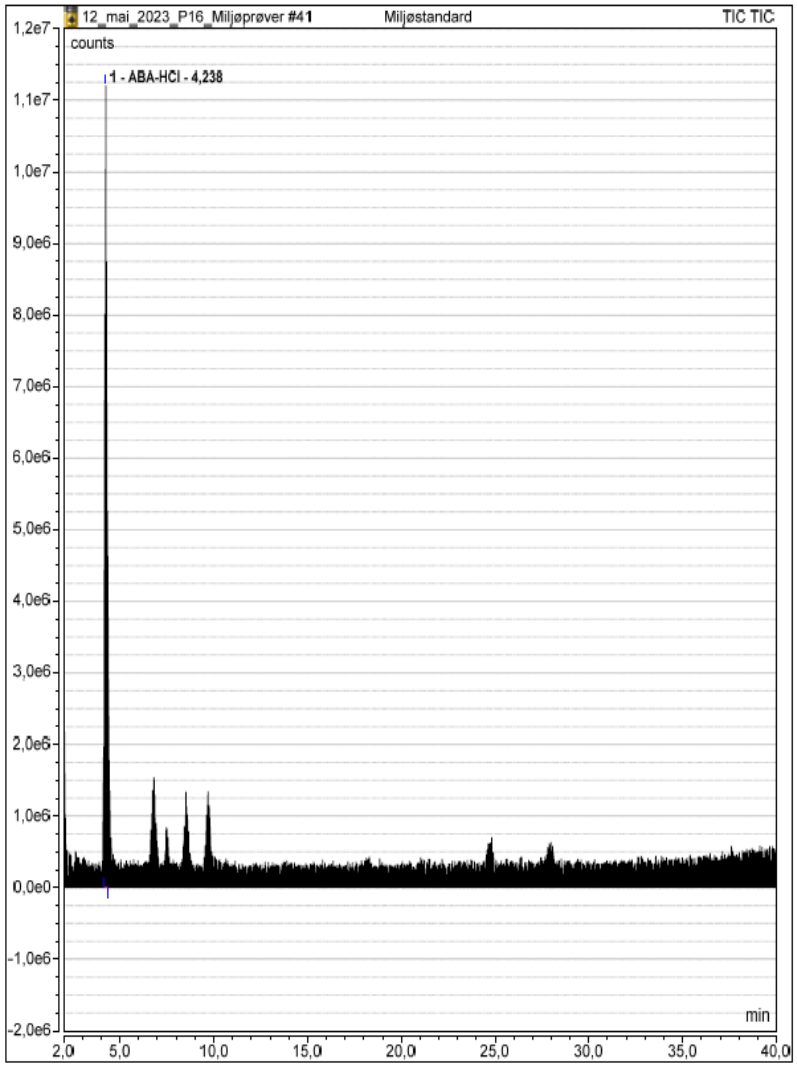

Figure 4.2: TIC- chromatogram standard solution.

Iodixanol is barely visible on the TIC, making resolution difficult.

Table 4.2: Reference standard of ICM and intermediates data from MS and UV.

Peak nr	Standard analyte	Retention time	Molecular mass	m/z from MS M +H^+	Comment
1	ABA-HCl	*4,147*	328	328,1 /655,2/656,3	*655 = dimer*
2	541	*6,683*	747	747,8 /792,9/1494,8	*1494,8 = dimer of intermediate 541*
3	Endo-iohexol	*7,407*	821,13	821,9 / 822,8	*Endo and Exo iohexol are isomers with slight difference in retention time on HPLC.*
4	Exo-iohexol	*8,450*	821,13	821,8 / 822,8	
5	540	*9,593*	705,2	705,7 /750,9 /1410,8	*1410,8 = dimer intermediate Azo-540*
6	Iodixanol-1	*26,670*	1550,13	1551,0	*Identified as two masses, as the bond between the dimers are fragile.*
7	Iodixanol-2	*27,893*	1550,13	775,9 /1552	

Figur 4.3: MS-specter of identified peaks of ICM-standard. A) ABA-HCl b) 541 c) and d) iohexol e) 540 f) and g) iodixanol

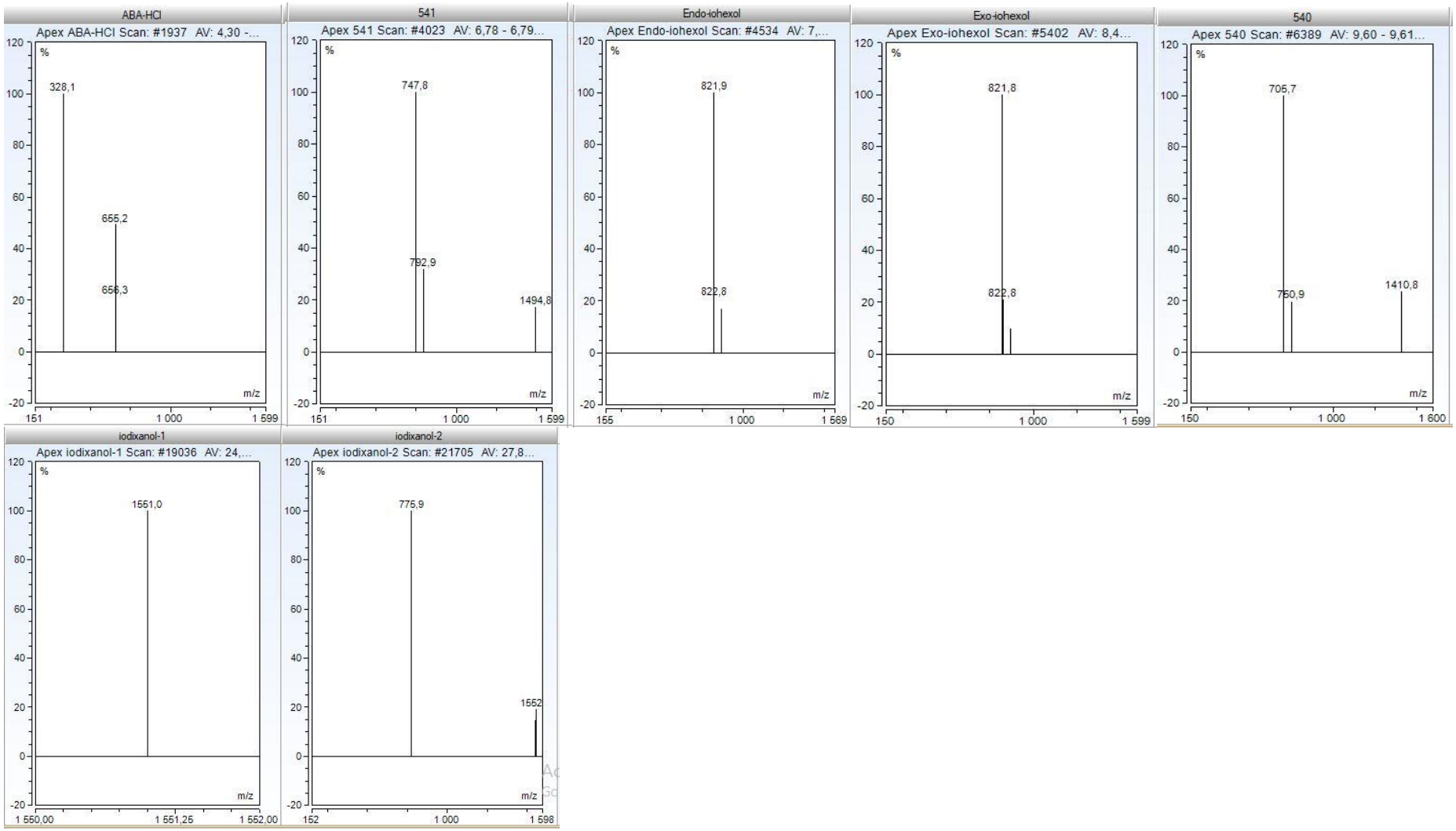

4.1.5 Testing of MS-detector parameters

Sample SP36 was used to test the MS-methods. Samples was performed in the same sequence using the same batch of eluents. The same 11 peaks was evaluated for m/z and peak counts/ ion abundance (Appendix I). Method 1 is a default method with a moderate temperature on the Ione-transfertube, Aux and Sheath-gas pressure. Method 1 (Table 3.3) was chosen as it had the second best peak count and the least noise in the baseline.

HESI ionization is considered a soft ionization method, and no fragmentation was detected in the sample when the temperature in the ion transfer tube was increased from 150 ℃ to 400 ℃. Reducing the aux-gas had negative effect on the robustness of the method. Reducing the intensity of the TIC-signal. Evaluation the overall TIC of the methods showed that increasing the sensitivity cased less ionization and higher signal to noise. Since ICM is thermostabile, but TPs might be less thermostabile, the default method was consideres the safer choice.

No significant diffrences in m/z of the 11 tops was observed when comparing the methods.

4.2 LC-MS analysis of samples form biological treatment plant (P-16)

4.2.1 Quantitative HPLC analysis of ICM.

Only iohexol and was detectable in the effluent from the EGSBs (Table 4.3). The MS-specter confirmed the presence of mass 821,9/822 m/z. Iohexol degradation observed in the samples was 96-98 %. After CFIC (SP29) iohexol was no longer detected (under detection limit). The levels of ICM in the feed (SP3) corresponded with the levels normally seen in feed (Table 2.1).

Table 4.3: Quantification of ICM in samples for WWTP using HPLC-UV with calibration standard. Nd= not detected

Sample point	Iohexol (mg/L)	541	540	iodixanol
SP3 (feed)	*48*	21	25	17
SP9	1	n.d	n.d	n.d
SP 10	2	n.d	n.d	n.d
SP36	1	n.d	n.d	n.d
SP39	2	n.d	n.d	n.d
SP 29	n.d	**nd**	**nd**	**nd**

4.2.2 MS-analysis of the feed solution to the biological treatment plant.

Analysis of the influent to EGSBs showed that iohexol, iodixanol and the intermediates 541 and 540 was present. The retention time and masses from the MS correlated with that of the substances in the calibration standard. In peak 1 the mass of di-iodide 540 (579 m/z) and ABA-HCl (328 m/z) was detected. Quantification of ABA-HCl was not possible because of the co-elution with di-iodinated 540.

The observations are natural in the side-stream from the production. The intermediates and final product do contain a range of known impurities. However, the levels are relatively small. All the observed masses in the feed solution represent known masses from the production. Table 4.4 shows an overview of the compounds naturally found in the feed tank to the WWTP.

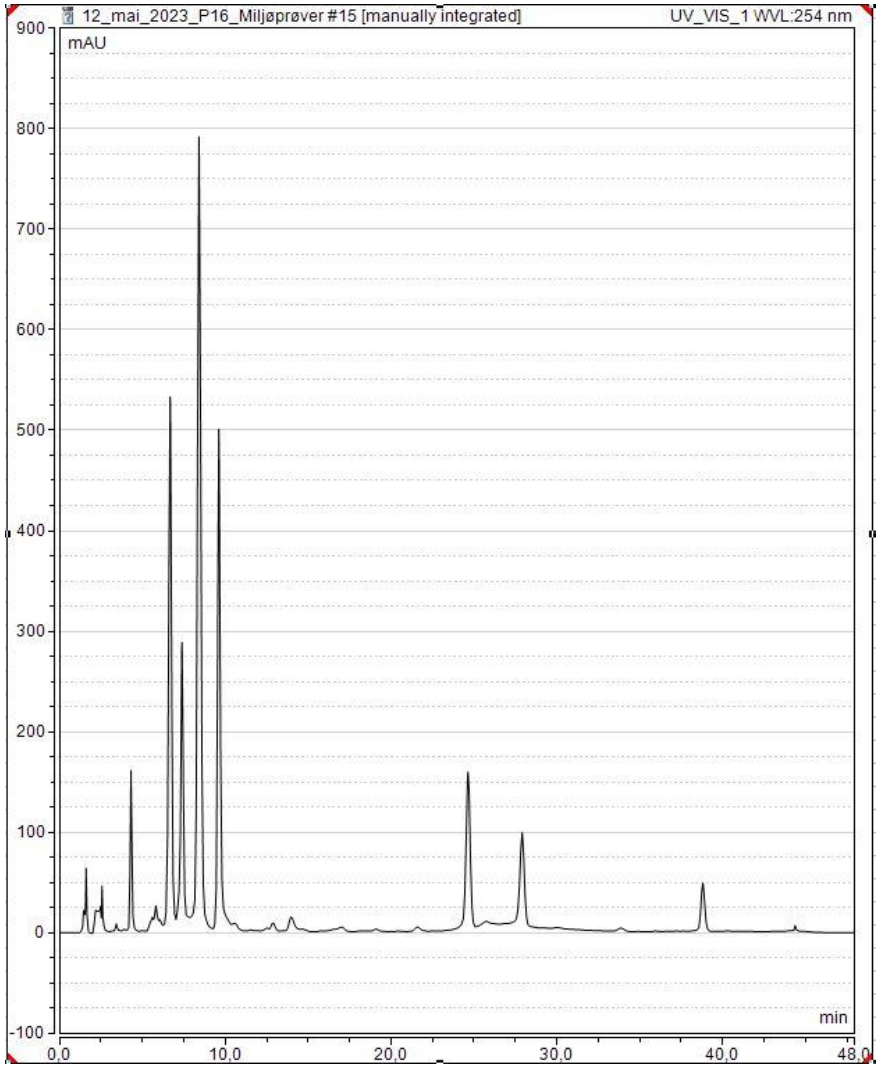

Figure 4.4: HPLC-Chromatogram BC-70/71 feed tank EGSB

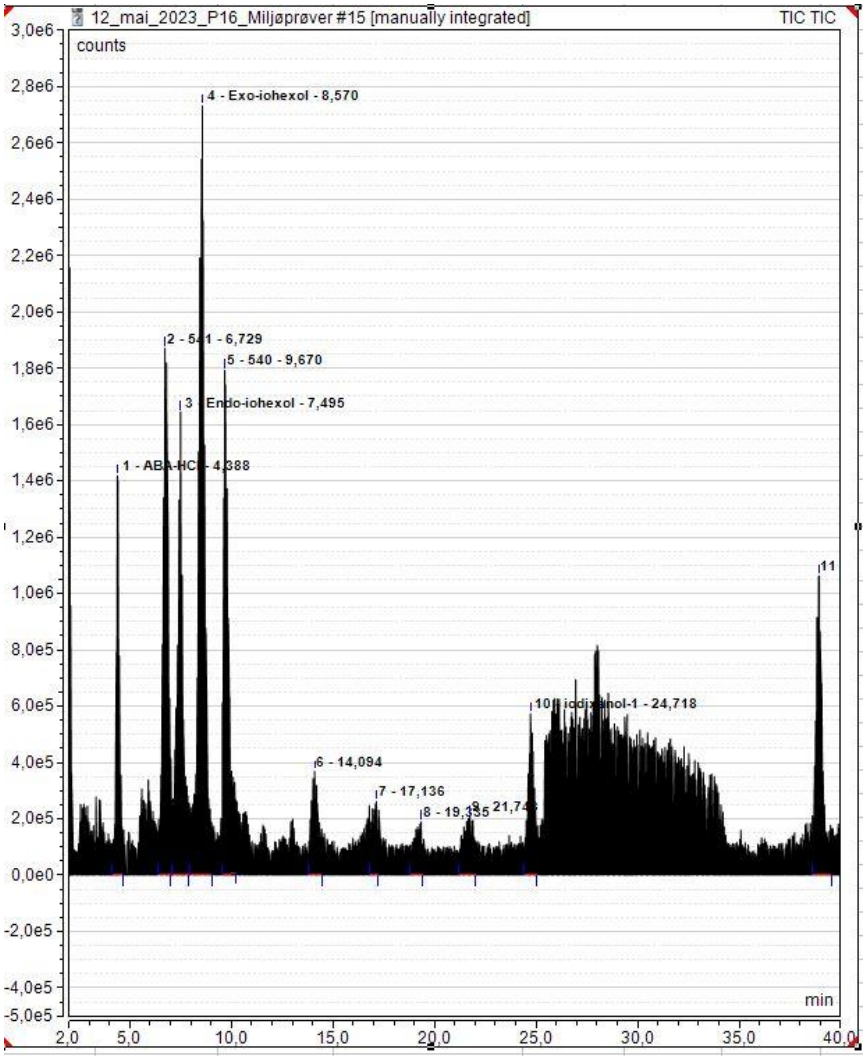

Figure 4.5: TIC-Chromatogram BC-70/71 feed tank EGSB

The noise seen after 25 minutes in TIC (figure 4.5) conforms with the gradient increase of water in the mobile phase.

Table 4.4: All detected masses in peaks from TIC-chromatogram from sample SP3 (feed)

Peak number	Retention time (min)	m/z (mass to charge) [M + H^+]	Comment
1	*4,388*	328,2 /579,9/601,9	ABA-HCl + 540-diiodated
2	6,729	748,2/747,7/749,2	541
3	7,495	822,2/821,7/828,1	Iohexol
4	8,570	822,0/823,0	Iohexol
5	9,670	705,9/707,0	540
6	14,694	730,0/730,9	
7	*17,136*	586,2/587,2	
8	19,335	460,3/699,5/367,7	
9	21,743	790,0/811,9/835,0	
10	24,718	776,2/775,7	
11	38,932	688,9/706,8/705,2	

4.2.3 MS-analysis of the EGSB 1, 2 and 3 (anaerobic biological treatment plant).

Analysis of all EGSBs showed multiple peaks with good resolution. The Peaks in the TIC chromatograms corresponded with the peaks from the UV-chromatogram, except for peaks eluted after 30 minutes, where no UV-signal was detected using 254 nm wavelength.

Figure 4.6 and figure 4.7 shows HPLC-UV specter and TIC-chromatogram of EGSB 1.

Table 4 gives an overview of the time vs *m/z* form HPLC-MS analysis of EGSB1.

Main TPs detected with highest relative abundance was TP 696, TP 887, TP 371, TP 740, TP 767, TP795, TP 593, TP 342, TP711, TP796, TP725, TP 586 and TP 643. In total 25 peaks were detected in the TIC, with several masses present associated with each peak.

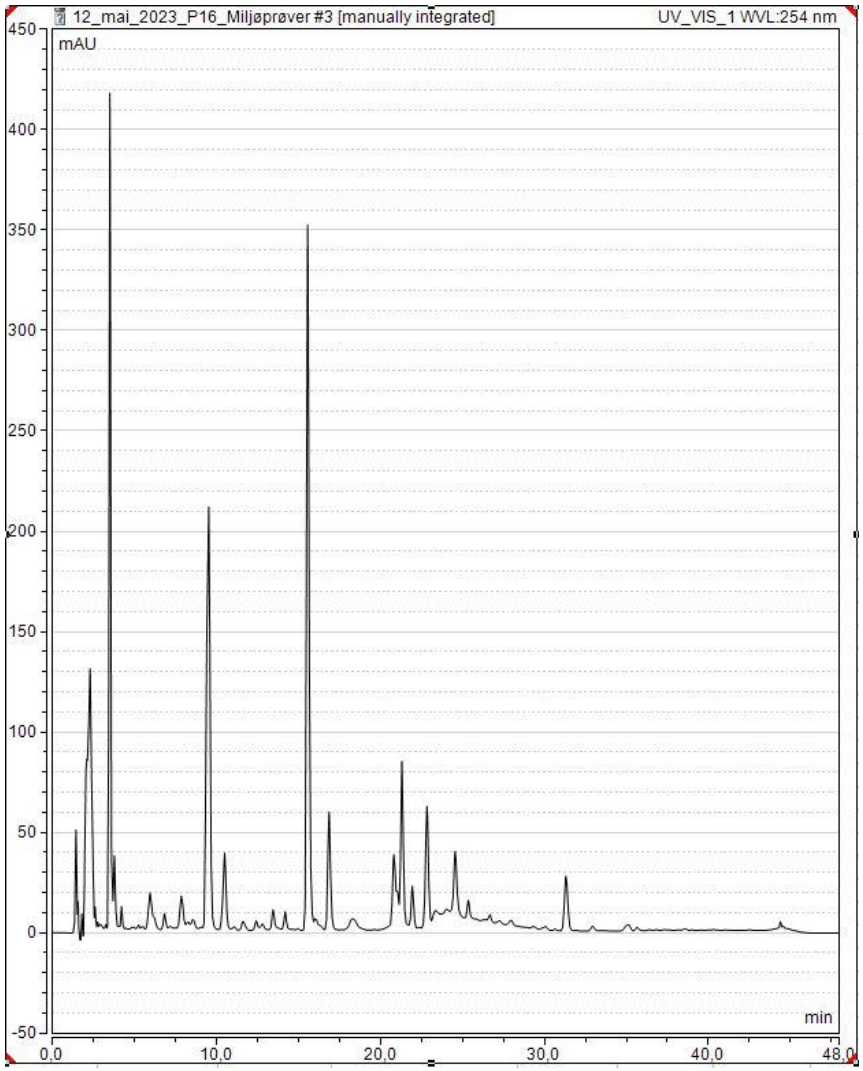

Figure 4.6: HPLC chromatogram EGSB 1 (SP9)

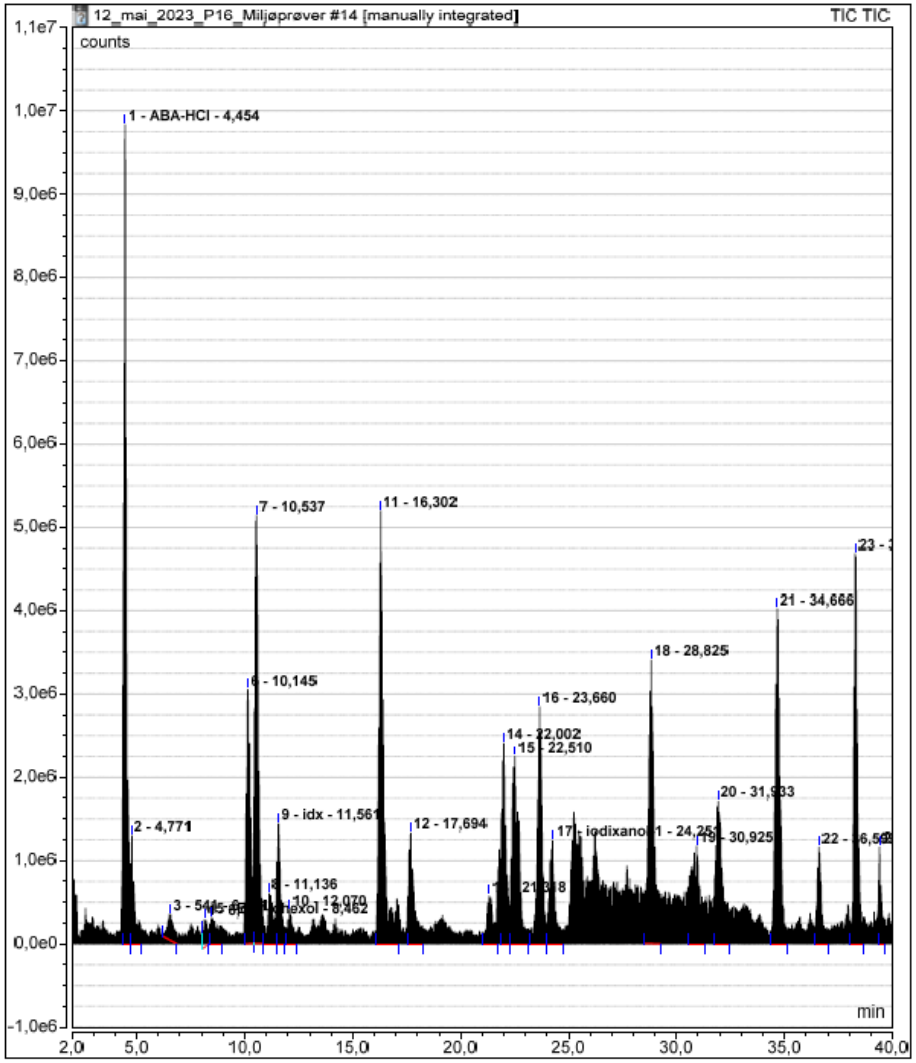

Figure 4.7: TIC-chromatogram EGSB 1 (SP9)

several peaks had positively charged adducts. The amount of sodium in the sample and the relatively common appearance of sodium adducts when using positive mode during HESI, makes the results plausible. Multiple charged peaks did also occur to a large extent in sample from SP3 (feed). The observation from EGSBs shows similar patterns for all reactors. Only double charged molecules was positively observed. The presence of double charge indicated that the molecule could accept charge on two locations. The m/z = the mass /charge will result in the mass being divided by two, which is seen in the mass-specter. All masses that were detected are listed in tables to the specific samples.

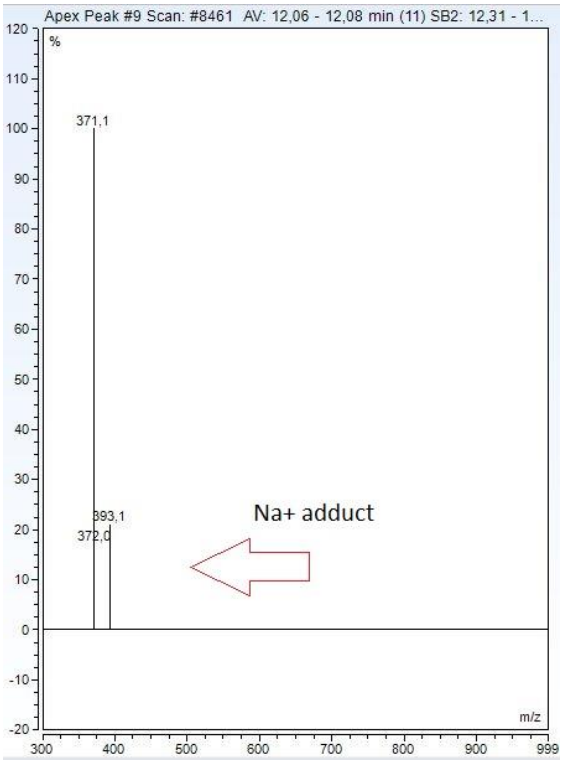

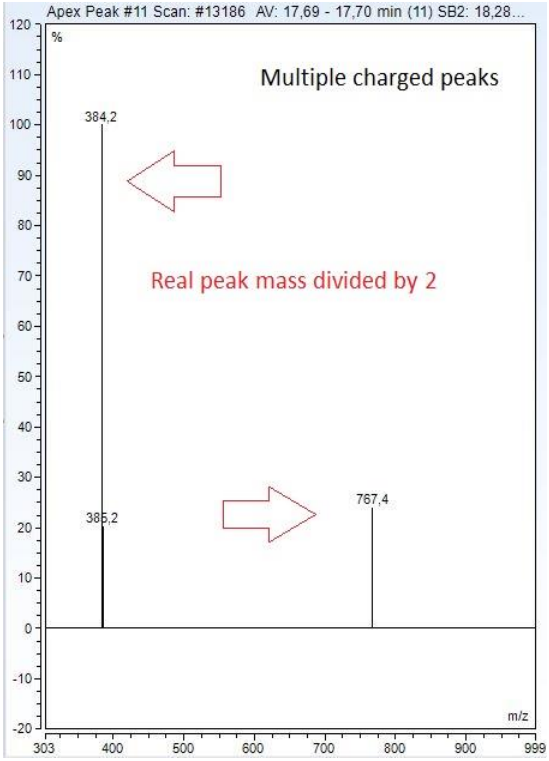

Figure 4.8: Na+ adduct peak 9 EGSB 1. *Figure 4.9: Double charge observed in peak 11 in EGSB1*

Table 4.5: All detected masses in peaks from TIC-chromatogram from sample SP9 (effluent from EGSB 1)

	Retention time (min)	m/z (mass to charge) [M + H^+]	Comment	Peak number	Retention time (min)	m/z (mass to charge) [M + H^+]	Comment
1	*4,454*	328 / 655,3	655 is a known dimer.	14	22,510	300,3 /328,3 /305,2	
2	*4,562*	342,2		15	23,660	444,2 /445,3 /887,5	444,2 and 445,3 (half mass) suspected double charge
3	*6,595*	696 / 718,3/696/717	717 and 718 suspected Na+ adduct	16	24,255	314,2 /342,4 /319,2 /341,9 /384,1	
4	*8,562*	821,8	iohexol	17	25,245	386,2 /431,3 /385,7 /387,3	
5	*10,211*	444,3 /445,3/887,4/888,6	444,3 and 445,3 suspected double charge	18	26,235	356,4 /711,3 /552,1 /355,8 /712,2 /357,0 /733,2	Mass 733,2 suspected Na+ adduct
6	*10,595*	402,3 /403,3 /803,4		19	28,825	344,3 /327,3 /372,1	
7	*11,236*	458,2 /459,3		20	30,925	358,2 /341,2 /386,3 /359,2	
8	*11,620*	416,2		21	31,935	398,4 /795,4 /796,2	398,4 (half mass) suspected double charge
9	*12,161*	371,1 /393,1 /372,0	Mass 393,1 suspected Na+ adduct	22	34,665	388,3 /371,3 /416,3 /389,3	
10	*16,300*	370,2 /739,4 /740,5	370,2 (half mass) suspected double charge	23	36,600	402,3 /430,3 /385,3 /403,3	
11	*17,695*	384,2 /386,2 /767,4	384,2 and 386,2 (half mass) Suspected double charge	24	38,275	432,3/415,3 /433,4	
12	*21,315*	615,2/ 593,1 /616,2 /594,3 /342,2 /319,4	Mass 615,2 and 616,2 suspected Na+ adduct	25	39,400	446,5/ 474,3	
13	*22,005*	795,4 /796,6 /398,5 /398,0	398,5 and 398,0 (half mass) suspected double charge				

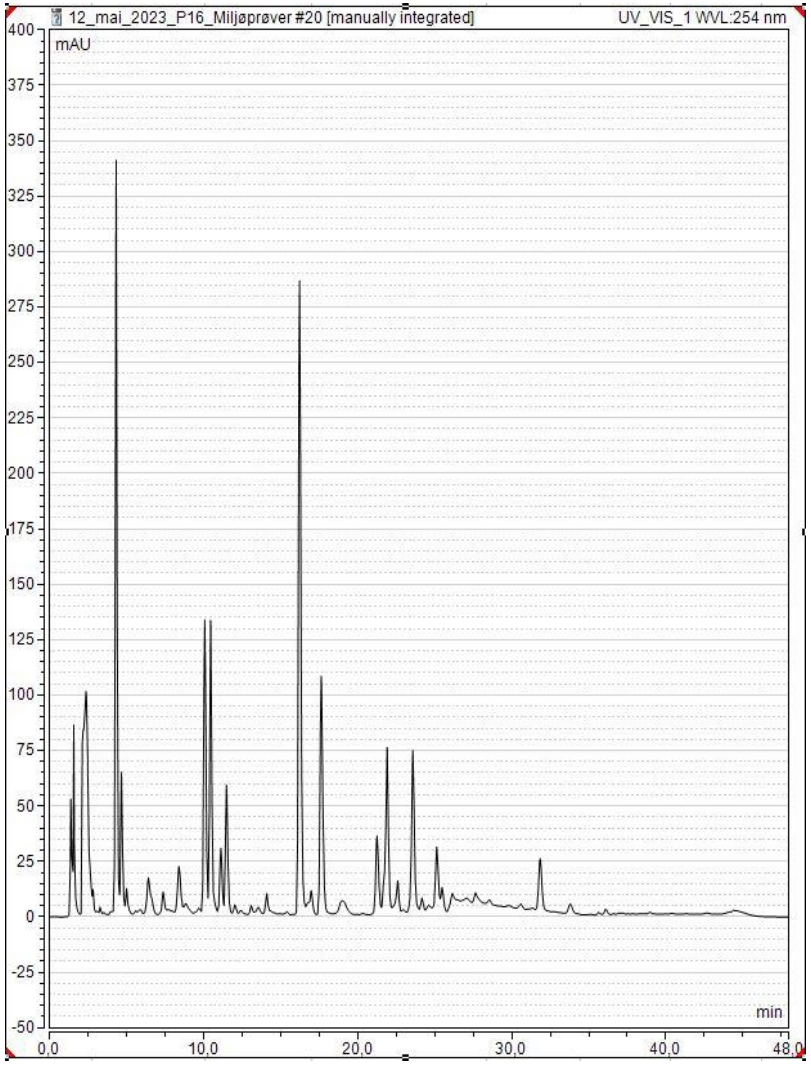

Figure 4.10: HPLC-chromatogram EGSB 2 (SP10)

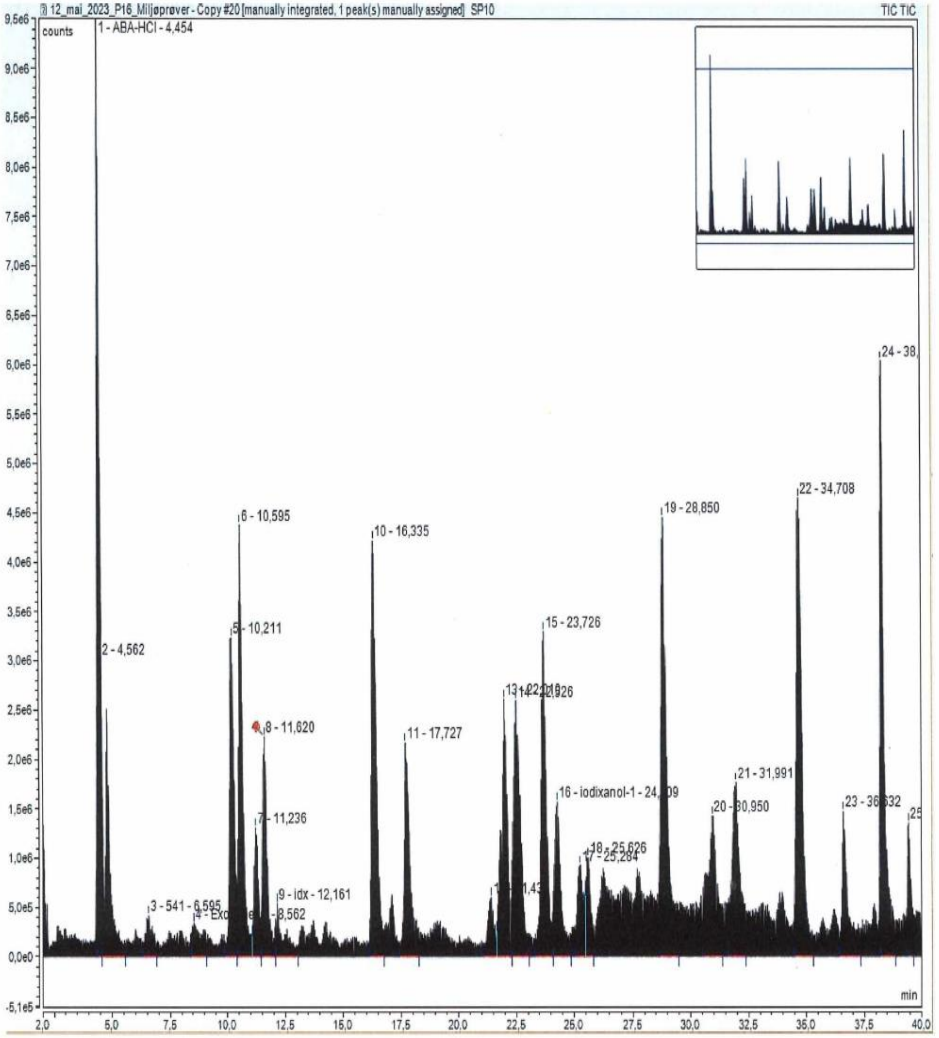

Figure 4.11: TIC- Chromatogram EGSB 2 (SP10)

Table 4.6: All detected masses in peaks from TIC-chromatogram from sample SP10 (EGSB 2)

Peak number	Retention time (min)	m/z (mass to charge) [M + H^+]	Comment	Peak number	Retention time (min)	m/z (mass to charge) [M + H^+]	Comment
1	*4,454*	328 ,2/ 329,3/ 655,3/655,4	Dimer av ABA-HCl (known component)	13	22,010	300,3 /328,3 /305,2	
2	*4,562*	328,2/329,2/677,3		14	22,525	444,5/444,0/445,3 /887,5	(Half mass) suspected double charge
3	*6,595*	696,2 / 695,6 / 718,1	Mass 718,1 suspected Na+ adduct	16	23,725	314,2 /342,2 /319,3/318,8 /384,2/384,9/767,4	Mass 342,2 suspected Na+ adduct of mass 319,2. Mass 384,2 /384,9 suspected double charge
4	*8,562*	821,6/ 822,2/823,1/ 843,8	Iohexol Mass 843,8 suspected Na+ adduct	17	24,305	386,2/ 793,3	Possible Na+ adduct followed in addition to double charge.
5	*10,211*	444,3 /445,3/887,4/888,6	(Half mass) suspected double charge	18	25,285	327,2 /344,2	Possible NH 4+ adduct
6	*10,595*	402,3 /403,3 /803,5		19	28,855	458,2/459,2	
7	*11,236*	458,3 /459,3		20	30,955	341,2/358,3/383,2/386,3	
8	*11,620*	416,2/ 417,3		21	31,990	398,4 /795,4 /795,1/817,3	Mass 817,3 Na+ adduct. 398,4 Half mass of 795,4 double charge present
9	*12,161*	371,2 /372,3		22	34,705	371,3 /388,3/393,2/416,3	Mass 416,2 suspected Na+ adduct
10	*16,335*	370,2 /371,3/739,4 /740,5/761,4	(Half mass) suspected double charge. Mass 761,4 suspected Na+ adduct	23	36,635	402,3 /430,6 /385,4 /407,4/406,9/403,3	
11	*17,725*	384,2 /386,2 /767,4	(Half mass) suspected double charge	24	38,305	415,3 /432,3/437,3/416,3	Mass 437,3 suspected Na+ adduct
12	*21,435*	615,2/ 593,1 /616,2 /594,3 /342,2 /319,4	Mass 615,1 and 616,0 4 suspected Na+ adduct	25	39,445	446,3/ 429,3/451,2/ 474,3	

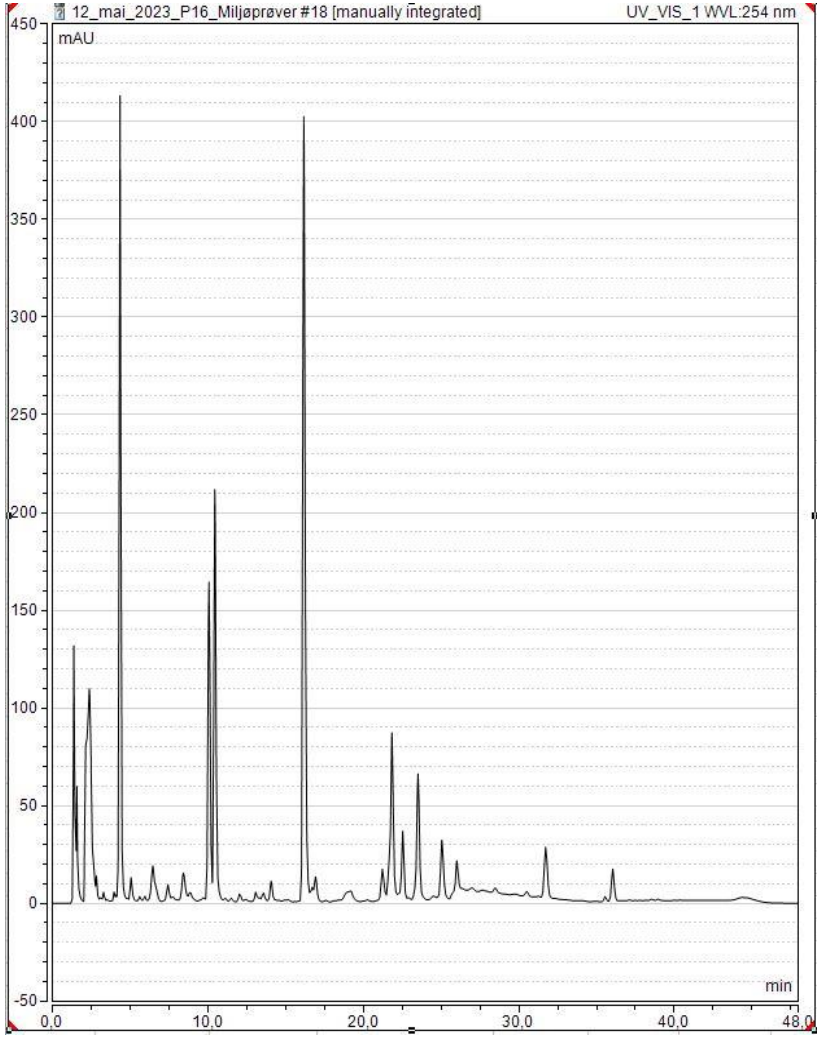

Figure 4.12: HPLC-Chromatogram EGSB 3 (SP36)

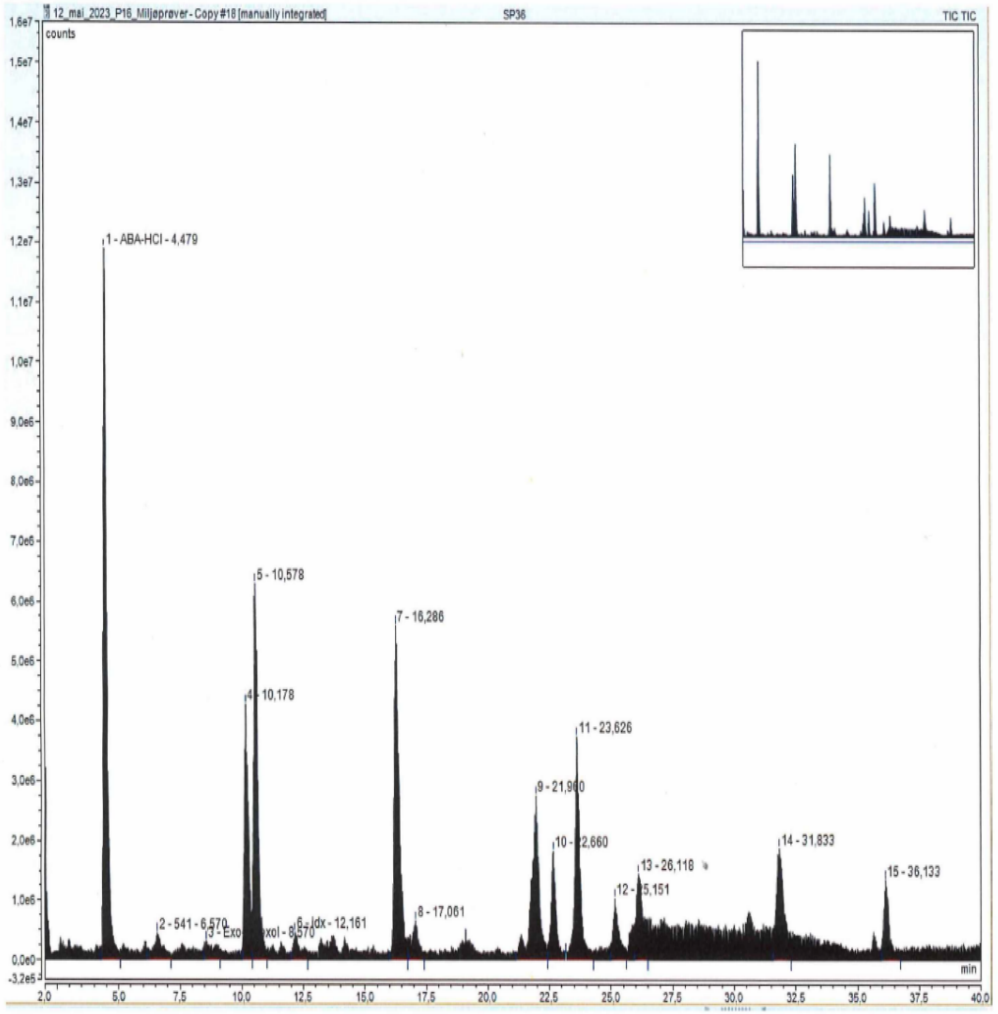

Figure 4.13: TIC-Chromatogram EGSB 3 (SP36)

Names in figures TIC were automatically assigned based on expected retention time of the ICM. However, in the EGSBs only the identity of iohexol was confirmed by mass-specter.

SP36 showed 11 dominant peaks. Peak nr 3 had the same retention time and m/z as the exo-iohexol. Showing that some iohexol leaves the EGSB 3 as intact parent molecule. No other ICM detected in the feed (SP3) was detected in the effluent of EGSB 3. A total of 15 peaks of interest was selected in the TIC-chromatogram.

Table 4.7: All detected masses in peaks from TIC-chromatogram from sample SP36 (effluent from EGSB 3)

Peak number	Retention time (min)	m/z (mass to charge) [M + H^+]	Comment	Peak number	Retention time (min)	m/z (mass to charge) [M + H^+]	Comment
1	*4,479*	328,2 / 655,3	Dimer (known contaminant)	9	*21,960*	398,2/796,4 /398,8/795,5/795,0	(Half mass) suspected double charge
2	*6,570*	696,0 /697,0/718,1	Na+ adduct	10	*22,660*	377,2/753,6	(Half mass) suspected double charge
3	*8,570*	821,9 /822,6 /844,9/843,5	Na+ adduct 821,9/822,6 (iohexol)	11	*23,626*	444,2 / 445,3	Possible double charge, but positive identification of larger mass not present.
4	*10,178*	887,5/888,5/ 444,2/445,3	(Half mass) suspected double charge	12	*25,151*	386,3/385,8/387,2/771,4/793,4	(Half mass) suspected double charge
5	*10,578*	402,2/403,3/803,4		13	*26,118*	356,3/711,2/733,4	733,4 **suspected** Na+ adduct Mass 356,3 (Half mass) suspected double charge
6	*12,161*	371,2 / 372,3		14	*31,833*	398,7/398,0/795,3/796,0/796,7/ 817,3	Mass 817,3 **suspected** Na+ adduct. Mass 398,7/398,0 3 (Half mass) suspected double charge
7	*16,286*	739,3 / 740,4/370,4/369,8	(Half mass) suspected double charge	15	*36,133*	643,2 / 311,1	
8	*17,061*	352,2 /358,2 /586,1/725,3					

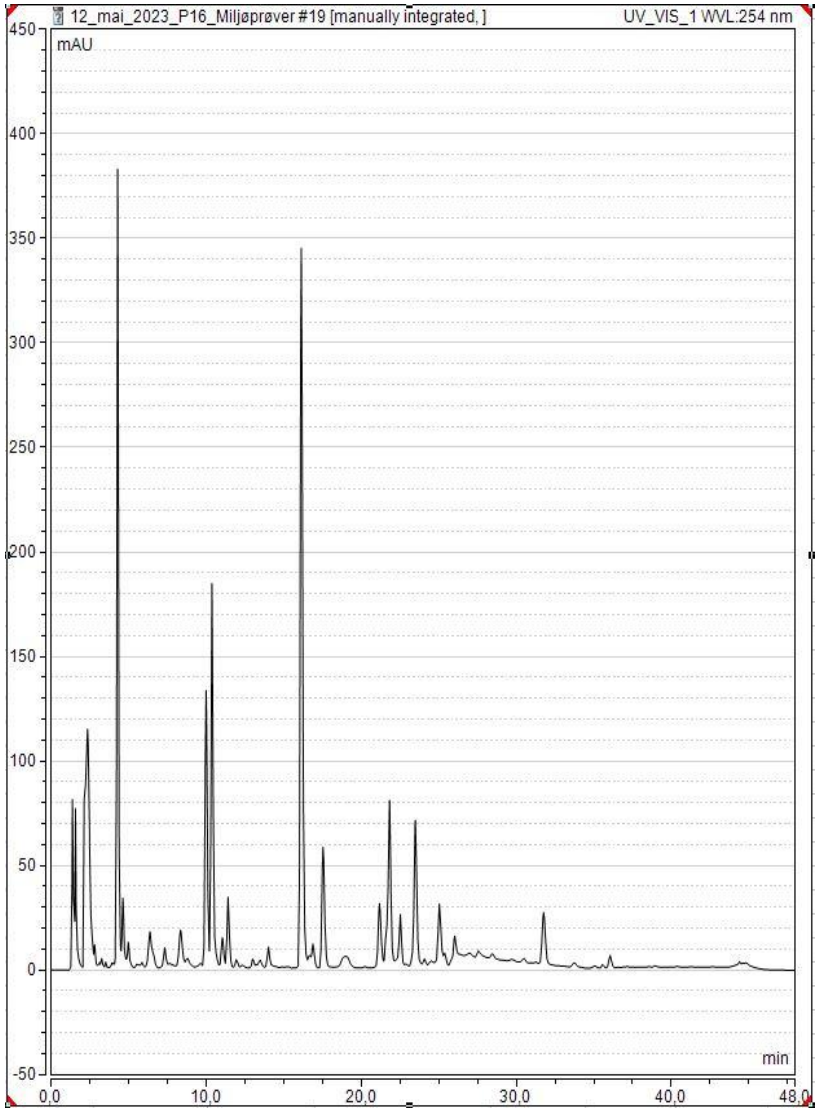

Figure 4.14: HPLC-Chromatogram Effluent from all EGSB (SP39)

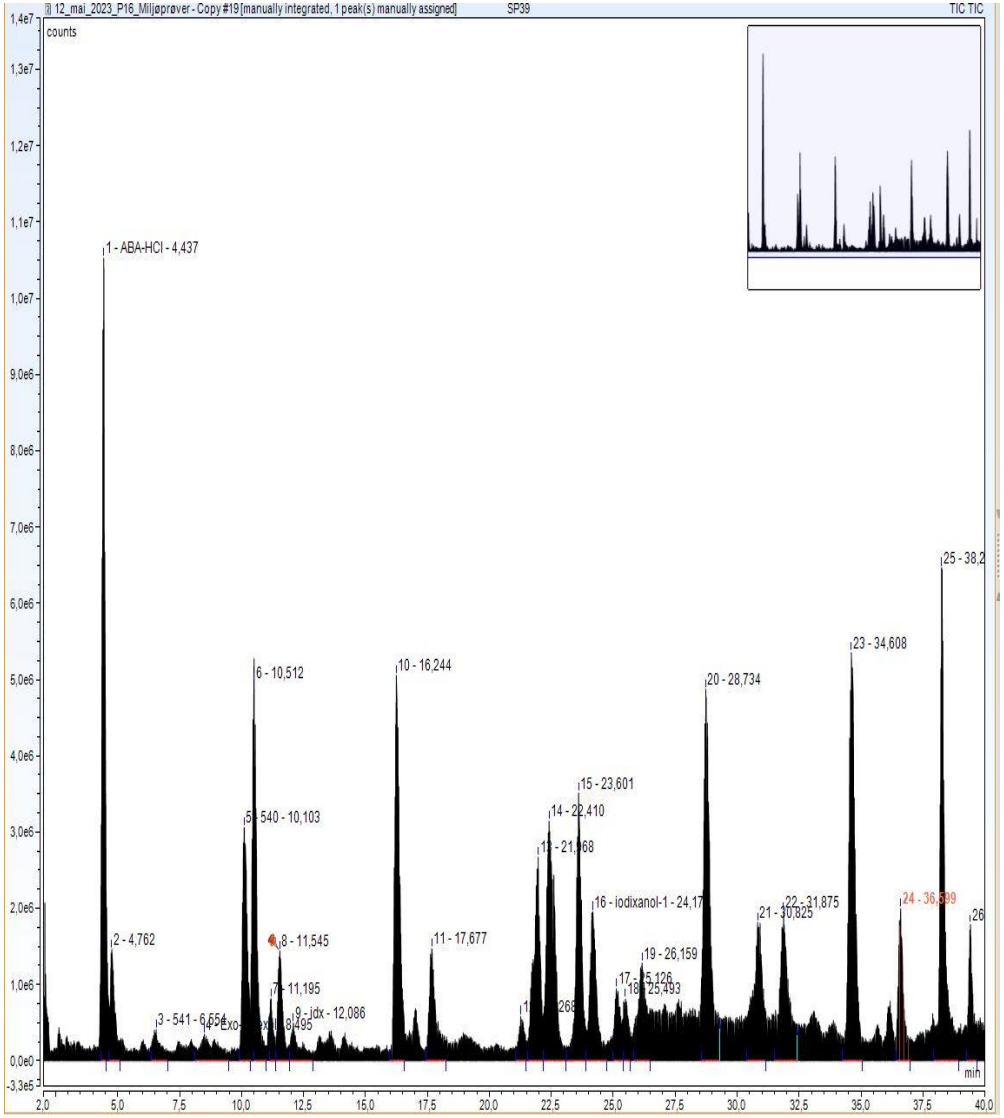

Figure 4.15: TIC-Chromatogram Effluent from all EGSB (SP39)

Table 4.8: All detected masses in peaks from TIC-chromatogram from sample SP39 (effluent from all EGSBs).

Peak number	Retention time (min)	m/z (mass to charge) [M + H^+]	Comment	Peak number	Retention time (min)	m/z (mass to charge) [M + H^+]	Comment
1	4,*435*	328,2/655,4/656,4		12	*21,265*	615,2/593,2/616,1/342,1	Mass 615,2 and 616,1 suspected Na+ adduct.
2	*4,765*	342,2/343,2		13	21,965	398,4/795,3/796,0	(Half mass) suspected double charge
3	*6,555*	696,0/718,1	Mass 718,2 suspected Na+ adduct	14	22,410	305,2/328,3/300,3	
4	*8,495*	822,0/823,0	Iohexol	15	23,605	444,2	Possible double charge, but positive identification of larger mass not present.
5	*10,105*	444,2/445,4/887,4/888,4	(Half mass) suspected double charge	16	24,175	342,4/314,2/384,2	
6	*10,505*	402,2/403,3/803,3		17	25,125	386,2/793,2	(Half mass) suspected double charge
7	1*1,195*	458,2/459,2/457,7	Possible double charge, but positive identification of larger mass not present.	18	25,495	458,2/459,2/333,1	Possible double charge, but positive identification of larger mass not present.
8	*11,545*	416,2/417,3		19	26,155	356,0/356,6/711,3/370,2/733,2/480,2/357,3	Mass 733,2 suspected Na+ adduct 356,0/356,6 (half mass) suspected double charge.
9	*12,085*	371,3/370,7	Possible double charge, but positive identification of larger mass not present.	20	28,735	327,3/372,3	

Peak number	Retention time (min)	m/z (mass to charge) [M + H^+]	Comment	Peak number	Retention time (min)	m/z (mass to charge) [M + H^+]	Comment
10	*16,245*	739,4/370,2/740,5/371,2	(Half mass) suspected double charge	21	30,825	341,2/386,2/358,3/383,3/342,2	
11	*17,675*	384,3/767,3	(Half mass) suspected double charge	22	31,8 75	398,6/396,0/795,3/796,3	(Half mass) suspected double charge
				23	34,605	371,3/388,3/393,2	Mass 371,3 2 suspected Na+ adduct
				24	36,595	402,3/430,3/385,2/407,2/405,3/431,4	No UV-detection at 254 nm
				25	38,245	415,3/432,3/460,3	No UV-detection at 254 nm
				26	39,415	446,2/429,3/474,3/451,2	No UV-detection at 254 nm

26 TPs was detected in SP39. No changes in masses were observed between EGSBs and connective sample point (SP39). The peak counts of masses only found in EGSB 1 and 2 were reduced because of dilution effect when mixed with effluent from EGSB 3.

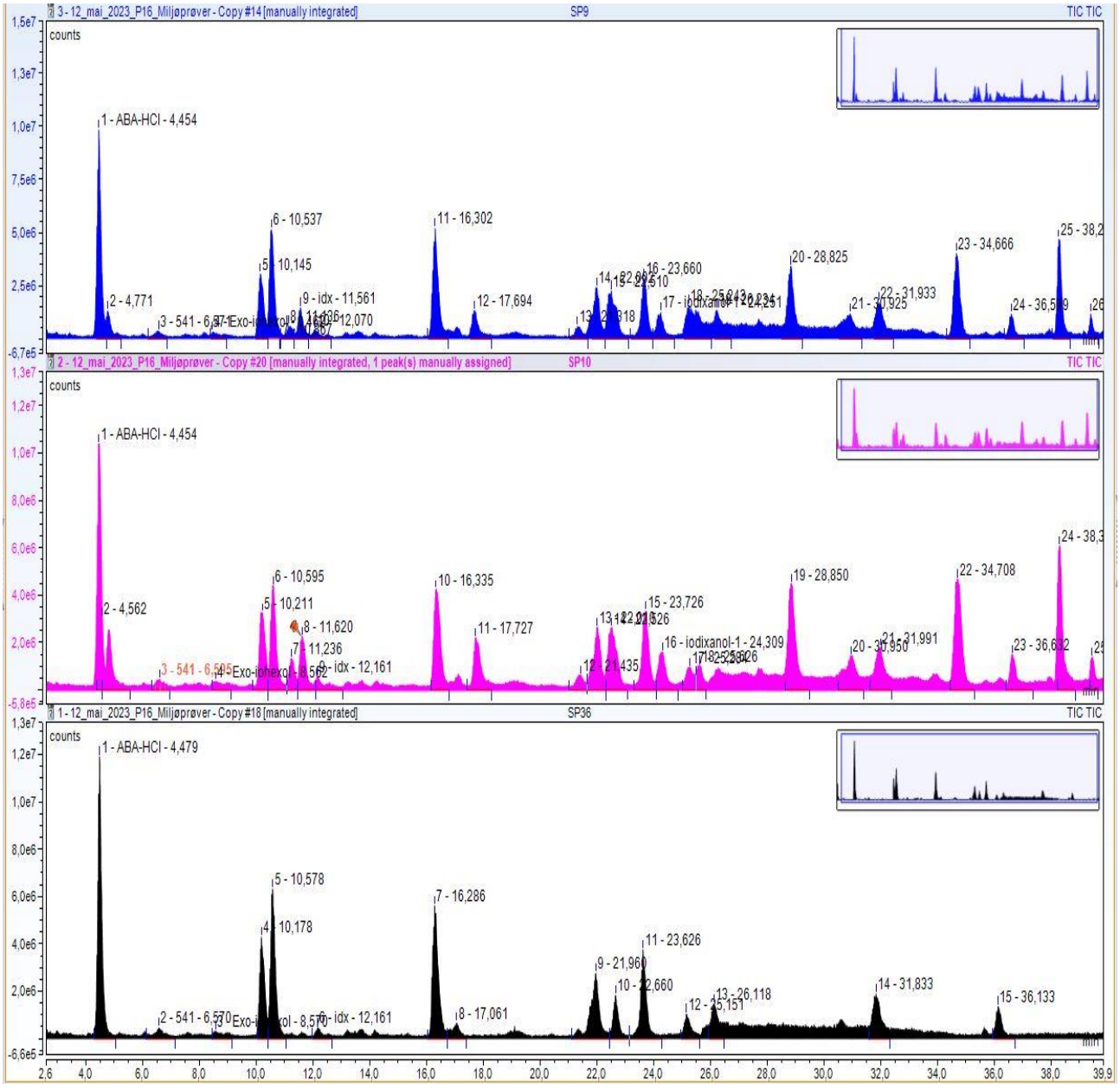

Figure 4.16: Comparison of TIC chromatograms from analysis of EGSB 1 (SP9) EGSB 2 (SP10) and EGSB 3 (SP36).

EGSB 3 show fewer peaks in the TIC chromatogram than EGSB 1 and 2. Overview of retention time and identified mass for the peaks, show that EGSB 1 and 2 are identical. In

total 9 peaks that were found in EGSB 1 and 2, was not found in EGSB 3 whereas 5 of them were not detected by UV at the used wavelength (254 nm). The lack of chromophore in the TP can indicate a breakage in the aromatic ring structure. All the masses not detected in UV-spectrum at 254 nm, had relatively lower mass than peaks detected by in the UV-specter.

4.2.4 Suggested Structures of observed TPs form EGSB (anaerobic reactor)

Masses detected in all EGSBs was TP 696, TP 887, TP 371, TP 740, TP 767, TP795, TP 593, TP 458, TP 342, TP711, TP796, TP725, TP 586 and TP 643. Structures was suggested for four of them. The structures are TPs of iohexol, which is the most abundant ICM in the feed to the EGSB. Chemdraw software was used to draw molecules presented in figure 4.17. Following structures have not been described in environmental samples from literature studies cited in this study.

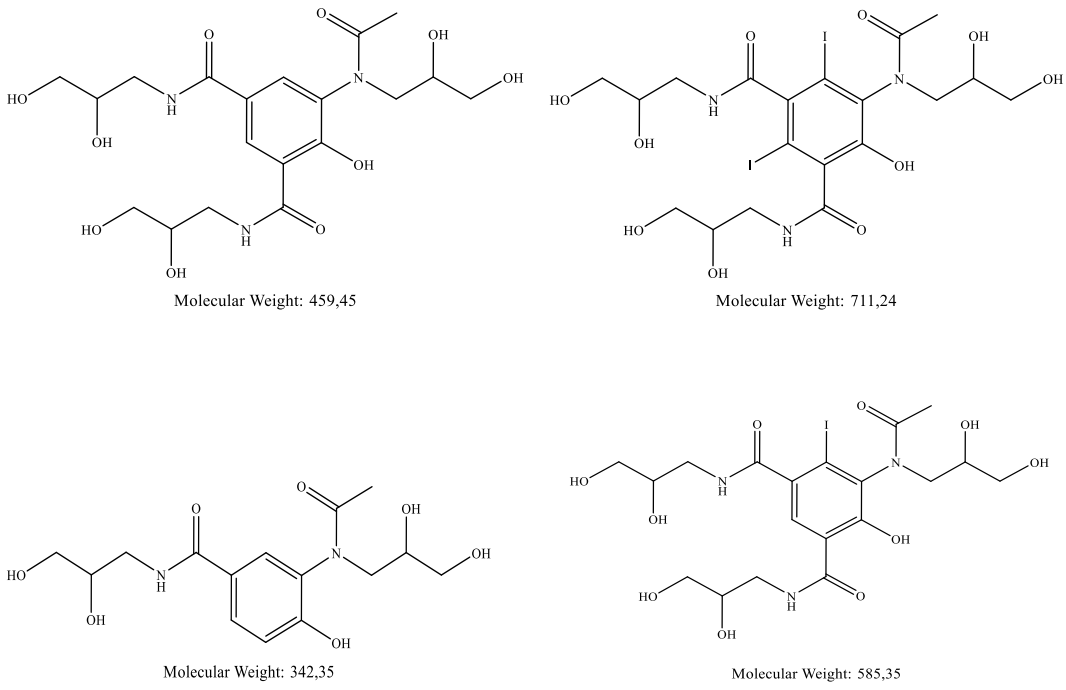

Figure 4.17: Structures new TPs based on degradation of iohexol.

All structures have lost one or more iodide ions, with TP 343 having lost all iodide. In all structures a hydroxyl group has been added.

4.3 HPLC-MS results from aerobic reactor (CFIC/SP29)

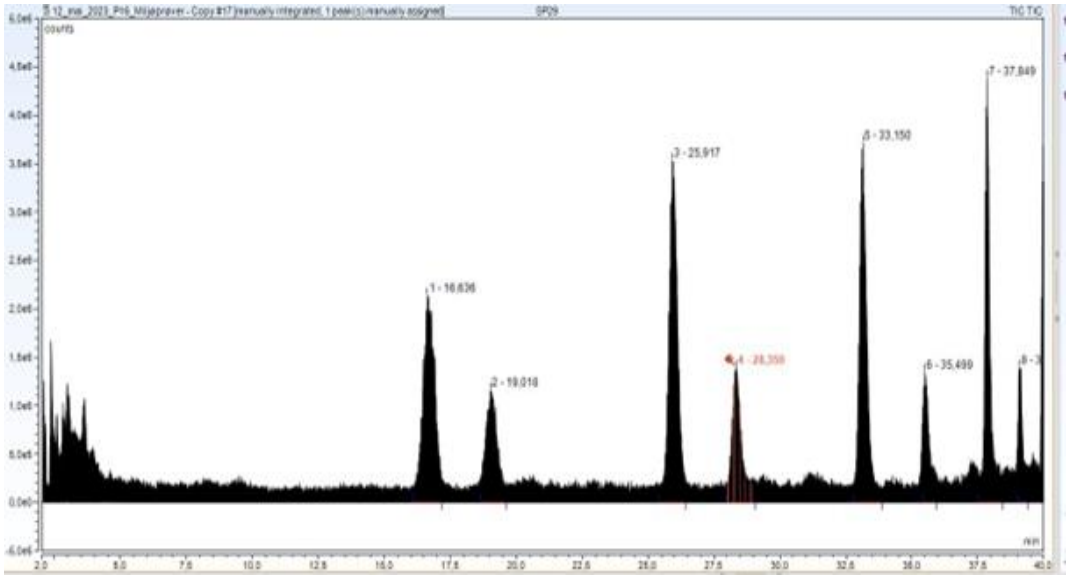

Figure 4.18: SP29 (Effluent after aerobic treatment) TIC.

Peaks detected in the TIC chromatogram at retention time after 5 minutes was not detected in the UV-chromatogram. The substances in question do not have a chromophore that can be detected by ordinary HPLC analysis using 254 nm wavelength in the UV-detector. The cluster of peaks in the first 4 minutes contains a variative of molecular weights. The molecules are expected to be highly hydrophilic and interact poorly with the C18 stationary phase of the HPLC column. Tops late in the chromatogram interacted more strongly with the stationary phase and was eluted from the column after the mobile phase gradient was 50:50 of Acetonitrile and MilliQ-water.

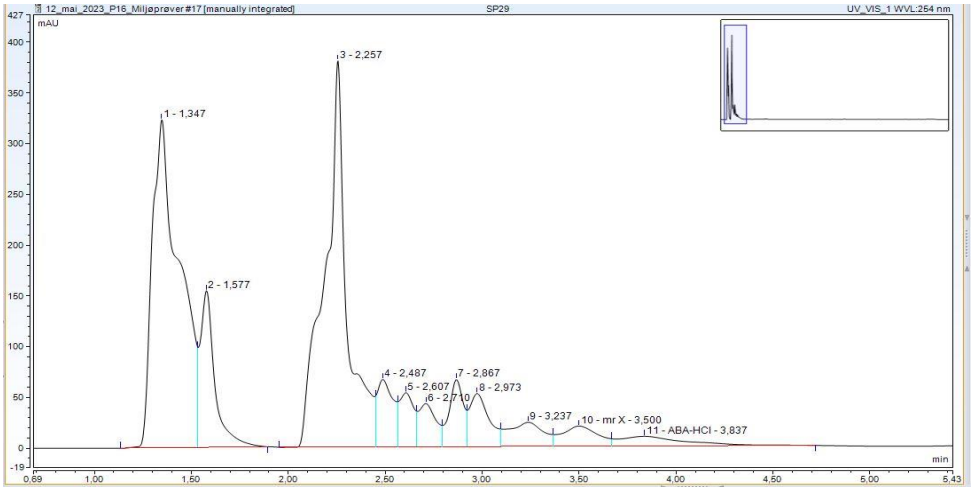

Figure 4.19: SP29 (effluent after aerobic treatment) UV. Only the cluster of peaks the first 4 minutes are visible in the UV-chromatogram. No observable peaks in the range 15-40 min in contrast to the TIC-chromatogram.

Table 4.9: SP29 analysis of peaks by MS-spectrometer.

Peak number	Retention time (min)	m/z (mass to charge) $M + H^+$	Comment	Peak number	Retention time (min)	m/z (mass to charge) $M + H^+$	Comment
1	*16,635*	328,3/305,2	Mass 328,3 suspected Na+ adduct	5	33,145	416,3/388,3/371,1/393,2/371,8	Mass 416,3 suspected Na+ adduct of mass 393,2
2	*19,015*	342,2/319,2	Mass 342,2 suspected Na+ adduct.	6	35,495	430,2/385,2/402,3/407,3/430,9	
3	*25,915*	327,3/372,5/344,3/372,0		7	37,850	415,3/460,3/432,3/437,3/461,4	
4	*28,355*	386,2/341,2/363,2/387,3	Mass 363,2 suspected Na+ adduct of mass 341,1	8	39,065	474,4/446,2/451,3/452,3/429,3/428,7	Mass 474,4 Suspected Na+ adduct of mass 452,4

All observed peaks have a m/z small relative to the parent ICM compounds. The mass size is a strong indication of deiodination since the size of iodide (126,9 mw) must be removed full or partly to give TPs with the observed masses.

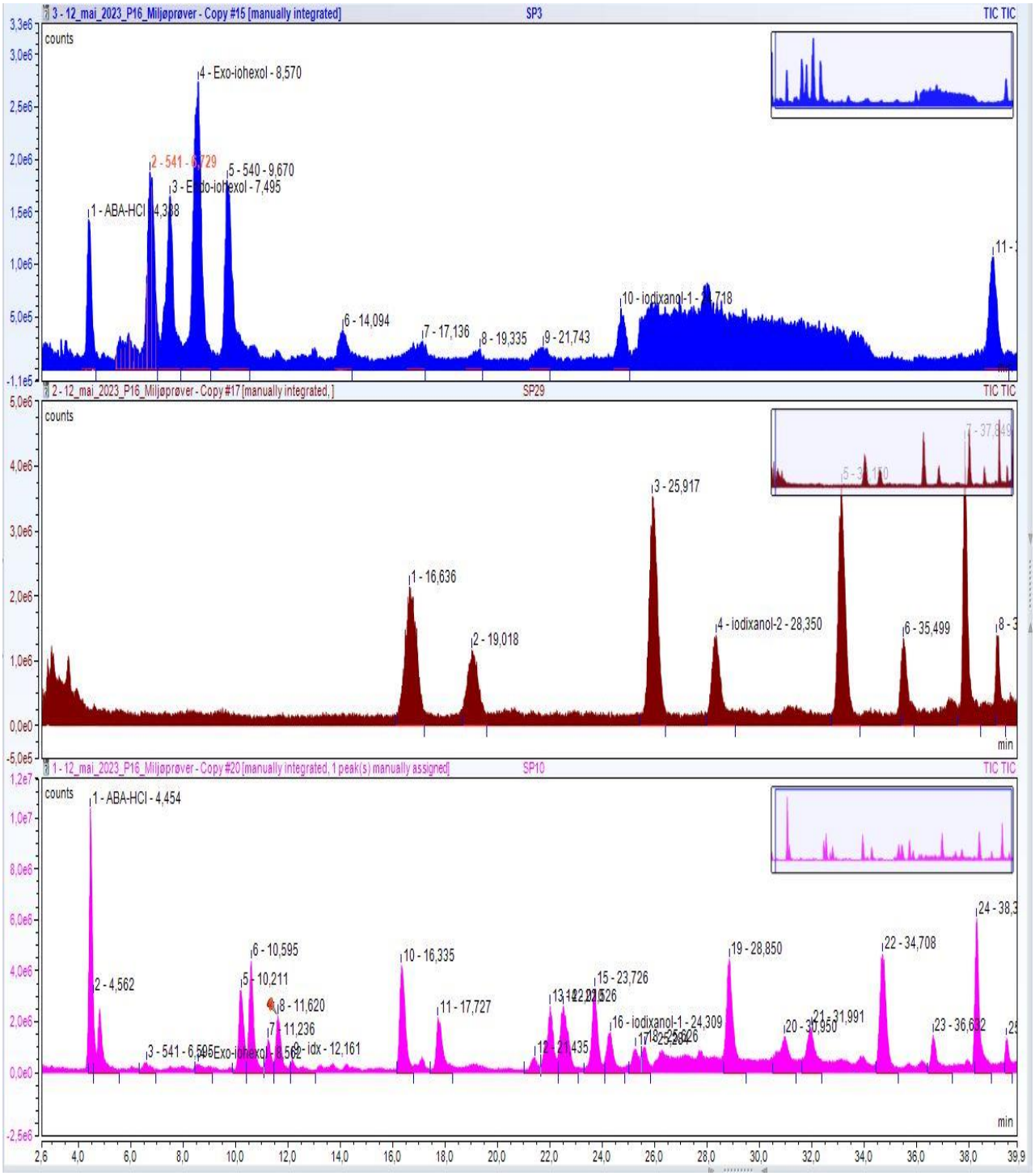

Figure 4.20: Comparing results from Feed SP3 (top), EGSB SP10 (bottom) and CFIC SP29 (middle) shows that parent ICM is not detectable after CFIC (SP29). Small amount of iohexol was detected in the after the EGSB (retention time 7-8 min).

4.4 Single ion mass (SIM) scan targeting known deiodinated ICM.

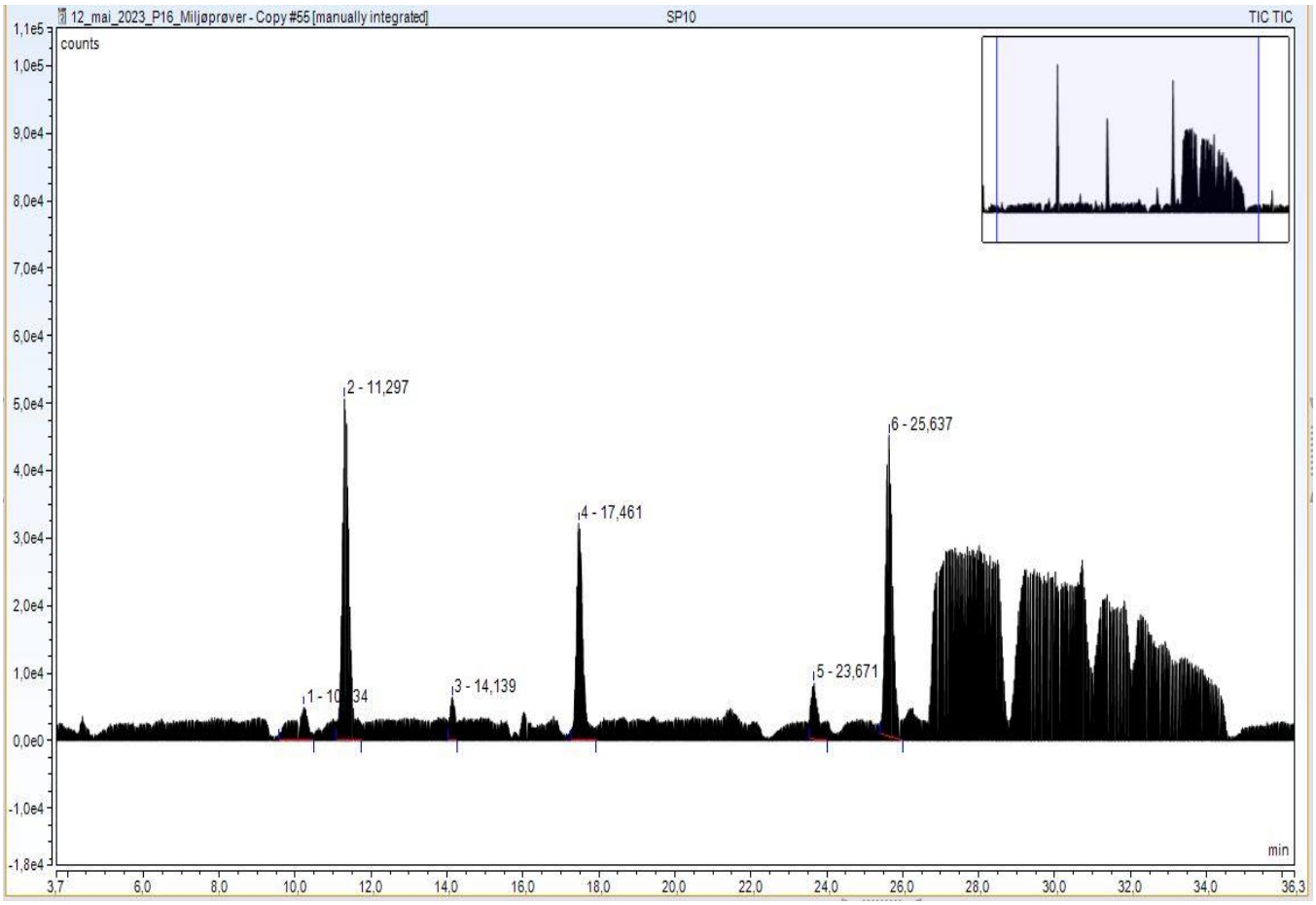

Figure 4.21 : SIM- measurement targeting 9 deiodinated ICM in EGSB 2 (SP10)

SIM measurement over a full time range of 2 min -40 min showed 6 peaks of interest. Peak 2, 4, and 6 were the dominant peaks. The m/z was TP 694,3 (peak 1) TP 451 (peak 2, 3, 5 and 6)and TP 366 (peak 4). Peak 1 showed a mass coherent with iohexol molecule with loss of one iodide ion. TP 451 is coherent with mono-iodiated intermediate 540. Positioning of the iodide on the aromatic ring structure (Otho-Ortho-Para) affect the retention time of the isomer. The identification of TP 451 in multiple peaks may be because of iodide at para or orto position of the molecule. Of the 9 target structures, only 3 was detected.

In SP 29 (effluent from CFIC) only TP 451 was detected.

4.5 SIM targeting TPs of iohexol known form litterature.

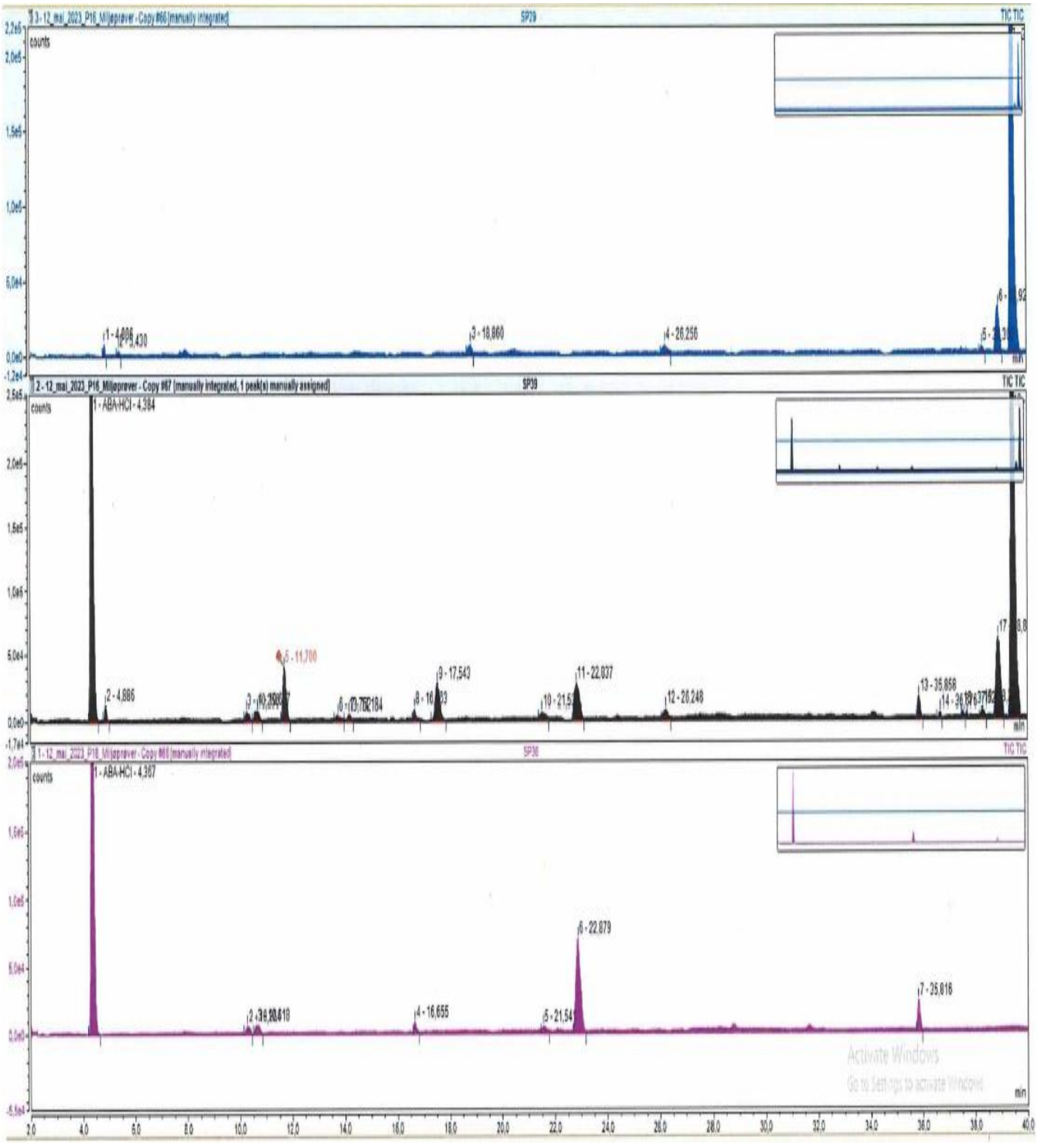

Figure 4.22: Peaks observed in a) SP29 b) SP39 and c) SP36 after SIM analysis.

TPs from chapter 4.4 was applied in addition to TP 868, TP 849, TP 835, TP 833, TP 775, TP 745, TP 687, TP 657, TP 629, and TP 599 identified in literature [12].

In SP39 (effluent from all EGSBs) 7 TP (TP 657, TP 451A, TP 833, TP 366, TP 775A, TP 451B and TP 775B) was identified. In SP36 6 TPs (TP 657, TP 451A, TP 833, TP 366, TP 775, TP 451B) was identified. The structure of TP 755 corresponds to iohexol parent molecule with cleavage of sidechain A1 and a carboxylation of side-chain B [4, 12, 24].

In SP29 (effluent from CFIC) none of the selected iohexol TPs was observed.

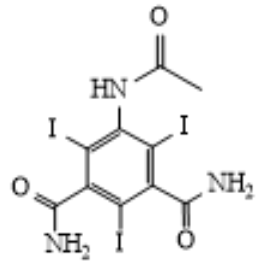

a) TP 599

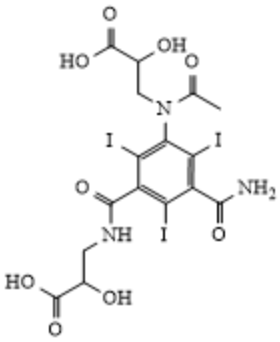

b) TP 775

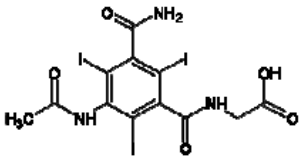

c) TP 657

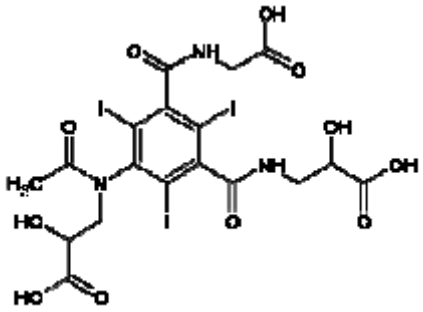

d) TP 833

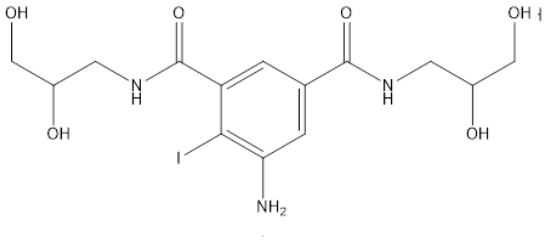

e) TP 451

Figure 4.23: a) b) c) d) Structures of TPs from iohexol identified in literature [12, 17]

e) 540-monojod (own figure)

4.6 Analysis of free iodide by ion-chromatography.

The initial inlet value of free iodide in SP3 was measured to be 16 mg/L. Assuming 30 m^3/h flow through the system, the daily amount of free iodide in the influent is 11,52 kg/day. Results in table 4.10 shows the concentration of free iodide increases to 80-85 mg/L in EGSB 1 and 2 respectively, while the level of free iodide in EGSB 3 was 55 mg/L. The reactors are feed form the same feed tank continuously. The increase in free iodide through the EGSB 1, 2, and 3 was 49,7/day, 47,5/day and 28,1 kg/day respectively. ICM are the only source of iodide to the EGSB reactors, indicating that dehalogenation of ICM occurs during the anaerobic step of the biological treatment plant. No increase in free iodide was observed between the EGSB effluent and the CFIC effluent.

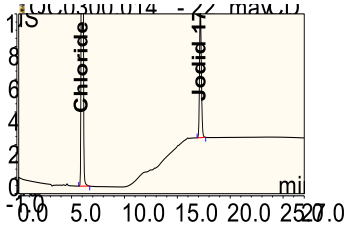

Figure 4.24: Calibration standard (I^- and Cl^-)

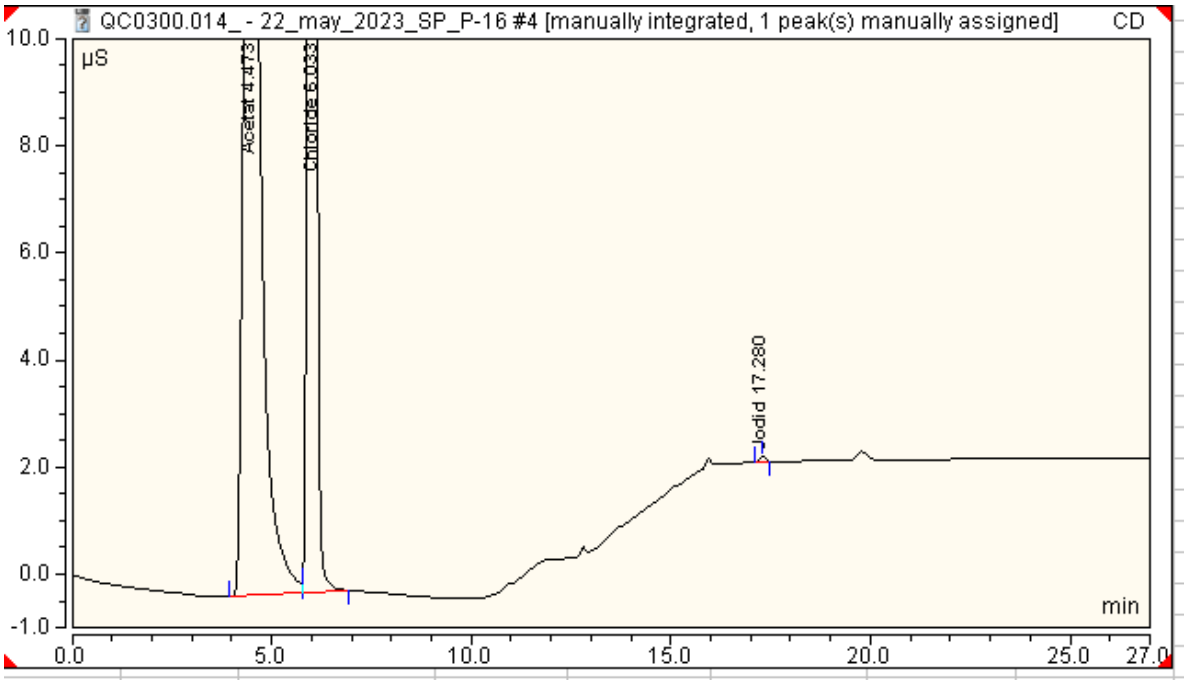

Figure 4.25: Free iodide in feed solution (SP3)

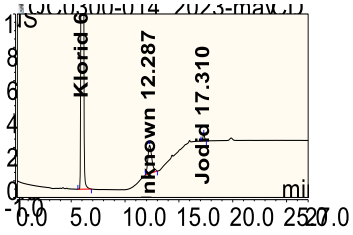

Figure 4.26: Free iodide levels in SP36 (EGSB 3)

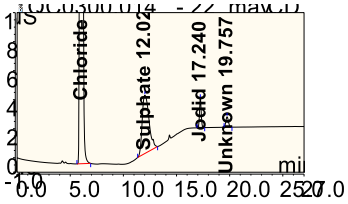

Figure 4.27: Free iodide in effluent from EGSB 1 (SP9)

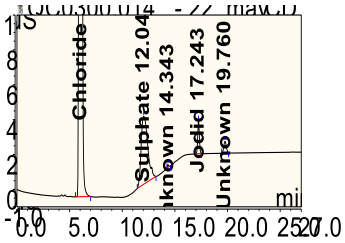

Figure 4.28:Free iodide in effluent form EGSB 2 (SP10)

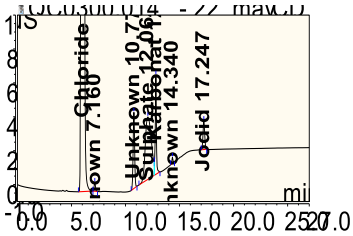

Figure 4.29 : Free iodide in effluent form CFIC (SP29)

Table 4.10: Results from IC analysis of free iodide (I⁻) in the effluent from the EGSB 1, 2, 3 and after the aerobic reactor. No standards for acetate, sulphate or carbonate were used during the analysis. The template of the method automatically assigned the names. However, the presence of the ions is likely.

Sample	Chloride (g/L)	Iodide (mg/L)	Other identified peaks
SP3	5,56	16	Acetate
SP9	6,45	85	Sulphate, Carbonate
SP10	6,34	80	Sulphate, Carbonate
SP36	5,44	55	Sulphate
SP29	5,70	71	Carbonate, Sulphate

Sulfur is added to the EGSB, while the level of sulfur in the feed is limited to small residuals of para toluene sulfonic acid (PTSA), from production. Carbonate increases because of CO_2 generated in the solution at pH 8,2-8,4 in the CFIC.

4.7 Removal of TPs from effluent using Ion-exchange resins or activated carbon (MCN)

4.7.1 Removal of TPs using ion-exchange resin.

LC-MS was performed after treatment with ion-exchange resin. Testing was performed on effluent with neutral pH (pH 6,7), and acidic pH (pH 2). Figure 4.30 and 4.31 shows the MS-specter of samples after both test set-ups.

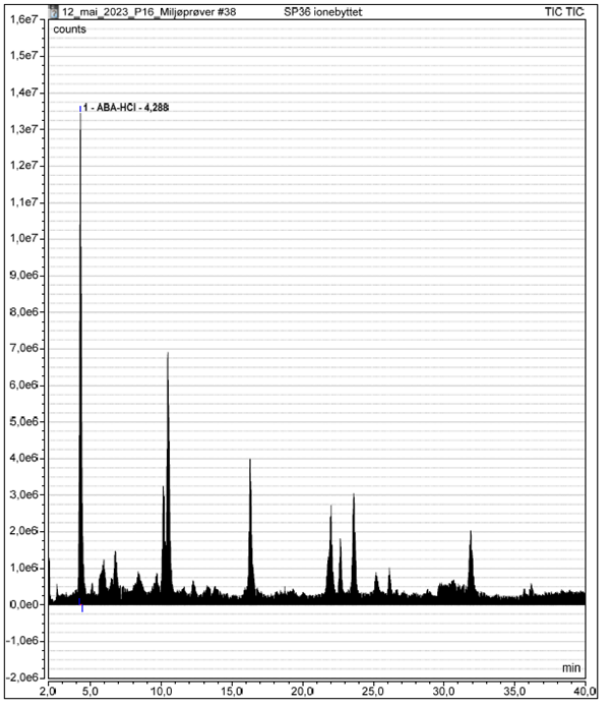

Figure 4.30: SP36 (pH 6,7) after Ion exchange.

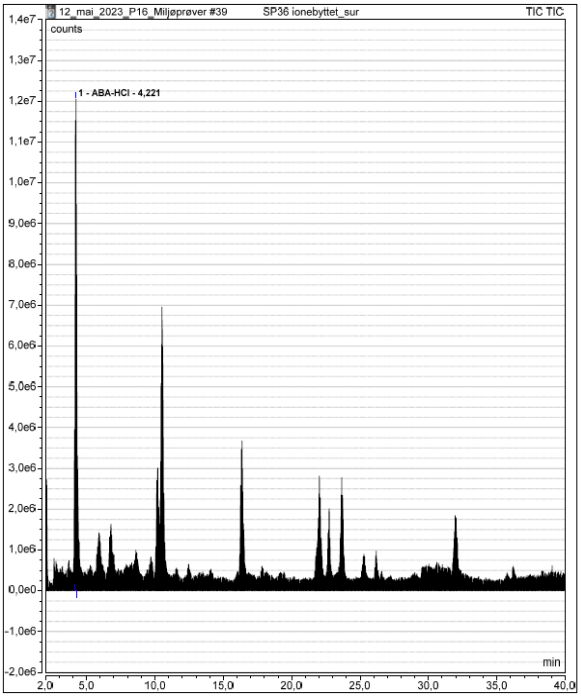

Figure 4.31: SP36 (pH2) after ion-exchange.

In test sample with neutral pH, 540 and 541 was detected while iohexol was not observed. Iohexol are not expected to adhere to the resin. However, the background noise in the TIC area could have suppressed the detection of iohexol. Under neutral pH, 15 peaks of interest were detected. Na+ adduct formation and observed low masses because of double charge ions, was detected in 7 out of 15 TIC peaks. Table 4.11 shows the result form after ion-exchange under neural pH conditions. Under pH 2, iohexol and 540 was not detected while 541 and ABA-HCl was observed. Table 4.12 shows the results under acidic pH (pH 2). Ion-exchange after pH adjustment of the solution did not change the MS-specter. If protonation had occurred prior to ion-exchange, it's expected that less affinity to the ion-exchange resin and subsequent more tops in the TIC chromatogram. The peaks in SP36 are therefore suspected not to be acidic moieties. The minimal variations observed in the masses observed

in the MS-spectrometer, are likely more an effect of sampling and analytical variance, as the amount of these compounds is limited. The detection of m/z of 540 and 541 in the sample indicate that reduction of noise by ion-exchange resin, uncovered residual intermediates that was undetectable in the HPLC-MS method described in chapter 4.2.

Table 4.11: Results from analysis from sample from EGSB 3 (SP36) after treatment with ion-exchange resin (neutral pH). Double charges ions and Na+ adduct formation is observed in several peaks. 540 and 541 (intermediate) was detected, while iohexol was not detected.

Peak number	**Retention time (min)**	**m/z (mass to charge) M + H^+**	**Comment**
1	*4,288*	328,2 /655,3	655,3 = known contaminant in ABA-HCl
2	5,929	673,9 / 690,9 / 718,9 /674,8	673,9 and 674,8 likely isomers
3	6,754	748,0 /749,0	541(intermediate)
4	8,354	674,8/ 692,8 /698,0	
5	9,678	705,8 /707,0	540 (intermediate)
6	10,412	402,2/ 403,3 /803,3	
7	*10,478*	402,2/ 403,3/803,2	
8	12,236	371,1/ 393,4 / 764,2/ 409,2	Mass 393,4 = Suspected Na+ adduct of mass 371,1
9	16,286	370,2 / 371,2 / 739,5/ 740,4	Suspected double charged ion
10	22,010	795,4/ 398,2 / 399,0/ 796,4	Suspected double charged ion
11	22,660	377,3/ 753,2	Suspected double charged ion
12	23,601	444,2/ 445,4/ 887,4	Suspected double charged ion
13	26,126	386,1 /387,0/793,4/771,4	Mass 793,4= Suspected Na+ adduct of mass 771,4 Mass 386,1 and 387,0 =Suspected double charged ion
14	31,875	398,1/398,9/795,2/795,9	Suspected double charged ion
15	36,149	311,1/ 348,9/ 643,2/356,3	

Table 4.12: Results from analysis from sample from EGSB 3 (SP36) after treatment with ion-exchange resin (pH 2). Double charges ions and Na+ adduct formation is observed in several peaks. 541 (intermediate) was detected, while iohexol and 540 was not detected.

Peak number	Retention time (min)	m/z (mass to charge) $M + H^+$	Comment
1	*4,221*	328,2 /327,7/655,3/656,4	655,3 = known contaminant in ABA-HCl
2	5,912	673,7/718,8/692,1/695,8	
3	6,795	506,9/747,9	541(intermediate)
4	8,612	678,8/692,8/675,3/511,8	
5	10,070	444,2/445,3	
6	10,203	444,2/445,3/887,5	Suspected double charged ion
7	*10,503*	402,2/403,3/803,5	
8	12,469	371,0/371,5/763,8/372,3	
9	16,361	370,3/739,6/739,0/740,4	Suspected double charged ion
10	22,026	398,1/399,0/795,4/796,5	Suspected double charged ion
11	22,743	377,2/753,3/754,4	Suspected double charged ion
12	23,659	444,2/445,3/887,3	Suspected double charged ion
13	26,176	356,1/356,7/711,4	Suspected double charged ion
14	31,950	398,3/795,5/794,9	Suspected double charged ion
15	36,199	311,1/356,2/349,2/643,3	

4.7.2 Removal of TPs using activated carbon (MCN).

Activated carbon (MCN) is routinely used in the iohexol process as a purification step. The carbon is not expected to remove iohexol or iodixanol form the sample. The TIC chromatogram shows a drastic reduction in number of peaks and ion-abundance in the TIC chromatogram in sample from EGSB 3(SP36) (figure 4.32) and CFIC (SP29) (Figure 4.33). Table 4.13 shows that 2 peaks remaining in the sample was identified as iohexol isomers. In sample from CFIC (SP29) one peak was visible on the TIC chromatogram (table 4.14). The low peak number and relative high background noise compared to the peak, makes it difficult to separate the masses form the noise.

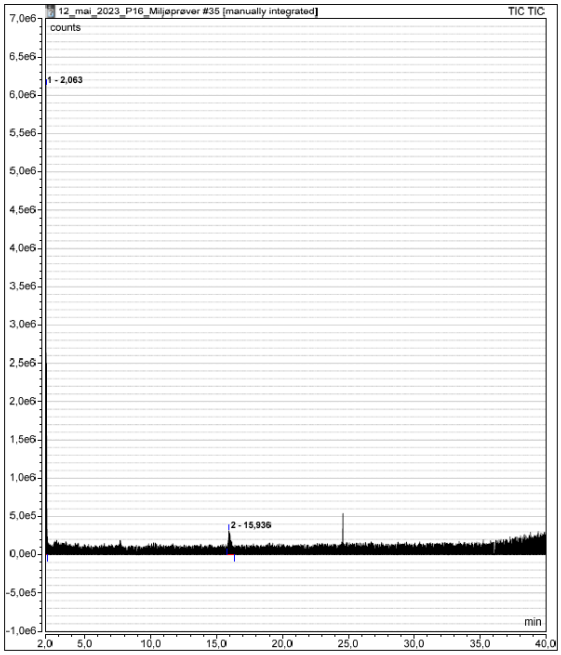

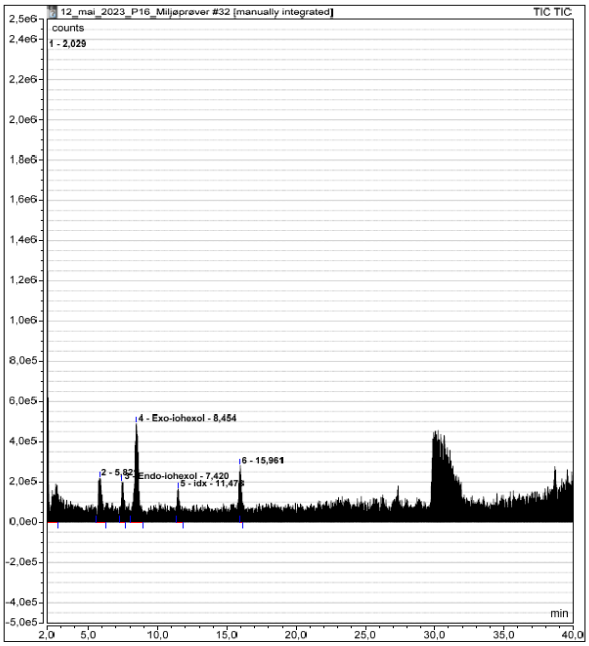

Figure 4.32: SP29 treatment with activated carbon *Figure 4.33: SP36 treatment with activated carbon*

The amount of activated carbon was rather high in this test (1 g/L effluent). Accurate amounts needed to remove TPs is probably lower. It's also possible that other types of carbon are more suitable for the purpose of removing TPs in an industrial scale.

Table 4.13: Peaks from TIC-chromatogram detected in effluent from EGSB 3 (SP36) after treatment with activated carbon.

Peak number	Retention time (min)	m/z (mass to charge) $M + H^+$	Comment
1	*5,82*	312,2/ 367,0/370,4/443,1/315,1	Low peak count /possible contaminants /background noise
2	7,420	821,9/822,6/844,7/342,3	Endo isomer Iohexol detected Mass 844,7 suspected Na+ adduct of iohexol.
3	8,454	821,9/823,2	Exo-isomer iohexol detected.
4	11,475	316,3	
5	15,961	480,7/706,1/992,6/534,2	

Table 4.14: Peak from TIC- chromatogram observed in effluent from CFIC (SP29) after treatment with activated carbon.

Peak number	Retention time (min)	m/z (mass to charge) $M + H^+$	Comment
1	*15,936*	356,3/536,0/309,0/775,1/919,2	Low peak counts Interference of background noise.

5. Discussion

5.1 Discussion of results

ICM was degraded in all EGSBs to yield multiple TPs. Small amounts of iohexol were detected in effluent from EGSBs. Removal of 96-98 % of iohexol was observed in EGSBs, Iohexol was not detected in effluent from CFIC. Iodixanol was not observed in effluent from EGSBs. TPs with high m/z are suspected to originated from iodixanol Samples from December 2020 showed a minor reduction in iodixanol with subsequent elevated 541 concentration. This elevation of 541 was not seen in current study. The first intermediate 540 was not detected after EGSBs.

TP 696, TP 887, TP 371, TP 740, TP 767, TP795, TP 593, TP 342, TP711, TP796, TP725, TP 586 and TP 643 was detected in all EGSBs.

Four new TPs suspected to originate from iohexol (TP 342, TP 711, TP586 and TP 458). The TPs structure indicate dehalogenation by hydrolysis, were an OH group replace a halogen.

EGSB 3 was commissioned in April 2023. EGSB 1 and 2 was commissioned in 3Q 2020. Results from LC-MS showed a clear difference between EGSB 3 and EGSB 1 and 2. In EGSB 3 only 15 TPs was detected (25 TPs in EGSB 1 and 2). Peak nr 2, 7, 8, 11, 16, 19, 20, 22, 24 and 25 present in TIC-chromatogram from EGSB 1 and 2 was not observed in EGSB 3. Degradation of compounds and the mechanisms that are used, depends on the microbial community present, the chemical environment [25, 27]. Study of the microbial community in the 3 EGSB reactors showed that there was a significant difference between the first two EGSBs and EGSB 3. One of the main differences was the abundance of Geobacter.*spp* and Tenuifilum *spp,* which was abundant in EGSB 1 and 2, but not in EGSB 3 [35].

Geobacter species are specialized in making electrical contact with extracellular electron acceptors and other organisms. Geobacter fills an anaerobic diversity niche as a primary agent for coupling oxidation of organic compounds to the reduction of metals like Fe (II) and Mn (IV) [39]. Anaerobic oxidation of aromatic hydrocarbons and specific oxidation of benzene by route of phenol under anaerobic conditions has been seen [40, 41] supports the possible structure of TPs identified in this thesis.

Geobacter.spp uses simple organics like ethanol and acetate as electron donors to reduce Fe (II) and Mn (IV). Degradation of the nitroaromatic antibiotic Chloramphenicol was seen by *Geobacter.spp* using acetate as sole organic electron donor. 20 mg/L was degraded by reductive dehalogenation with 97, 6 % efficiency. Concentration of the substrate affected the removal efficiency as toxic levels was reached at 80 mg /L Chloramphenicol [42]. *Geobacter.spp* have been shown to mineralize benzene to CO_2 in 5 days [28].

Tenuifilum spp found in EGSB 1 and 2 have shown the ability to degrade lignin cellulose under anaerobic conditions [43] Degradation of lignin occurs in 2 steps 1) non-specific extracellular depolymerization 2) mineralization by specific catabolic enzymes and pathways [43, 44]. ICM degradation by the white-rot fungi by extracellular ligninolytic enzymes has been observed [4, 6]. Enzymatic activity and reductive dehalogenation during anaerobic conditions, followed by oxidative reactions and specific catabolic pathways under aerobic step may enable the cleavage of the aromatic ring structure of ICM. It is further shown that breaking of the aromatic ring structure enzymatically to catechol, makes it possible reach mineralization as aerobic degradation of catechol produce compounds that readily enters the Krebs cycle [28, 45].

The high concentration of the ICM in the EGSBs in combination with easily available organic compounds like methanol, and acetate may stimulate the degradation. This is in coherence with a study showing that deiodination only occurred after addition of ethanol [23]. The effect of concentration in the system compared to other studies (ug/L /ng/L) the threshold value for biodegradation may also be a reason for the low rate of degradation seen in low concentration environments.

The acclimation for deiodination has been observed to be up to 6 months [27, 30]. The observed change in degradation from 2020 to 2023 may be a result of this. The EGSB 3 had been in operation for between 2 weeks and 1 month prior to sampling. Compared to EGSB 1 and 2 that used about 6 months before there was visual difference in effluent form the WWTP, the acclimatation time in EGSB 3 seems to be shorter. This is in accordance with findings in literature [27, 30]

Analysis of free iodide of the feed and the effluent from EGSBs and CFIC, showed an increase of iodide through the WWTP. The registered increase from 16 mg/L to maximum 85 mg/L in EGSB 1, 80 mg/L in EGSB 2 and 55 mg/L in EGSB 3, support reductive dehalogenation occurring. Chloride levels was used as a control ion in the analysis since it is expected to remain stable in the system. The observed difference may be because the sampling was done at the

same time and therefor lag in the system (from feed to EGSB effluent) is likely. Iodide was comparable in EGSB 1 and 2, while EGSB 3 had a lower level of free iodide in the effluent. The lower level of free iodide in the sample from EGSB support the data from the SIM analysis targeting TPs related to deiodination, where fewer peaks with less ion-abundance was found in EGSB 3. Iodide did not increase through the CFIC (SP29), indicating that dehalogenation only took place under anaerobic conditions.

SIM analysis showed that TPs for deiodinated compound was present in all EGSBs. Three known deiodinated masses TP 366 m/z, TP 451 m/z and TP 694 m/z was detected in EGSB 1 and 2. In EGSB 3 all but TP 694 was detected. In CFIC only TP 451 m/z was found.

Full scan using LC-MS showed that 9 peaks present in both EGSB 1 and 2 was not observed in EGSB 3. Two of these was visible on the UV-specter, while the other 7 was not. The mass detected in the TIC-chromatogram had small mass range (327 m/z – 477 m/z). TPs from ICM at this size range would indicate loss of minimum 1 iodide ion in addition to cleavage of sidechain. The loss of chromophore at 254 nm can indicate that 1) the substances are degraded is a way that results in no absorption in UV-spectrum 2) that the compound is not visible at 254 nm but would be detectable using another wavelength in the UV-detector. Catechol and its derivates however, has a UV-spectrum optimum at 277 nm and should be visible in the HPLC-chromatogram [45]. However, the total loss of detectability could indicate loss of C-C double bonds in a high degree. Since the Central structure of the ICM is a benzene ring (3 double bonds), it can be speculated that ring cleavage might be the reason for det observed peaks.

The loss of visible peaks in the HPLC-UV analysis is even more evident after aerobic degradation where 8 peaks was only identified in the TIC, while a cluster of peaks where eluted in the first 4 min of the 48 min run was observed in the UV-specter. Also indicating a significant change in structure of the detected compounds.

Intermediate and impurities from ICM production are not found in nature in the same way as the pharmaceutical itself. These compounds also generate TPs, making the puzzle of identification by looking at mass alone difficult. TPs for the intermediates 540 and 541 are not found in literature. The number of unknown TPs observed in this study is not unexpected.

In the last part of the test period effluent from EGSB and CFIC was treated using activated carbon and ion-exchange resins. Use of activated carbon have been used to treat micropollutant from hospitals effluents with positive effect [46].

MCN carbon did not remove iohexol or 541 from the effluent. The peaks became more visible in the TIC chromatogram, as the other TPs was readily removed from solution. The low peak counts in the unknown compounds remain after treatment makes it difficult to separate from the background noise. Treatment of effluent showed 1 peak in the TIC-chromatogram. However, noise to signal was high and the observed peak cluster might be mostly background noise.

5.2 Discussion of methods

The method for detection of ICM was made based on internal method used in the iodixanol process on site. The reason for this is a better resolution due to longer run using a gradient elution method. Separation in feed solution SP3 showed that all compound achieved baseline separation. As the chemical structure in the TPs differs from that of the parent compounds the method might be less suitable. After SP29 separation of the peaks visible in the UV-spectrum is poor. A method dedicated to analysis of this sample point might be necessary to evaluate degradation of ICM and TPs.

Sample was only filtered prior to injection on the LC-MS. The use of extraction like liquid-liquid extraction, SPE or other protocols are often used to remove contaminants. Omitting this step have been demonstrated in literature [47], but may reduce sensitivity in the MS. The matrix of the feed solution to the EGSB contain only alcohols, acetate and ICM residuals, whereas other studies have been centered around municipality WWTP, natural waters, soil, and sediment. The choice to omit the extraction was made due to sample matrix in SP3. However, contaminants from the EGSB of CFIC can have affected the analysis.

MS parameters selected to give the best results for ICM parent compounds. The highest overall performance was seen in method 1, which was the default parameters suggested by the Chromeleon 7.3 cobra wizard. Tests was performed on EGSBs, but not on the CFIC. Optimal MS- parameters for analysis of CFIC (SP29) might have been sub-optimal.

Single-quad methods have lower resolving power adding uncertainty in identifications of smaller peaks. Using SIM mode was more suitable for detecting TPs with known mass.

Repression of analytes with low abundance is possible due to the background noise in the system. The injection volume of the sample was increased from 10 µl to 50 µl, to increase the analyte/ noise ratio. This gave good results. However, the level of NaCl (1,5 %) and other salts in the sample, increased the background over time. It was necessary to clean the instrument with water and 50:50 water/acetonitrile for longer periods. The ion-transfer tube

that transfer the ions to the quadropoly in the MS, was cleaned to remove contaminants in the system. Replacement became necessary when separation in the TIC-chromatograms was no longer possible. The instrument was used by several operators and projects in the period. Therefor the much care was taken in cleaning the instrument.

Na + adduct formation and half mass due to double charge in the molecule was observed in all samples. This is known challenges when interpreting single-quad MS-data [37, 48].

6. Conclusion

Removal of up to 98 % of iohexol was observed in the EGSBs. ICM was not detected after CFIC. Compared to analysis form 2020 the increase in degradation have increased drastically. The acclimation period in EGSB 1 and 2 was higher than for EGSB 3. The difference in microbial community shown in the EGSBs are the most likely reason for the discrepancy between EGSB 3 and the other two. Free iodide increased through the EGSBs, but not in the CFIC. TPs for deiodinated known masses was detected in all EGSBs, but with lower peak counts in EGSB 3. Four new iohexol TP structures was suggested. All of which had lost one more iodide ion. This correlated with the relative observed increase in free iodide in the reactors. The levels of free iodide and the presence of TPs in EGSB effluent, indicates the occurrence of reductive dehalogenation and hydrolysis.

TPs from EGSB and CFIC was readily removed from solution using MCN activated carbon, while ion-exchange resins were less effective. An adapted and optimized biological treatment plant in combination with polish step for degradation of TPs generated in CFIC can reduce the emission of ICM to the environment.

7. Further work

To fully determine the structure of the data from the single-quad MS, further analysis is needed. Separation of TPs by preparative HPLC followed by triple quadrupole MS and NMR can be the next step to fully understand the processes in the WWTP, which is unique in terms of ICM degradation. Isolation of TPs for making calibration standards is necessary to create a quantitative method to be used routinely at the plant. Further surveillance of the iodide mass-balance can be a good method to follow the change of reductive dehalogenation over time.

Last the isolation of TPs makes it possible to perform specific toxicity testing that will become vital to make a risk assessment for the release of observed TPs to the environment.

8 References

1. https://reports.valuates.com/market-reports/QYRE-Auto-22G10562/global-iohexol-api

2. https://farmasihistorie.com/w/index.php?title=Nyegaard_%26_Co_A/S

3. https://www.gehealthcare.in/products/contrast-media/omnipaque

4. Zhang, W.; Fourcade, F.; Amrane, A.; Geneste, F. Iodinated X-Ray Contrast Media in the Environment. Encyclopedia. Available online: https://encyclopedia.pub/entry/40201 (accessed on 11 June 2023).

5. *NIVA report 2006LNR 5236-2006 "Forsøk med biologisk nedbrytning av røntgenkontrastmidlet iohexol i ferskvann og sjøvann»*

6. *Nowak Agnieszka"Transformation and ecotoxicological effects of iodinated X-ray contrast media" Rev Environ Sci Biotechnol (2020) 19:337–354 https://doi.org/10.1007/s11157-020-09534-0(0123456789().,-volV)(01234567*

7. Ternes, T. A.; Hirsch, R. Occurrence, and behavior of X-ray contrast media in sewage facilities and the aquatic environment. *Environ. Sci. Technol.* **2000**, *34* (13), 2741-2748.

8. https://www.ntnu.no/nv/sf/ge-healthcare/bedriftspres

9. Tahri N, Bahafid W, Sayel H, et al. (2013) Biodegradation: Involved Microorganisms and Genetically Engineered Microorganisms. Biodegradation - Life of Science. InTech. DOI: 10.5772/56194.

10. Søknad om tillatelse til forurensende virksomhet GE Healthcare AS, Lindesnes April 2020. Miljødirektoretet.no (avaliable as PDF online)

11. https://www.regjeringen.no/no/sub/eos-notatbasen/notatene/2008/nov/industriutslippsdirektivet-ied-tidl.-ippc/id2434854/

12. Kormos JL, Schulz M, Kohler HP, Ternes TA. Biotransformation of selected iodinated X-ray contrast media and characterization of microbial transformation pathways. Environ Sci Technol. 2010 Jul 1;44(13):4998-5007. doi: 10.1021/es1007214. PMID: 20509647

13. Carballa, M.; Omil, F.; Lema, J.M.; Llompart, M.; García-Jares, C.; Rodríguez, I.; Gómez, M.; Ternes, T. Behavior of pharmaceuticals,cosmetics and hormones in a sewage treatment plant. Water Res. **2004**, 38, 2918–2926.

14. 15. Drewes, J.E.; Fox, P.; Jekel, M. Occurrence of iodinated X-ray contrast media in domestic effluents and their fate during indirect potable reuse. J. Environ. Sci. Health Part A **2001**, 36, 1633–1645.

15. Xu, Z.; Li, X.; Hu, X.; Yin, D. Distribution, and relevance of iodinated X-ray contrast media and iodinated trihalomethanes in an aquatic environment. Chemosphere **2017**, 184, 253–260.

16. Meiru Hou, Xiaodie Li, Yu Fu, Lingli Wang, Dagang Lin, Zhaohui Wang. Degradation of iodinated X-ray contrast media by advanced oxidation processes: A literature review with a focus on degradation pathways[J]. *Chinese Chemical Letters*, 2023, 34(4): 107723-1-107723-10. doi: 10.1016/j.cclet.2022.08.003

17. Kormos, J. L.; Schulz, M.; Wagner, M.; Ternes, T. A. Multistep approach for the structural identification of biotransformation products of iodinated X-ray contrast media by liquidchromatography/hybrid triple quadrupole linear ion trap mass spectrometry and 1H and 13C nuclear magnetic resonance. *Anal. Chem.* **2009**, *81* (22), 9216-9224.

18. Steger-Hartmann T, Länge R, Schweinfurth H. Environmental risk assessment for the widely used iodinated X-ray contrast agent iopromide (Ultravist). Ecotoxicol Environ Saf. 1999 Mar;42(3):274-81. doi: 10.1006/eesa.1998.1759. PMID: 10090816

19. Borowska E, Felis E, Żabczyński S. Degradation of Iodinated Contrast Media in Aquatic Environment by Means of UV, UV/TiO_2 Process, and by Activated Sludge. Water Air Soil Pollut. 2015;226(5):151. doi: 10.1007/s11270-015-2383-9. Epub 2015 Apr 17. PMID: 25960580; PMCID: PMC4412684.

20. Li, M.; Zhang, T.-Y.; Xu, B.; Hu, C.-Y.; Dong, Z.-Y.; Wang, Z.; Tang, Y.-L.; Yu, S.-L.; Pan, Y.; Xian, Q. Iodinated trihalomethanes formation in iopamidol-contained water during ferrate/chlor(am)ination treatment. Chemosphere 2021, 272, 129568.

21. https://echa.europa.eu/documents/10162/a5ae9101-7a5d-49cc-af75-d14d1162b3f8 retrieved may 14 2023.

22. Strehl, C.; Thoene, V.; Heymann, L.; Schwesig, D.; Boergers, A.; Bloser, M.; Fligge, F.; Merkel, W.; Tuerk, J. Cost-effective reduction of micro pollutants in the water cycle—Case study on iodinated contrast media. Sci. Total Environ. 2019, 688, 10–17.

23. Lecouturier, D.; Rochex, A.; Lebeault, J.-M. Enrichment and properties of an anaerobic mixedculture that reductively deiodinated 5-amino-2,4,6-triiodophthalic acid, an X-ray contrast agentprecursor. *Appl. Microbiol. Biotechnol.* **2003**, *63* (5-6), 550-556.

24. Kormos JL, Schulz M, Ternes TA Occurrence of iodinated X-ray contrast media and their biotransformation products in the urban water cycle. Environ Sci Technol (2011) 45:8723–8732. https://doi.org/10.1021/es2018187

25. M. Alexander “Biodegradation and Bioremediation “second edition 1999, Academic press chapter 11, (p 179-182)

26. M. Alexander “Biodegradation and Bioremediation “second edition 1999 Academic press, Chapter 1, p (4-7)

27. Mohn WW, Tiedje JM. Microbial reductive dehalogenation. Microbiol Rev. 1992 Sep;56(3):482-507. doi: 10.1128/mr.56.3.482-507.1992. PMID: 1406492; PMCID: PMC372880

28. Bin Cao & Karthiga Nagarajan & Kai-Chee “Biodegradation of aromatic compounds: Current statusand opportunities for biomolecular approaches” Loh Appl Microbiol Biotechnol (2009) 85:207–228 DOI 10.1007/s00253-009-2192-4

29. M. Alexander “Biodegradation and Bioremediation “second edition 1999 Academic press, Chapter 7 (p 105-115)

30. Judith L Sims, Joseph M Sulfite and Hugh H. Russell “Reductive Dehalogenation of Organic Contaminants in Soils and Ground Water” Jan 1991 EPA Ground Water Issue EPA/540/4-90/054

31. Lecouturier, D.; Rochex, A.; Lebeault, J.-M. The mineralization of 5-amino-2,4,6-triiodoisophthalic acid by a two-stage fixed-bed reactor. *Water Res.* **2008**, *42* (10-11), 2491-2498.
32. M. Alexander “Biodegradation and Bioremediation “second edition 1999 Academic press, Chapter 12 (p 200-203)

33. Edwards EA, Grbić-Galić D. Anaerobic degradation of toluene and o-xylene by a methanogenic consortium. Appl Environ Microbiol. 1994 Jan;60(1):313-22. doi: 10.1128/aem.60.1.313-322.1994. PMID: 8117084; PMCID: PMC201305

34. https://www.biowater.no/case-studies/ge-healthcare/
35. Fasseland. C and Soteland. I. Mikrobiell sammensetning i biorenesanlegg, Bachelor Thesis, Institute for natural sciences, UIA, 2023 (avaliable on demand).

36. Hirsch, R.; Ternes, T. A.; Lindart, A.; Haberer, K.; Wilken, R-D. A sensitive method for the determination of iodine containing diagnostic agents in aqueous matrices using LC-electrospraytandem-MS detection. *Fresenius J Anal Chem.* **2000**, *366* (8), 835-841.

37. M.Sargent (Ed), Guide to achieving reliable quantitative LC-MS measurements, RSC Analytical Methods Committee, 2013. ISBN 978-0-948926-27-3

38. Mass Specter (MS) operation manual, Thermo Scientific, 102120591-0002 Revision E, February 2019.
39. Lovley DR, Ueki T, Zhang T, Malvankar NS, Shrestha PM, Flanagan KA, Aklujkar M, Butler JE, Giloteaux L, Rotaru AE, Holmes DE, Franks AE, Orellana R, Risso C, Nevin KP. Geobacter: the microbe electric's physiology, ecology, and practical applications. Adv

Microb Physiol. 2011; 59:1-100. doi: 10.1016/B978-0-12-387661-4.00004-5. PMID: 22114840.

40. Zhang T, Tremblay PL, Chaurasia AK, Smith JA, Bain TS, Lovley DR. Anaerobic benzene oxidation via phenol in Geobacter metallireducens. Appl Environ Microbiol. 2013 Dec;79(24):7800-6. doi: 10.1128/AEM.03134-13. Epub 2013 Oct 4. PMID: 24096430; PMCID: PMC3837793.

41. Zhang T, Bain TS, Nevin KP, Barlett MA, Lovley DR. Anaerobic benzene oxidation by Geobacter species. Appl Environ Microbiol. 2012 Dec;78(23):8304-10. doi: 10.1128/AEM.02469-12. Epub 2012 Sep 21. PMID: 23001648; PMCID: PMC3497359

42. HengDuo Xu, LeiLei Xiao, ShiLing Zheng, YueChao Zhang, JiaJia Li & FangHua Liu "Reductive degradation of chloramphenicol by *Geobacter metallireducensScience China Technological Sciences* volume 62, pages1688–1694 (2019)

43. Podosokorskaya, O., A., Kochetkova, T., V., Novikov, A., A., Tochchakov, S., V., Elcheninov, A., G., Kublanov, I., V. (2020). Tenuifilum thalassicum gen. nov., sp. nov., a novel moderate thermophilic anaerobic bacterium from a Kunashir Island

44. https://www.microbiology.ubc.ca/research/labs/eltis/research/bacterial-lignin-degradation Retrieved 1. June 2023.

45. Ali Ahmad Aghapour, Gholamreza Moussavi, and Kamyar Yaghmaeian "Biological Degradation of Catechol in Wastewater using the Sequencing Continuous-inflow Reactor (SCR)" Article in Journal of Environmental Health Science and Engineering · May 2013
DOI: 10.1186/2052-336X-11- https://www.researchgate.net/publication/257885209
46. Metzger, S. & Kapp, H. & Seitz, W. & Weber, W.H. & Hiller, G. & Süßmuth, W. (2005). Removal of iodinated X-ray contrast media during municipal wastewater treatment using powdered activated carbon. GWF, Wasser - Abwasser. 146. 638-645

47. Seitz, W.; Schulz, W.; Weber, W. H. Novel applications of highly sensitive liquid chromatography/mass spectrometry/mass spectrometry for the direct detection of ultra-trace levels of contaminants in water. *Rapid Commun. Mass Spectrom.* **2006a**, *20* (15), 2281-2285

48. Van der Borg. N "Fundaments of single quadrupole Mass Spectrometry" Course material, Waters Cooperation 2018. Slide 1 (waters.com) Video seminar: Fundamentals of Mass Detection: Part I - What Is Single Quadrupole Mass Spectrometry and How Is It Used? - Waters Videos

49. Product description MCN carbon https://www.carlson.co.uk/wp-content/uploads/2017/09/Carlson-Carlcarb-

Appendix 1:

Table A_1: Results from optimization of MS method

Method 1		**Method 2**		**Method 3**		**Method 4**		**Method 5**		**Method 6**	
m/z	Height count	*m/z*	Height counts	*m/z*	Height counts	*m/z*	Height counts	*m/z*	Height counts	*m/z*	Height counts
328,1 /655,1	6722592	328,0	5795504	328,1	4063431	328,2/329,3	4622036	328,0 /655,1	9955405	328,0/655,0	4632519
444,1/887,3	2056639	444,2/466,0	2225602	444,1/466,0	1110303	444,1	1452280	444,1 /445,2	3161330	444,2/445,1/ 665,7	1537026
402,1/403,1/ 803,3	3909366	402,0/403,0	3312321	402,1	2592777	402,0/402,6	3015821	402,1/403,1/ 803,2	5634998	492,1/602,9	3647834
369,8/370,3/ 739,3	3339859	370,0	3231123	370,2/369,5/ 371,1	1368996	370,1/371,3/ 739,1	1823043	369,8/370,4/ 739,2	4931790	370,0/739,1	1965443
297,1	643532	444,2/466,1	581512	296,9/319,2/ 297,5	635362	795,4/796,1	693990	297,1/298,0	997730	444,2/443,6	881977
398, 5/ 397,9/795,4	1603063	398,1/795,0/ 796,0	1293954	398,3/795,4/ 794,9	578707	376,9/377,6/ 753,6	711110	398,1/795,2	2312958	377,5/376,8/ 753,1	686760
377,1/377,9/ 753,4	1271418	377,2/377,8/ 775,3	883460	377,2/753,3/ 774,2	1387308	444,2/443,6/ 445,1	558533	376,9/377,7/ 753,2	1942304	444,0/444,6/ 445,2	1721702
444,1/405,2	2196055	444,1/445,1	18664152	444,0/445,1	473915	194,1/166,1	1346762	444,1	3063033	194,1/166,3/ 151,1	582299
386,1	930582	386,1/408,0/ 423,0	648191	386,1	408072	385,7/386,3/ 280,9	657540	385,9/386,9/ 793,2	1211318	386,0/310,6/ 151,6	570948
356,0/356,6	857141	356,0/356,6/ 733,3	574394	356,2	443390	356,4/356;9/ 448,6	594274	356,0/356,5/ 711,2	1275632	356,2	528396
398,0/398,6/ 795,4	1297689	398,1/398,7/ 795,3	10335667	398,0/398,5/ 795,2	520503	398,5/484,0/ 822,6	484455	398,1/398,8/ 795,2	1883139	398,2/483,9/ 569,9	662532

Table A_2: Raw data used for calculation precision. Injection 1 in each was discarded du to HPLC pump error.

Inj. No.	Injection Name Selected Peak:	Type	Ret.Time min UV_VIS_1 540	Amount g/L UV_VIS_1 540	Rel.Area % UV_VIS_1 540	Area mAU*min UV_VIS_1 540	Height mAU UV_VIS_1 540	Type UV_VIS_1 540	Width (50%) min UV_VIS_1 540	Asym. EP UV_VIS_1 540	Resol. EP UV_VIS_1 540	Plates EP UV_VIS_1 540
1	*Miljø_standard*	*Unknown*	*11,380*	*0,0101*	*16,70*	*85,4784*	*393,14*	*M ^*	*0,180*	*1,24*	*n.a.*	*22205*
2	Miljø_standard	Unknown	9,764	0,0100	17,04	85,2749	457,28	MB*	0,155	1,23	41,92	22106
3	Miljø_standard	Unknown	9,580	0,0100	17,05	84,9099	452,20	MB*	0,157	1,24	41,91	20724
4	Miljø_standard	Unknown	9,607	0,0100	17,00	84,8431	451,35	MB*	0,157	1,23	41,81	20826
5	Miljø_standard	Unknown	9,633	0,0099	17,61	84,3686	450,17	BMB*	0,157	1,24	42,29	20870
6	Miljø_standard	Unknown	9,753	0,0097	17,19	82,7717	454,45	BMB*	0,155	1,22	41,92	21899

Inj. No.	Injection Name Selected Peak:	Type	Ret.Time min UV_VIS_1 Iodixanol	Amount g/L UV_VIS_1 Iodixanol	Rel.Area % UV_VIS_1 Iodixanol	Area mAU*min UV_VIS_1 Iodixanol	Height mAU UV_VIS_1 Iodixanol	Type UV_VIS_1 Iodixanol	Width (50%) min UV_VIS_1 Iodixanol	Asym. EP UV_VIS_1 Iodixanol	Resol. EP UV_VIS_1 Iodixanol	Plates EP UV_VIS_1 Iodixanol
1	*Miljø_standard*	*Unknown*	*28,817*	*0,0101*	*21,48*	*109,9322*	*197,53*	*BM *^*	*0,273*	*0,92*	*n.a.*	*61902*
2	Miljø_standard	Unknown	24,647	0,0102	22,04	110,2862	205,51	BMB*	0,264	0,92	n.a.	48150
3	Miljø_standard	Unknown	24,620	0,0100	21,75	108,3404	202,63	MB*	0,267	0,94	n.a.	47167
4	Miljø_standard	Unknown	24,637	0,0101	21,89	109,2313	202,15	BMB*	0,268	0,94	n.a.	46975
5	Miljø_standard	Unknown	24,693	0,0094	21,24	101,7701	201,45	BMB*	0,263	0,96	n.a.	48751
6	Miljø_standard	Unknown	24,737	0,0101	22,65	109,0485	203,12	BMB*	0,267	0,93	n.a.	47677

Inj. No.	Injection Name Selected Peak:	Type	Ret.Time min UV_VIS_1 Iohexol EXO	Amount g/L UV_VIS_1 Iohexol EXO	Rel.Area % UV_VIS_1 Iohexol EXO	Area mAU*min UV_VIS_1 Iohexol EXO	Height mAU UV_VIS_1 Iohexol EXO	Type UV_VIS_1 Iohexol EXO	Width (50%) min UV_VIS_1 Iohexol EXO	Asym. EP UV_VIS_1 Iohexol EXO	Resol. EP UV_VIS_1 Iohexol EXO	Plates EP UV_VIS_1 Iohexol EXO
1	*Miljø_standard*	*Unknown*	*10,257*	*0,0105*	*16,67*	*85,3150*	*314,41*	*M ^*	*0,237*	*0,98*	*3,18*	*10354*
2	Miljø_standard	Unknown	8,647	0,0104	16,75	83,8038	363,61	M *	0,205	1,00	3,66	9849
3	Miljø_standard	Unknown	8,417	0,0134	21,78	108,4960	355,21	M *	0,210	1,01	3,74	8878
4	Miljø_standard	Unknown	8,443	0,0104	16,90	84,3290	355,56	M *	0,210	1,01	3,74	8946
5	Miljø_standard	Unknown	8,473	0,0102	17,21	82,4813	353,64	MB*	0,210	1,01	3,73	9038
6	Miljø_standard	Unknown	8,627	0,0097	16,33	78,6177	355,33	BMB*	0,205	1,03	3,70	9847

Inj. No.	Injection Name Selected Peak:	Type	Ret.Time min UV_VIS_1 541	Amount g/L UV_VIS_1 541	Rel.Area % UV_VIS_1 541	Area mAU*min UV_VIS_1 541	Height mAU UV_VIS_1 541	Type UV_VIS_1 541	Width (50%) min UV_VIS_1 541	Asym. EP UV_VIS_1 541	Resol. EP UV_VIS_1 541	Plates EP UV_VIS_1 541
1	*Miljø_standard*	*Unknown*	*7,840*	*0,0102*	*25,11*	*128,5585*	*522,85*	*M ^*	*0,218*	*0,94*	*n.a.*	*7141*
2	Miljø_standard	Unknown	6,887	0,0105	26,22	131,1996	635,35	BM *	0,178	0,96	2,71	8295
3	Miljø_standard	Unknown	6,670	0,0103	25,89	128,9890	626,66	M *	0,181	0,95	5,27	7554
4	Miljø_standard	Unknown	6,690	0,0103	25,89	129,2065	624,88	M *	0,181	0,96	2,52	7548
5	Miljø_standard	Unknown	6,717	0,0099	25,82	123,7435	623,97	BMB*	0,179	0,96	2,59	7771

Calibration of HPLC-MS method.

Calibration curve made in Chromeleon 7.3 data handling system. For each compound used in the standard solution.

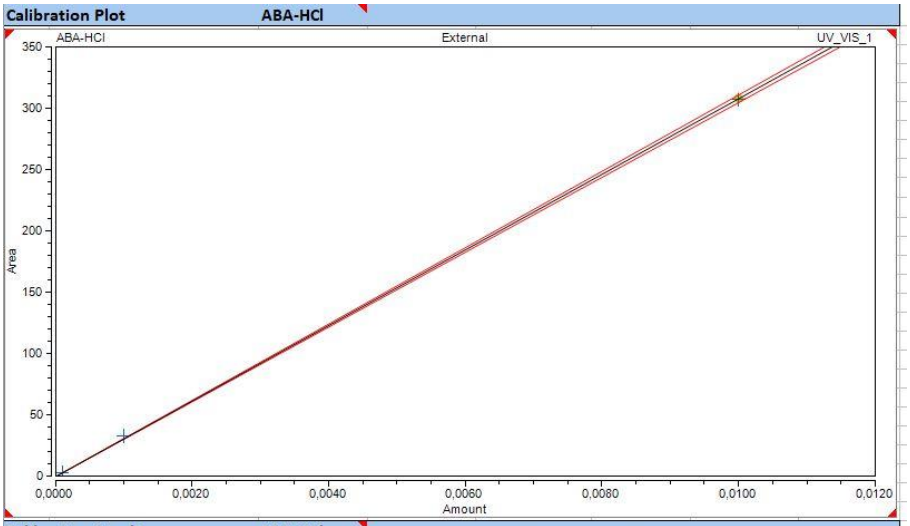

Calibration Results **ABA-HCl**

No.	Injection Name	Calibration Level	X Value UV_VIS_1 ABA-HCl	Y Value UV_VIS_1 ABA-HCl	Y Value UV_VIS_1 ABA-HCl	Area mAU*min UV_VIS_1 ABA-HCl	Height mAU UV_VIS_1 ABA-HCl
47	Standard 1	1	0,0100	308,0788	308,0788	308,079	2275,393
48	Standard 1	1	0,0100	307,2436	307,2436	307,244	2272,180
49	Standard 2	2	0,0010	33,1315	33,1315	33,131	291,654
50	Standard 2	2	0,0010	32,9948	32,9948	32,995	287,584
51	Standard 3	3	0,0001	3,3537	3,3537	3,354	29,102
52	Standard 3	3	0,0001	3,3489	3,3489	3,349	28,986
53	Standard 4	4	0,0000	0,3382	0,3382	0,338	2,913
54	Standard 4	4	0,0000	0,3388	0,3388	0,339	2,903

Figure A_1_1: Linearity ABA-HCl

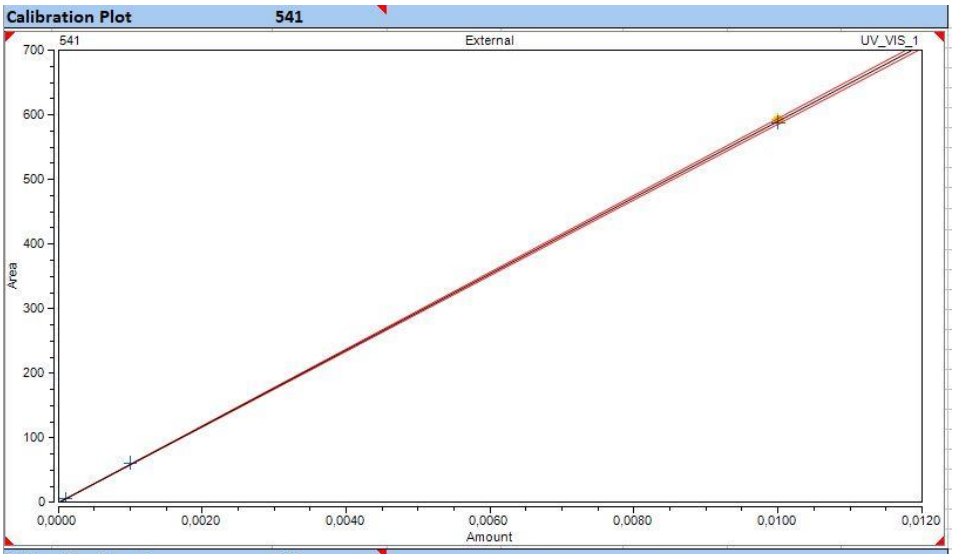

Calibration Results **541**

No.	Injection Name	Calibration Level	X Value UV_VIS_1 541	Y Value UV_VIS_1 541	Y Value UV_VIS_1 541	Area mAU*min UV_VIS_1 541	Height mAU UV_VIS_1 541
47	Standard 1	1	0,0100	592,0843	592,0843	592,084	2790,514
48	Standard 1	1	0,0100	587,9851	587,9851	587,985	2777,401
49	Standard 2	2	0,0010	61,6933	61,6933	61,693	297,663
50	Standard 2	2	0,0010	61,5332	61,5332	61,533	296,088
51	Standard 3	3	0,0001	6,2275	6,2275	6,227	30,083
52	Standard 3	3	0,0001	6,2370	6,2370	6,237	29,950
53	Standard 4	4	0,0000	0,6146	0,6146	0,615	3,099
54	Standard 4	4	0,0000	0,6198	0,6198	0,620	3,093

Figure A_1_2: Linearity 541

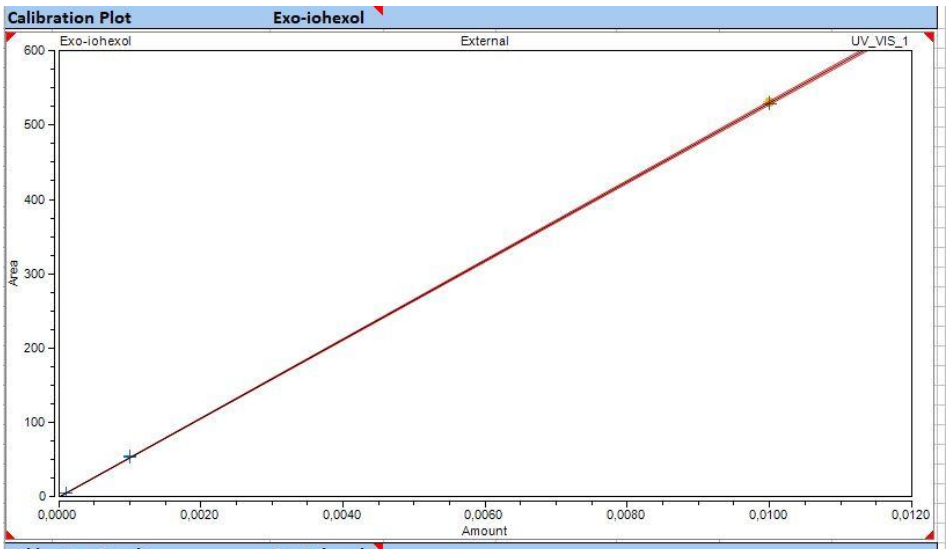

Calibration Results **Exo-iohexol**

No.	Injection Name	Calibration Level	X Value UV_VIS_1 Exo-iohexol	Y Value UV_VIS_1 Exo-iohexol	Y Value UV_VIS_1 Exo-iohexol	Area mAU*min UV_VIS_1 Exo-iohexol	Height mAU UV_VIS_1 Exo-iohexol
47	Standard 1	1	0,0100	531,0554	531,0554	531,055	1718,656
48	Standard 1	1	0,0100	528,5939	528,5939	528,594	1715,732
49	Standard 2	2	0,0010	54,4518	54,4518	54,452	178,618
50	Standard 2	2	0,0010	54,2021	54,2021	54,202	177,810
51	Standard 3	3	0,0001	5,5053	5,5053	5,505	17,964
52	Standard 3	3	0,0001	5,4813	5,4813	5,481	18,024
53	Standard 4	4	0,0000	0,5522	0,5522	0,552	1,869
54	Standard 4	4	0,0000	0,5589	0,5589	0,559	1,876

Figure A_1_3: Linearity Iohexol (endo and exo-isomers are combined in this standard)

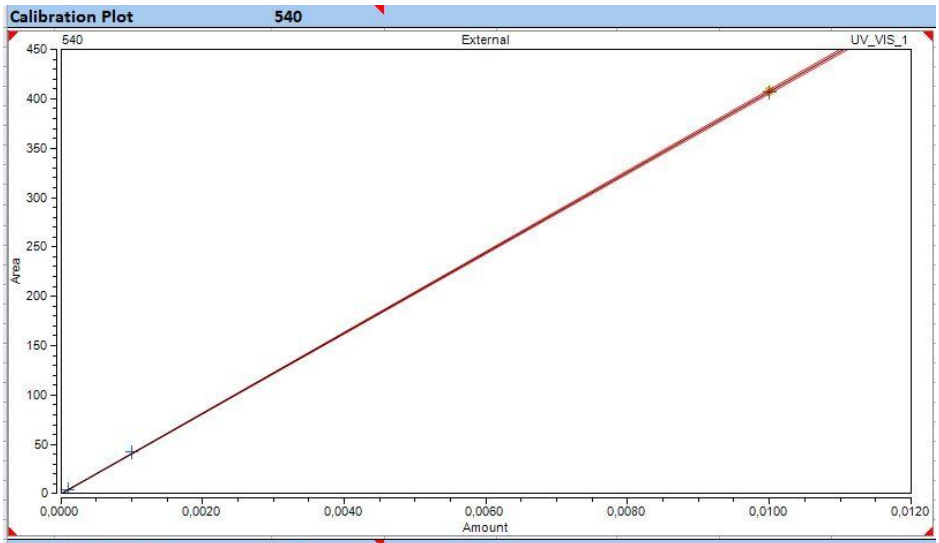

Calibration Results 540

No.	Injection Name	Calibration Level	X Value UV_VIS_1 540	Y Value UV_VIS_1 540	Y Value UV_VIS_1 540	Area mAU*min UV_VIS_1 540	Height mAU UV_VIS_1 540
47	Standard 1	1	0,0100	407,7251	407,7251	407,725	2174,141
48	Standard 1	1	0,0100	406,6945	406,6945	406,695	2173,755
49	Standard 2	2	0,0010	42,2093	42,2093	42,209	224,563
50	Standard 2	2	0,0010	42,1472	42,1472	42,147	224,742
51	Standard 3	3	0,0001	4,2824	4,2824	4,282	22,756
52	Standard 3	3	0,0001	4,2763	4,2763	4,276	22,839
53	Standard 4	4	0,0000	0,4212	0,4212	0,421	2,366
54	Standard 4	4	0,0000	0,4474	0,4474	0,447	2,380

Figure A_1_4: Linearity 540

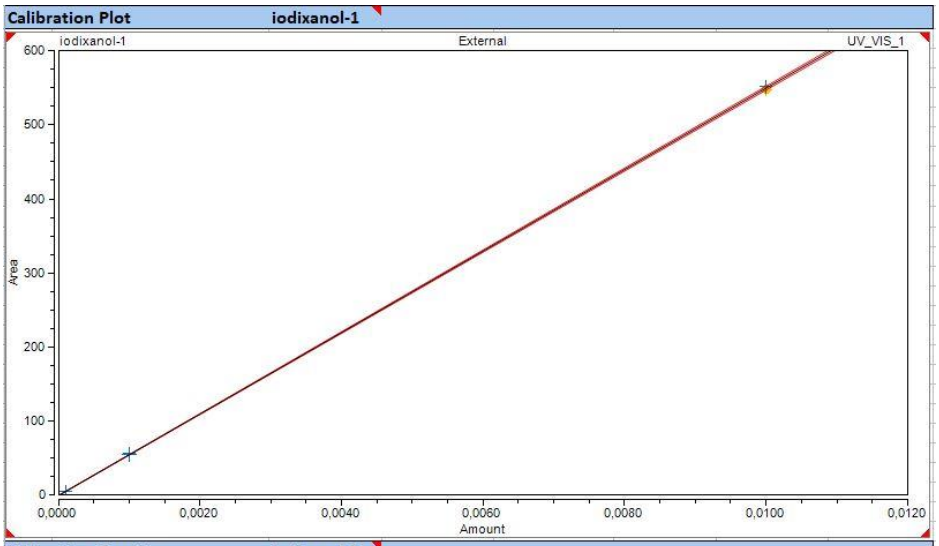

Calibration Results iodixanol-1

No.	Injection Name	Calibration Level	X Value UV_VIS_1 iodixanol-1	Y Value UV_VIS_1 iodixanol-1	Y Value UV_VIS_1 iodixanol-1	Area mAU*min UV_VIS_1 iodixanol-1	Height mAU UV_VIS_1 iodixanol-1
47	Standard 1	1	0,0100	547,8864	547,8864	547,886	1021,507
48	Standard 1	1	0,0100	551,2525	551,2525	551,252	1031,516
49	Standard 2	2	0,0010	56,2339	56,2339	56,234	105,039
50	Standard 2	2	0,0010	55,2760	55,2760	55,276	103,626
51	Standard 3	3	0,0001	5,5780	5,5780	5,578	10,376
52	Standard 3	3	0,0001	5,5231	5,5231	5,523	10,472
53	Standard 4	4	0,0000	0,5459	0,5459	0,546	1,106
54	Standard 4	4	0,0000	0,5969	0,5969	0,597	1,105

Figure A_1_5: Linearity Iodixanol

Appendix 2
Peaks TPs in SP9 (EGSB 1)

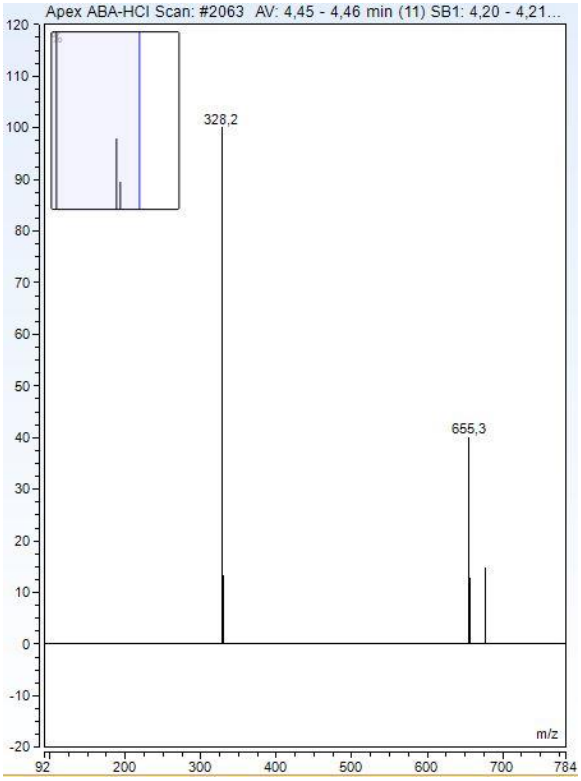

Figure A_2_1: SP9_peak 1_MS-specter

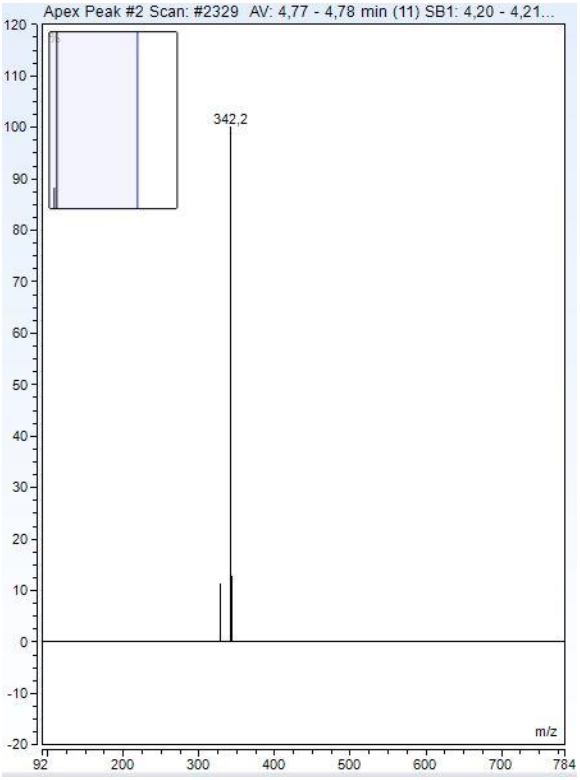

Figure: A_2_2 SP9_peak 2_MS-specter

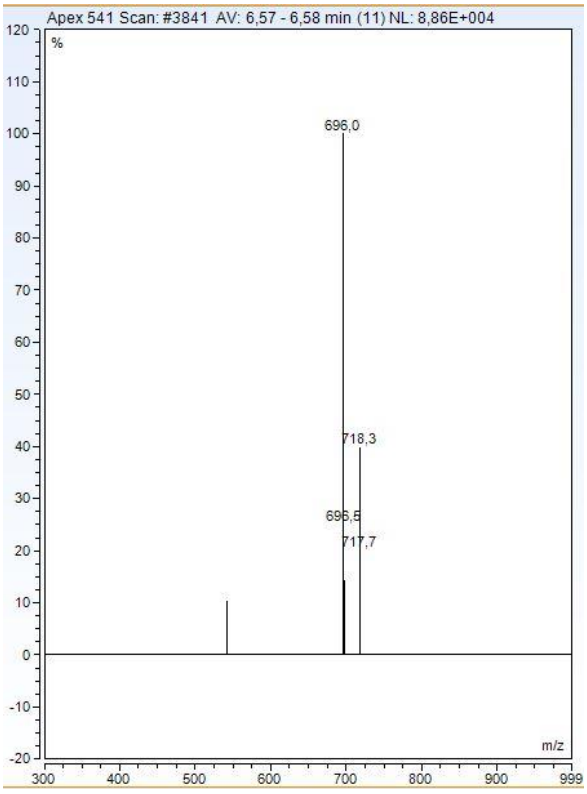

Figure: A_2_3 SP9_peak 3_MS-specter

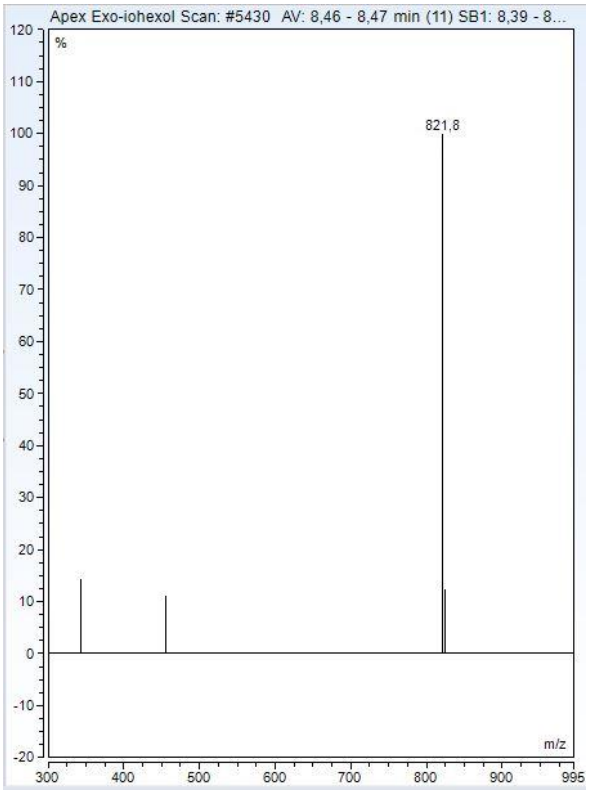

Figure A_2_4: SP9_peak 4_MS-specter

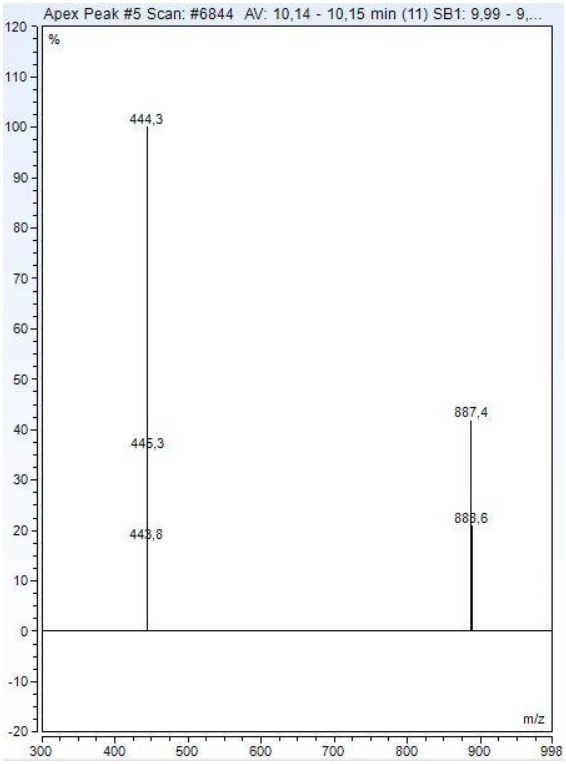

Figure A_2_5: SP9_peak 5_MS-specter

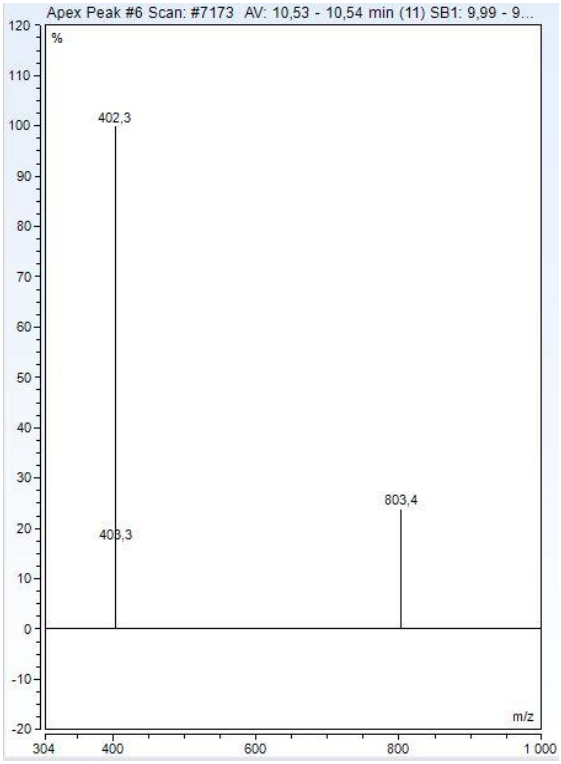

Figure: A_2_6: SP9_peak 6_MS-specter

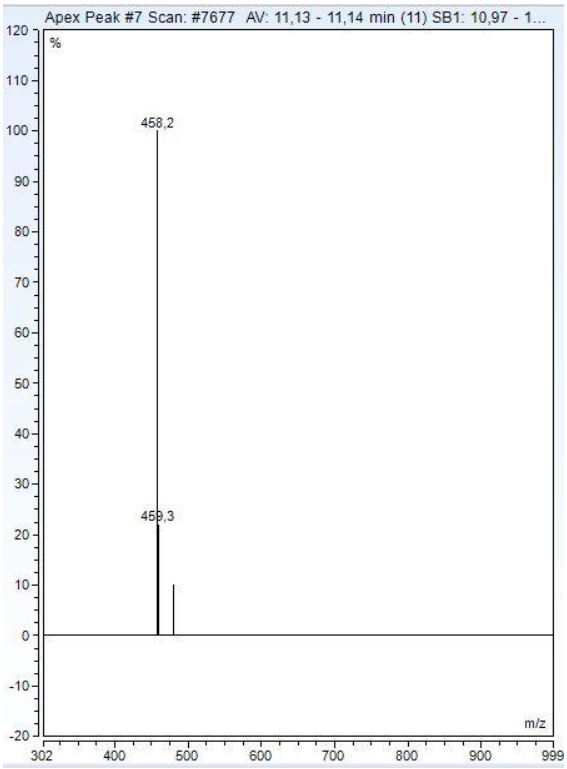

Figure: A_2_7: SP9_peak 7_MS-specter

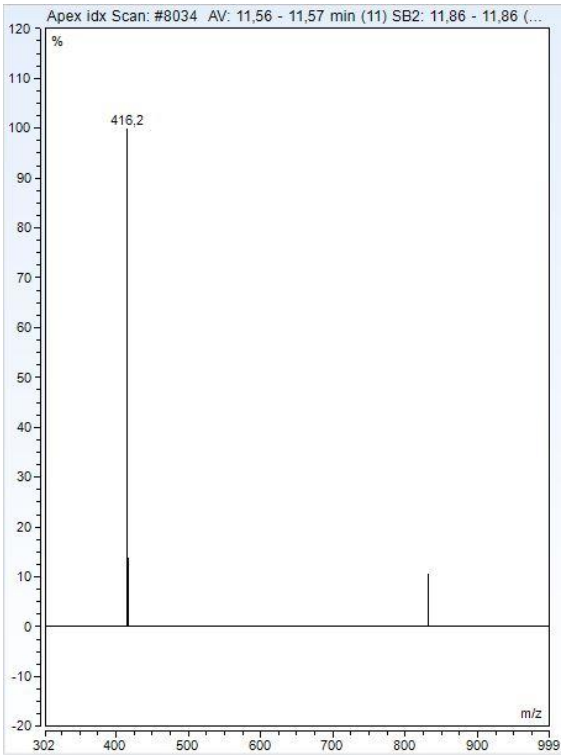

Figure: A_2_8: SP9_peak 8_MS-specter

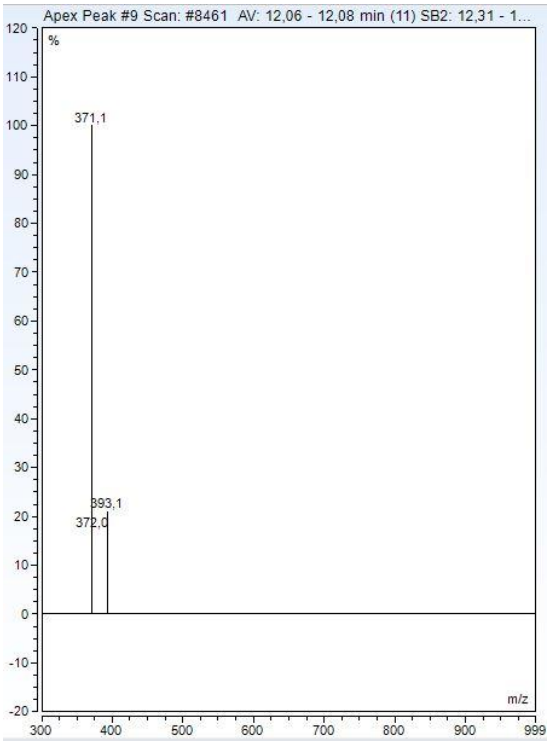

Figure: A_2_9: SP9_peak 9_MS-specter

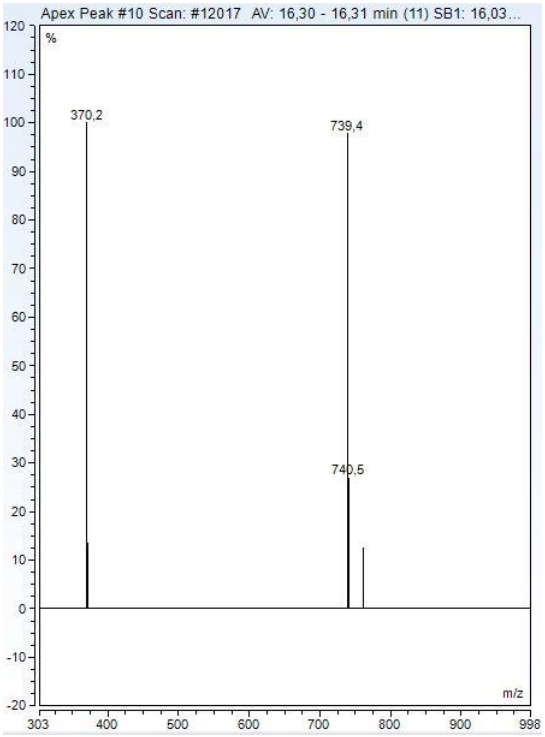

Figure: A_2_10: SP9_peak 10_MS-specter

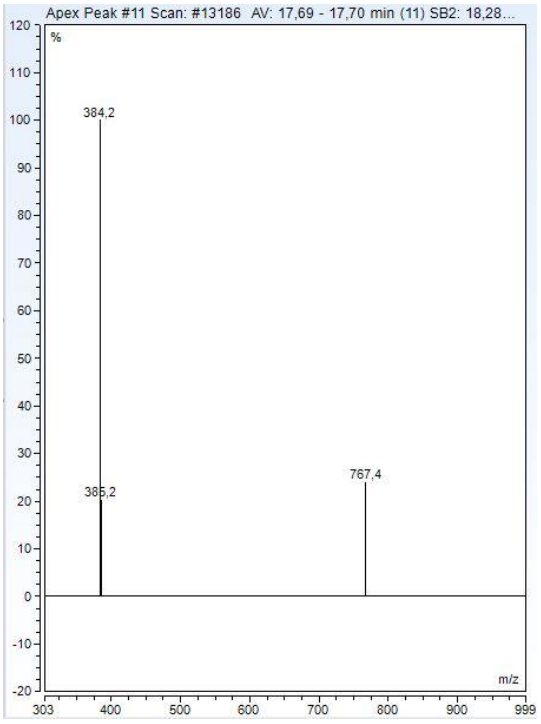

Figure: A_2_11: SP9_peak 11_MS-specter

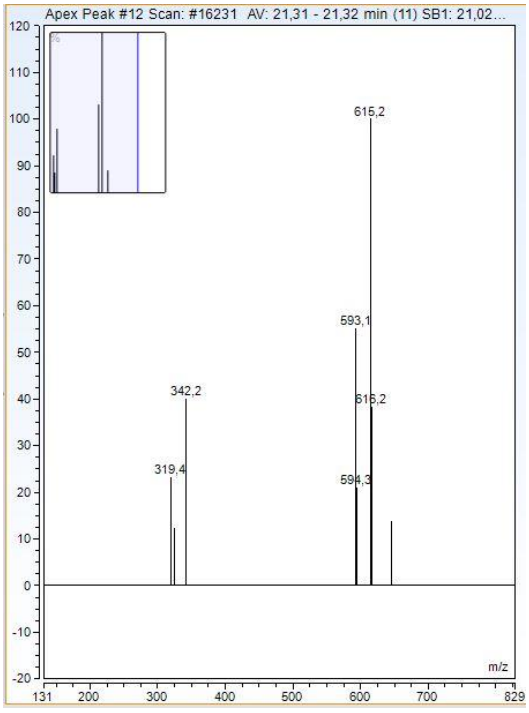

Figure: A_2_12: SP9_peak 12_MS-specter

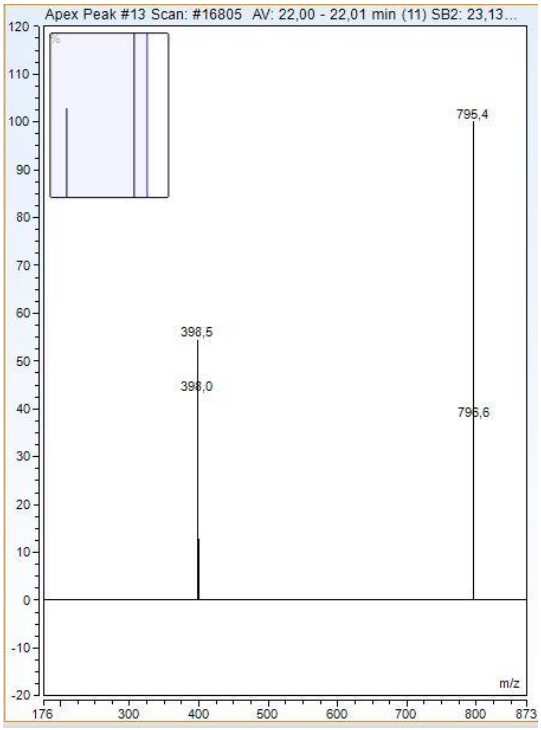

Figure: A_2_13: SP9_peak 13_MS-specter

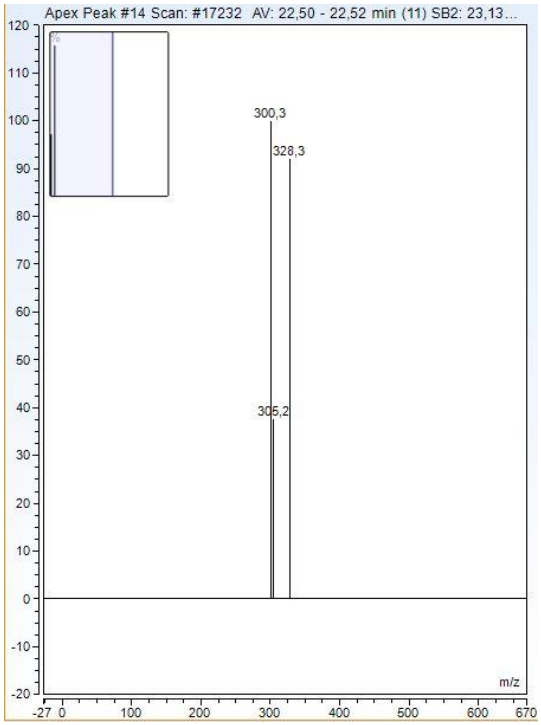

Figure: A_2_14: SP9_peak 14_MS-specter

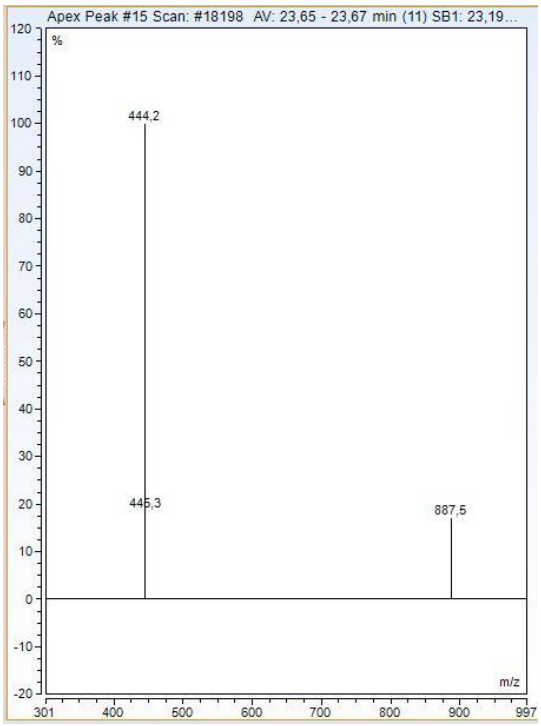

Figure: A_2_15: SP9_peak 15_MS-specter specter

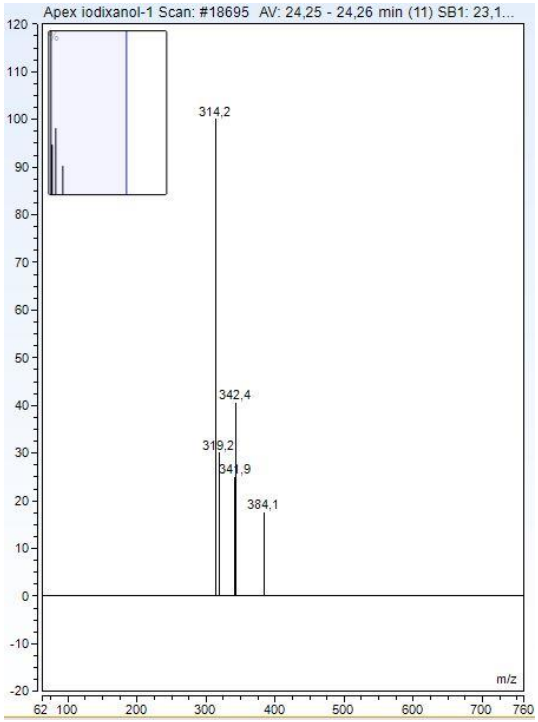

Figure: A_2_16: SP9_peak 16_MS-specter

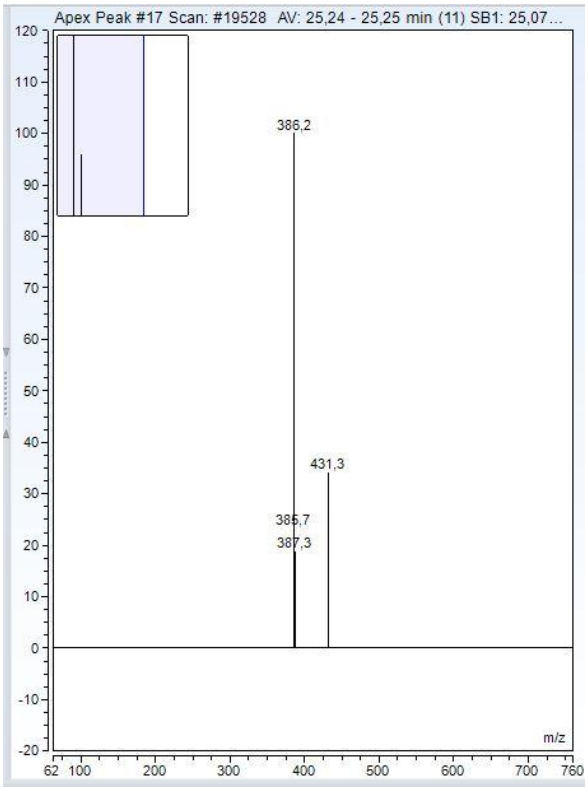

Figure: A_2_17: SP9_peak 17_MS-specter specter

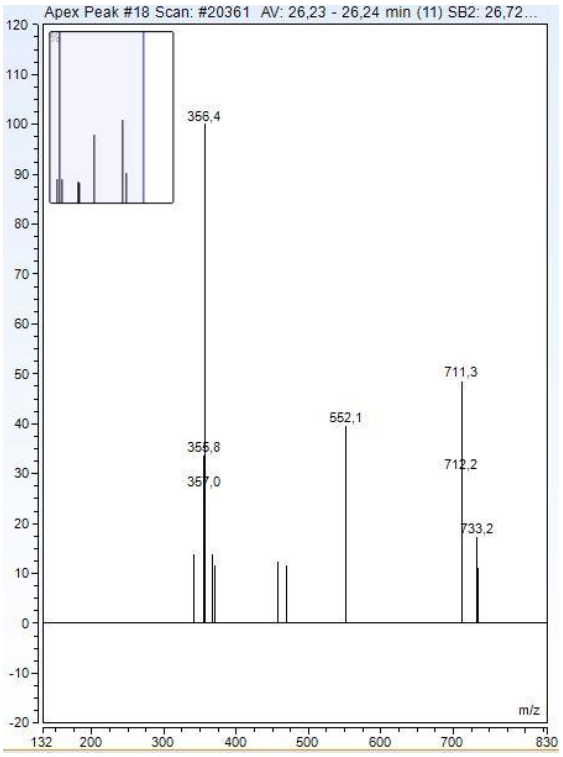

Figure: A_2_18: SP9_peak 18_MS-specter

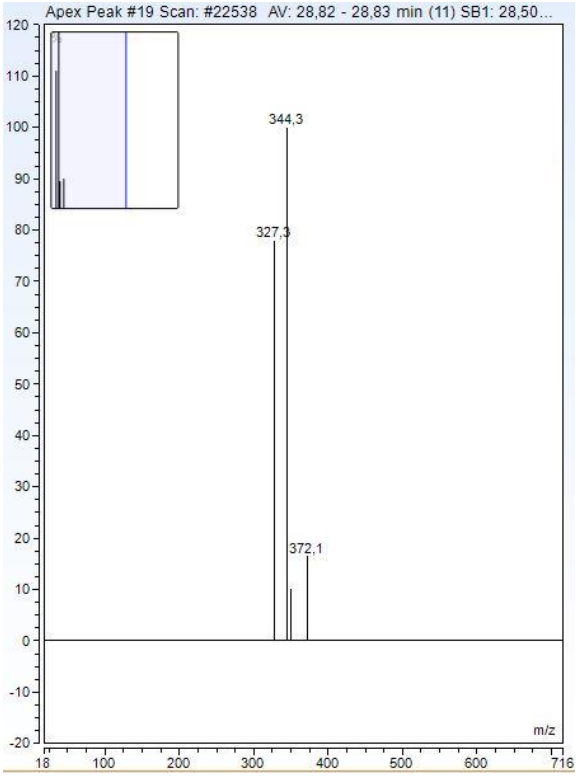

Figure: A_2_19: SP9_peak 19_MS-specter specter

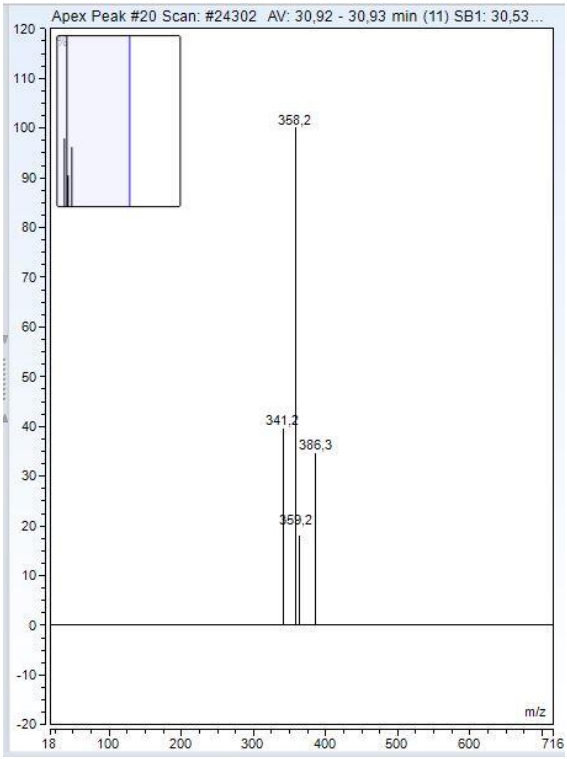

Figure: A_2_20: SP9_peak 20_MS-specter

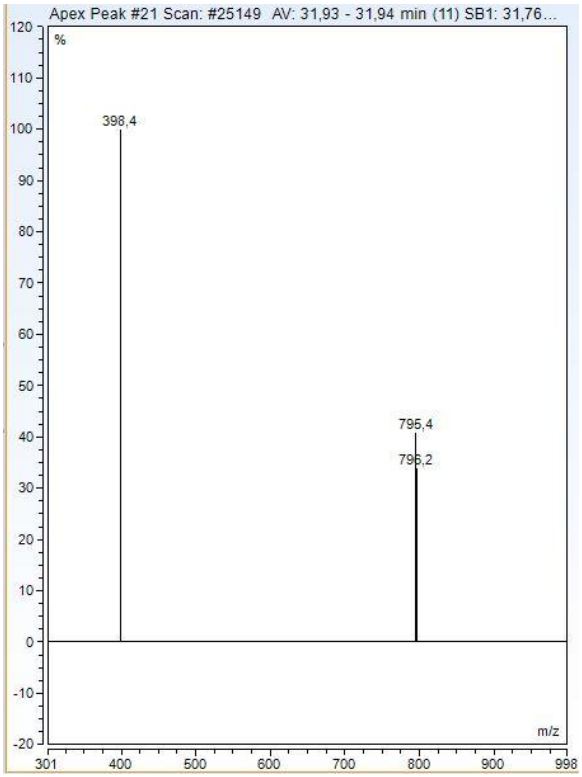

Figure: A_2_21: SP9_peak 21_MS-specter specter

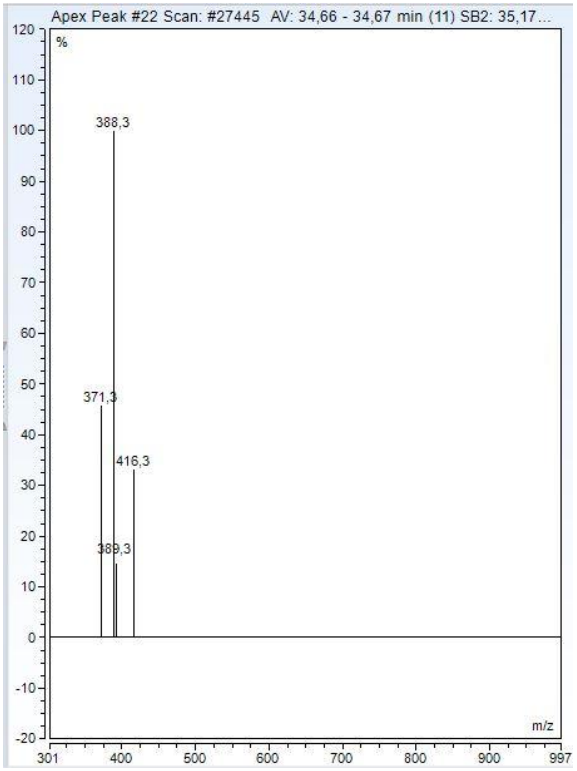

Figure: A_2_22: SP9_peak 22_MS-specter

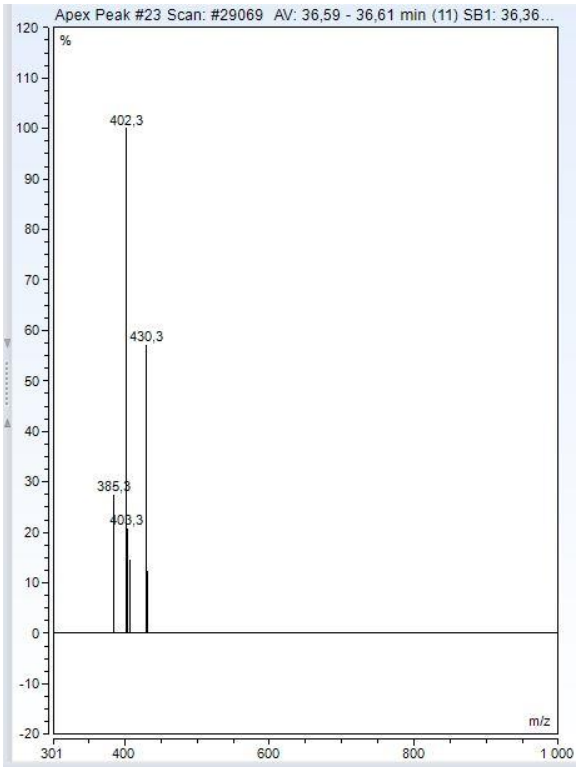

Figure: A_2_23: SP9_peak 23_MS-specter

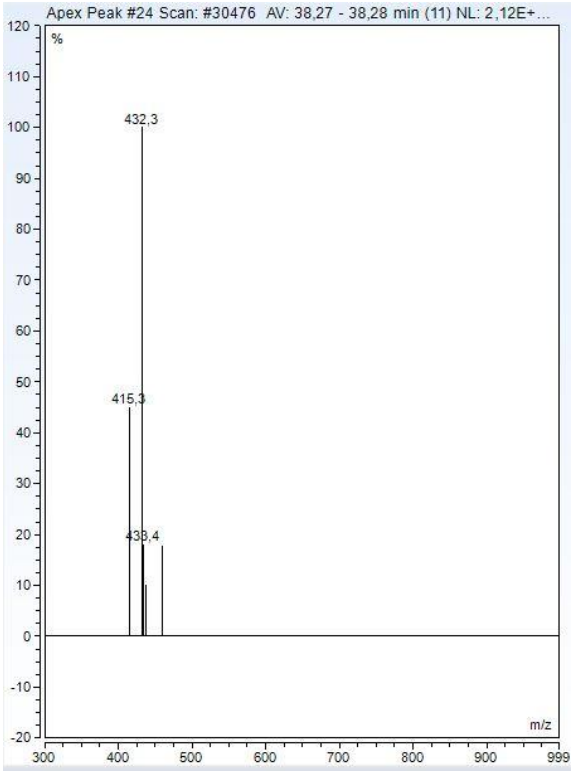

Figure: A_2_24: SP9_peak 24_MS-specter

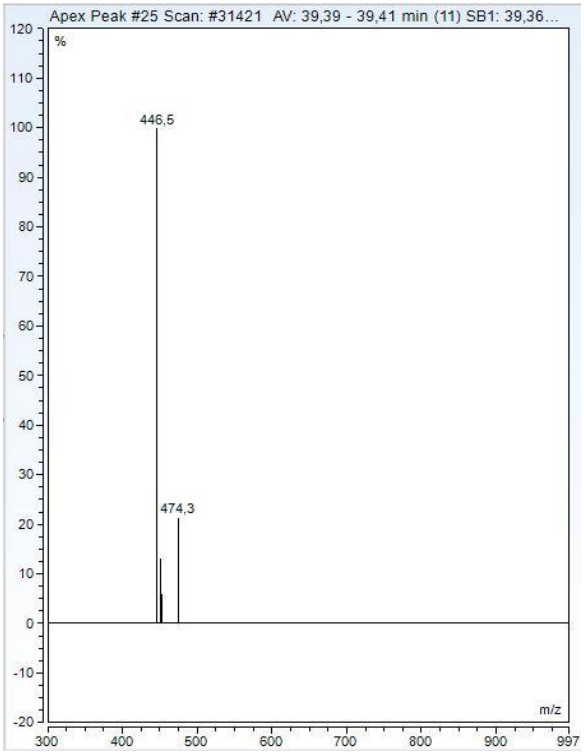

Figure: A_2_25: SP9_peak 25_MS-specter

Peaks TPs SP10 (EGSB 2)

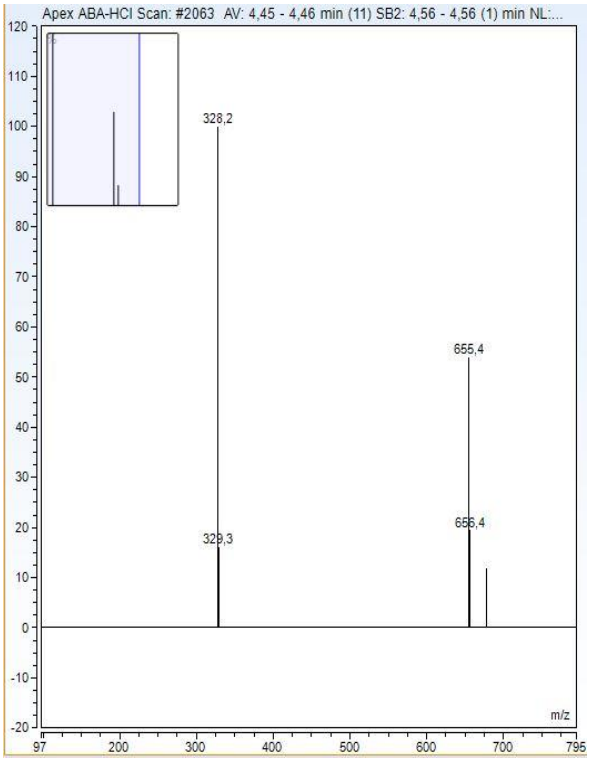

Figure: A_2_26:SP10_peak 1_MS-specter

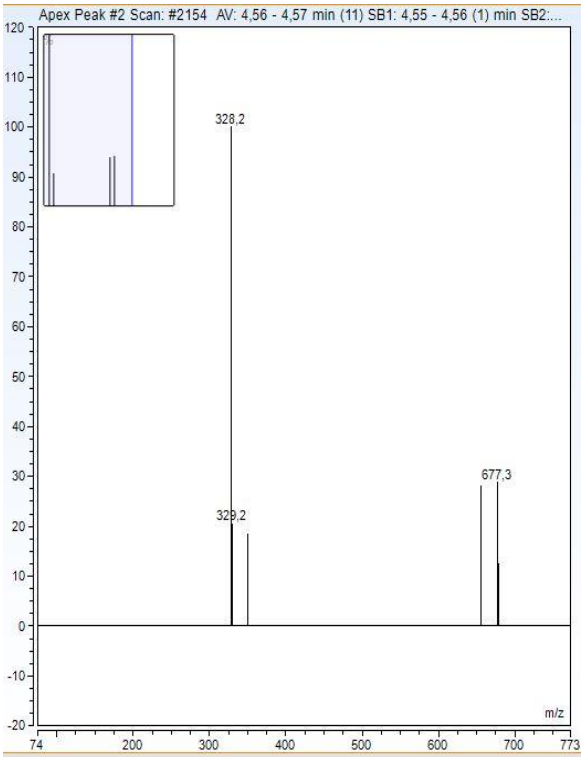

Figure: A_2_27: SP10_peak 2_MS-specter

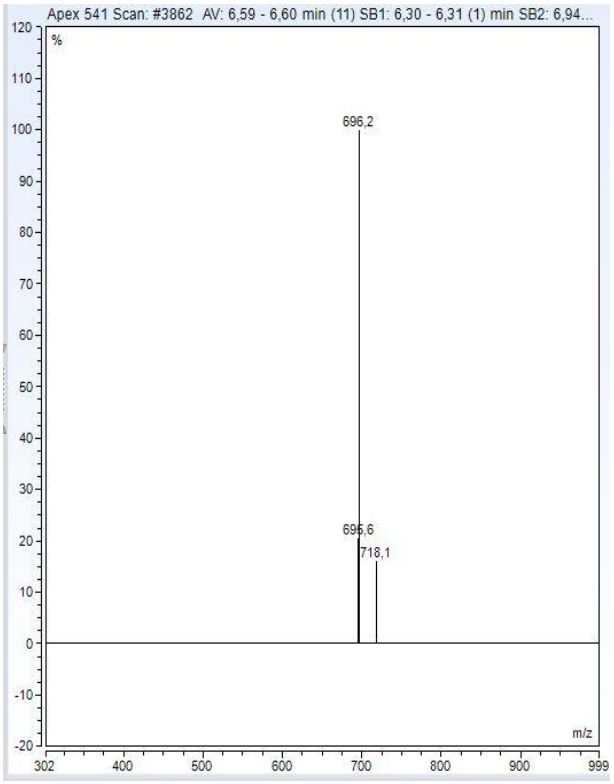

Figure: A_2_27: SP10_peak 3_MS-specter

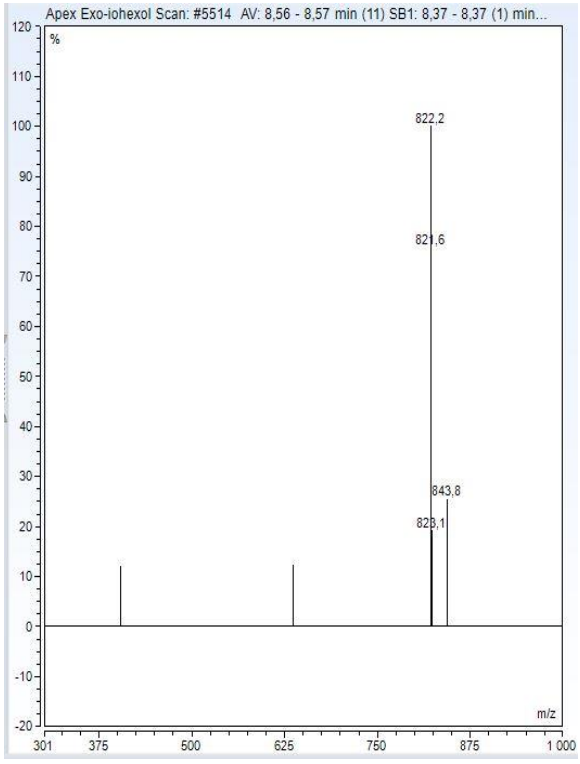

Figure: A_2_28: SP10_peak 4_MS-specter

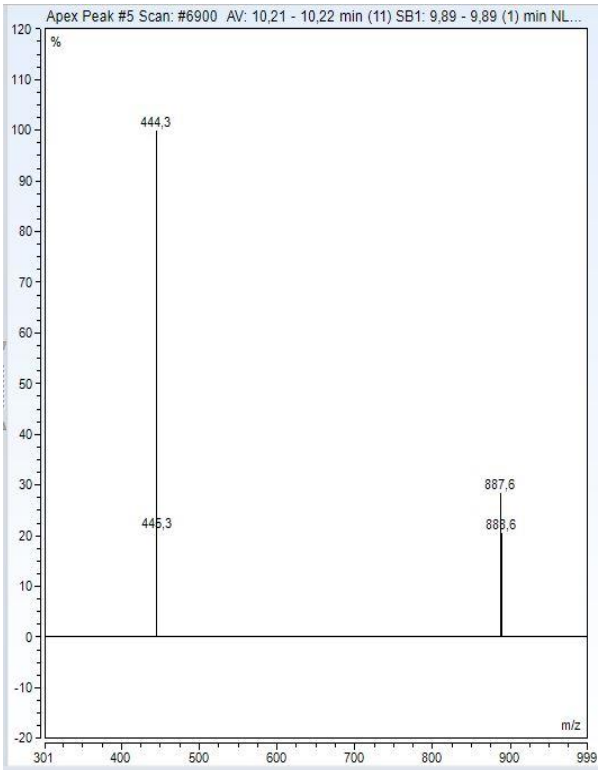

Figure: A_2_29: SP10_peak 5_MS-specter

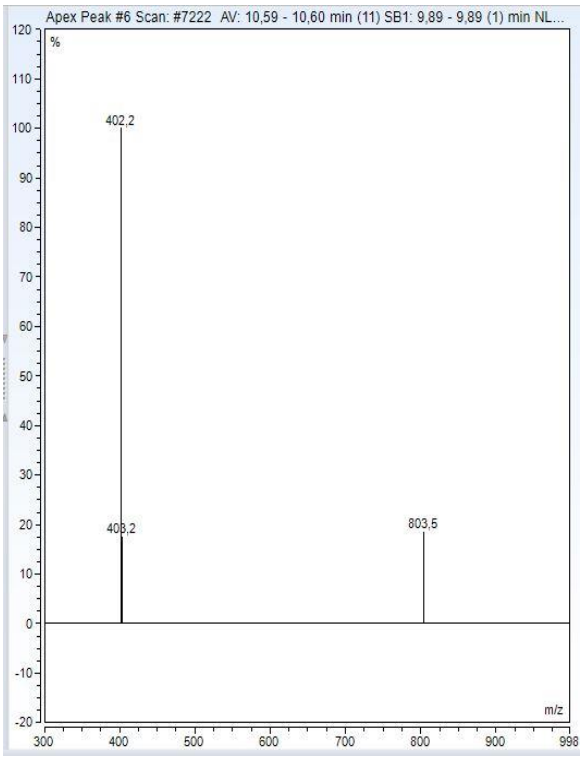

Figure: A_2_30: SP10_peak _6_MS-specter

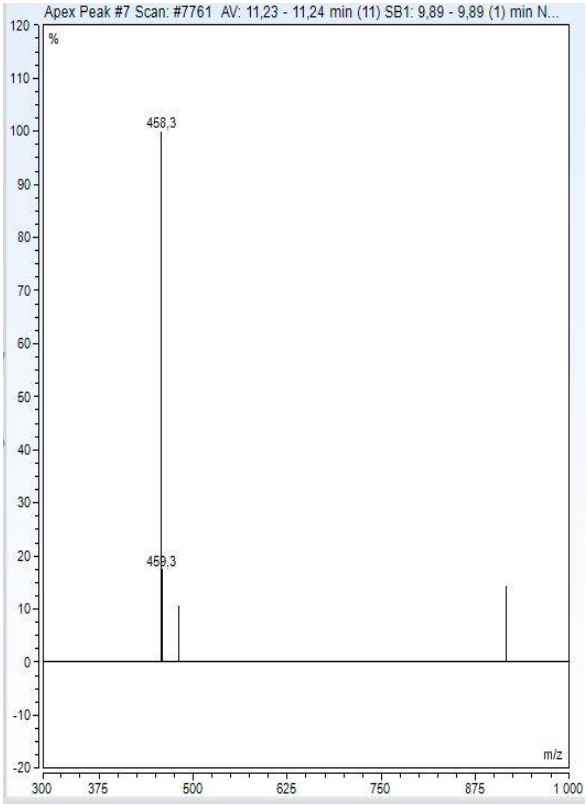

Figure: A_2_31: SP10_peak 7_MS-specter

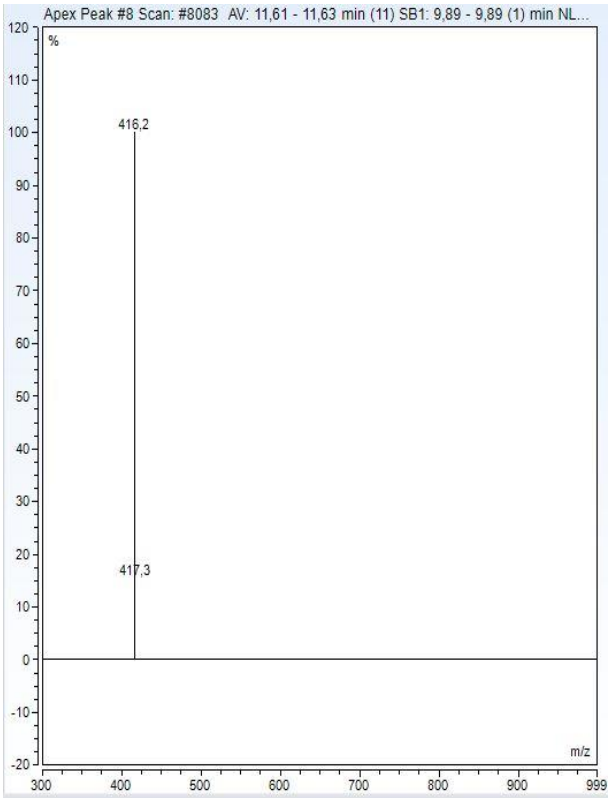

Figure: A_2_32: SP10_peak 8-MS_specter

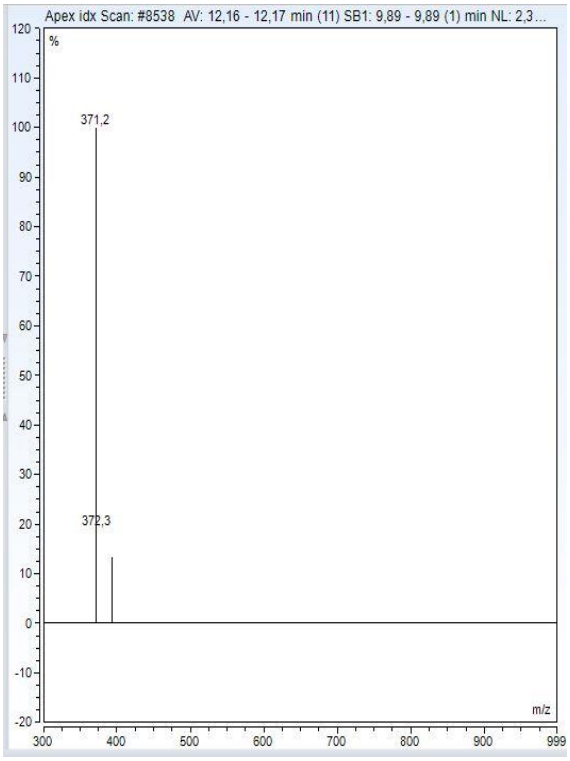

Figure: A_2_33: SP10_peak 9_MS-specter

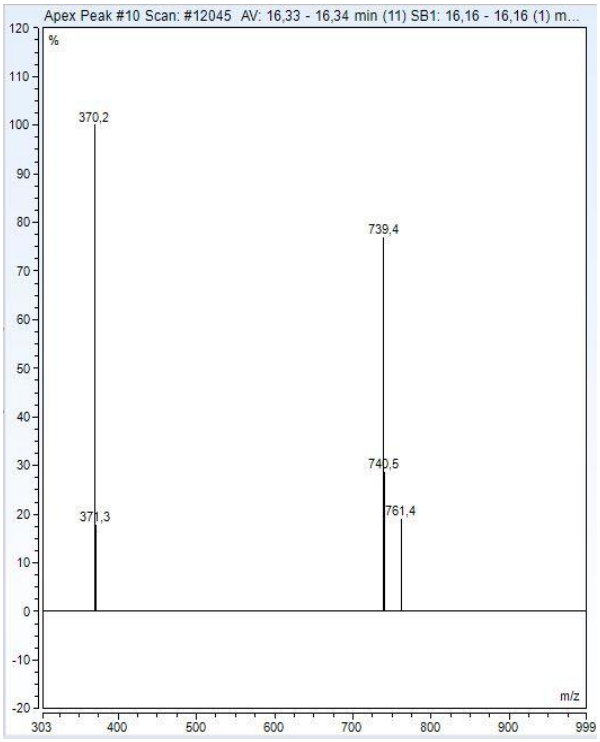

Figure: A_2_34: SP10_peak 10_MS-specter

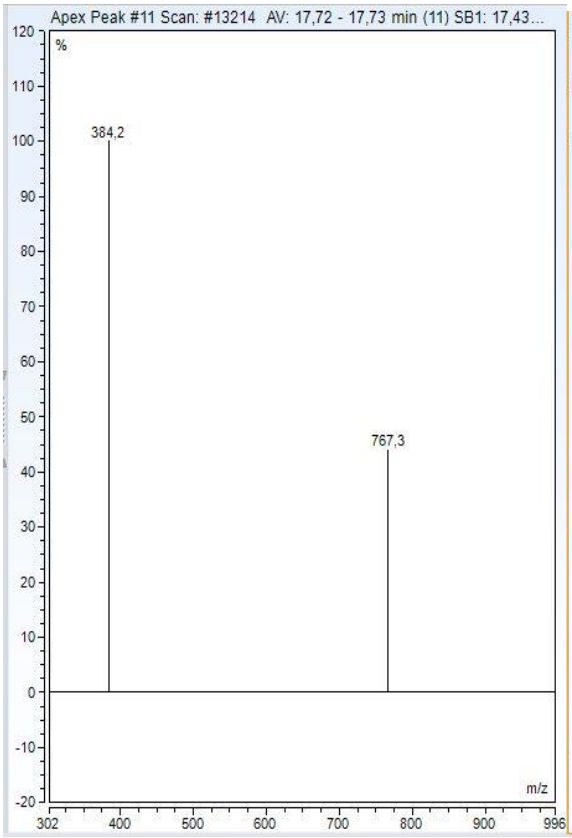

Figure: A_2_35: SP10_peak 11_MS-specter

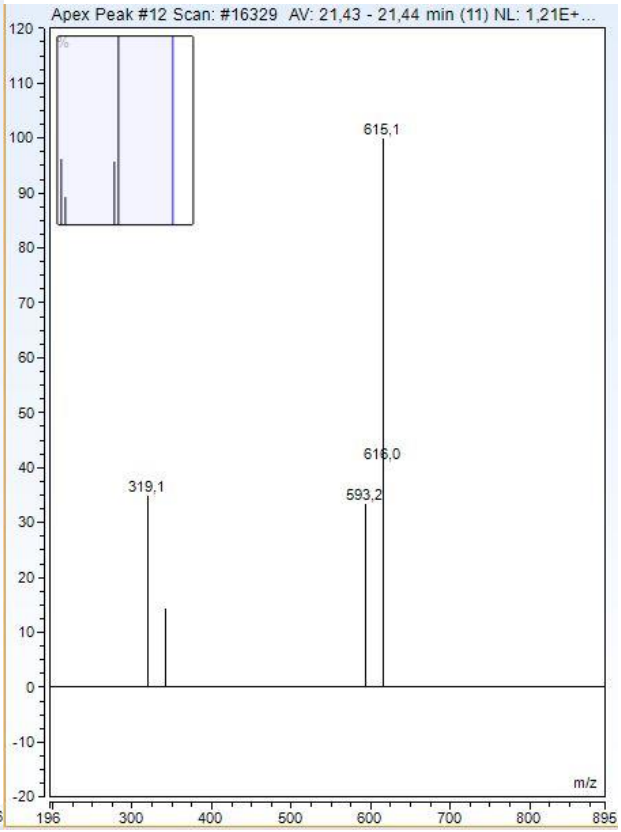

Figure: A_2_36: SP10_peak12_MSspecter

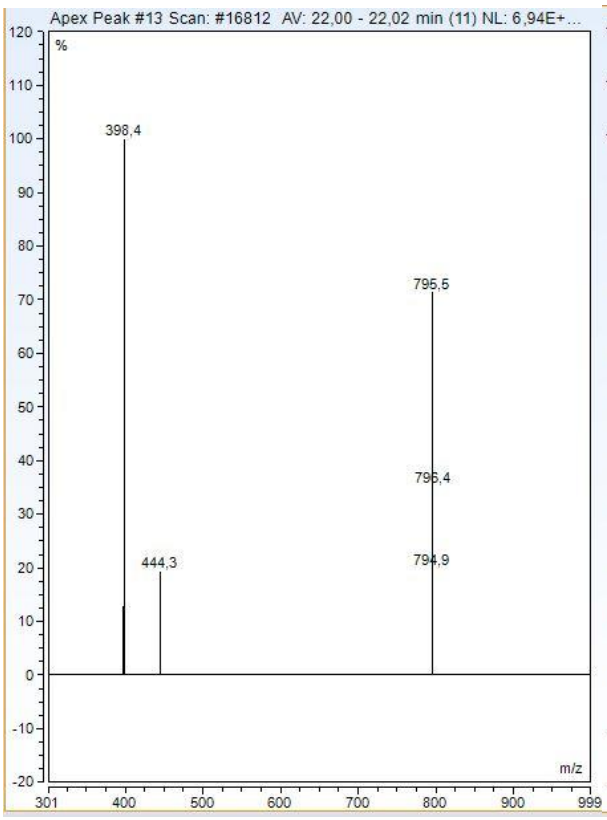

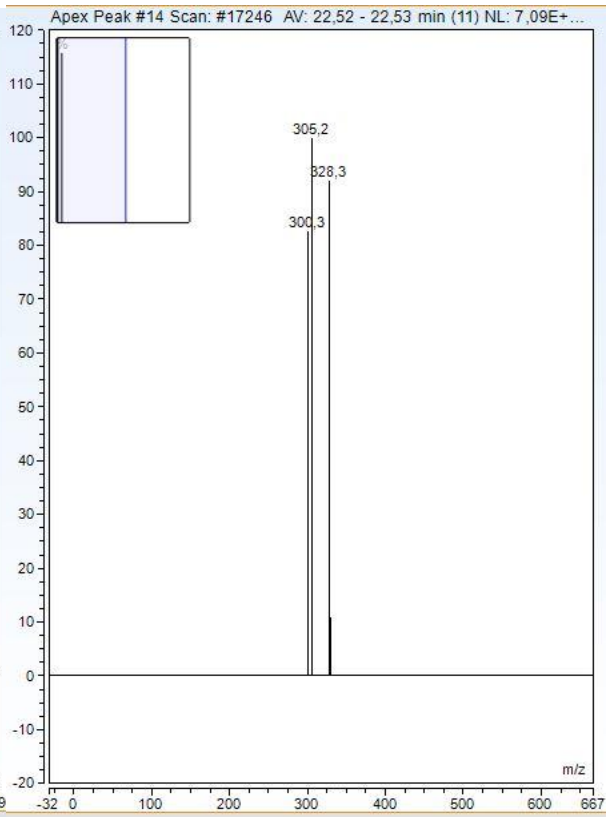

Figure: A_2_37: SP10_peak 13_MS-specter Figure: A_2_38: SP10_peak 14_MS_specter

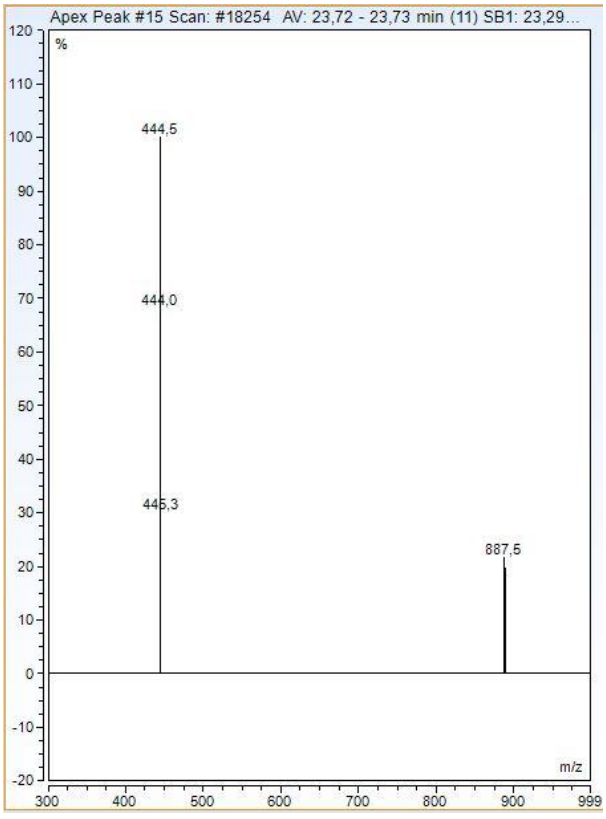

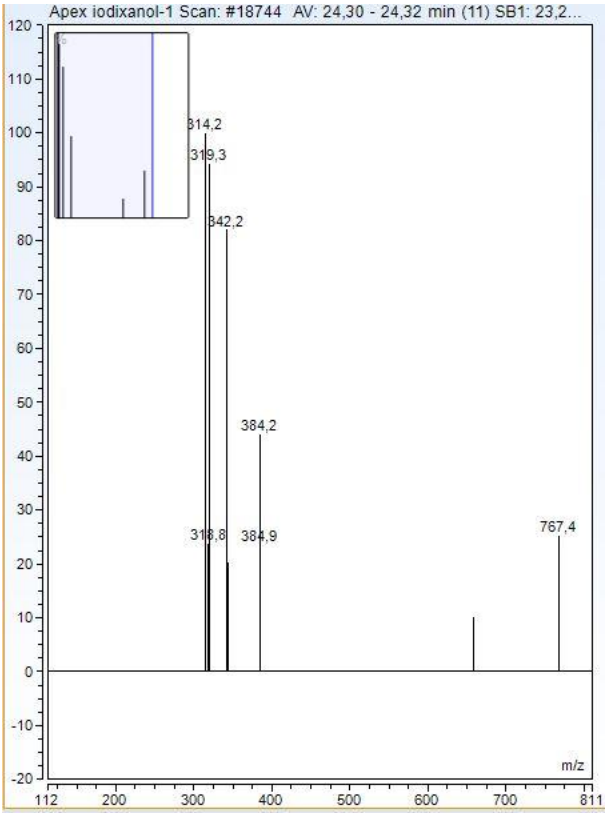

Figure: A_2_39: SP10_peak 15_MS-specter Figure: A_2_40: SP10_peak 16 _MS_specter

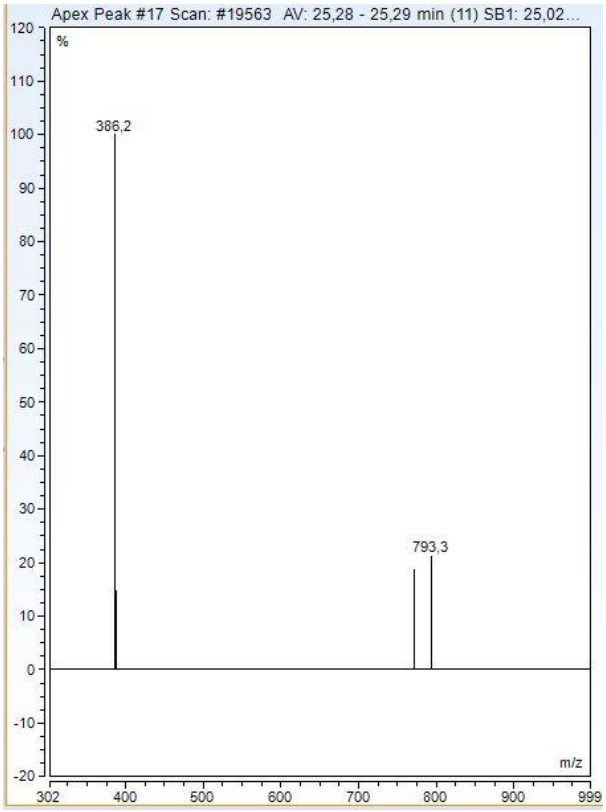

Figure: A_2_41: SP10_peak 17_MS-specter

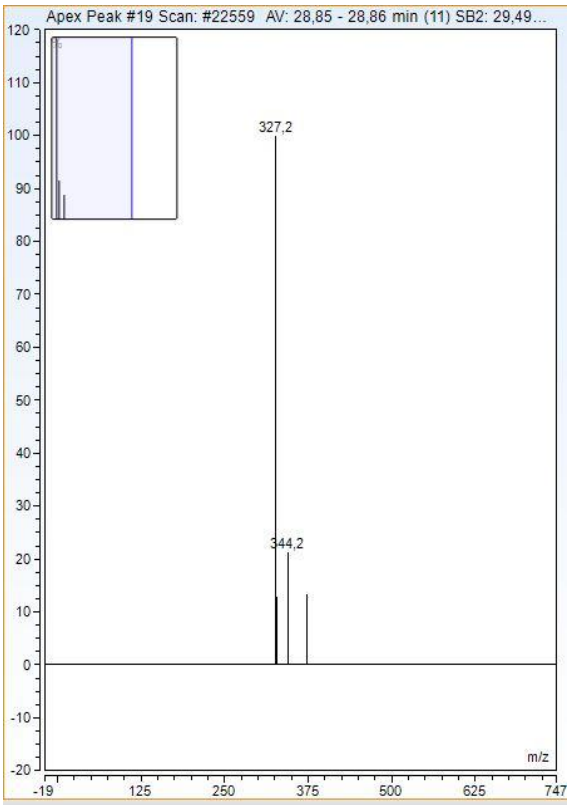

Figure: A_2_42: SP10_peak 18_MS-specter

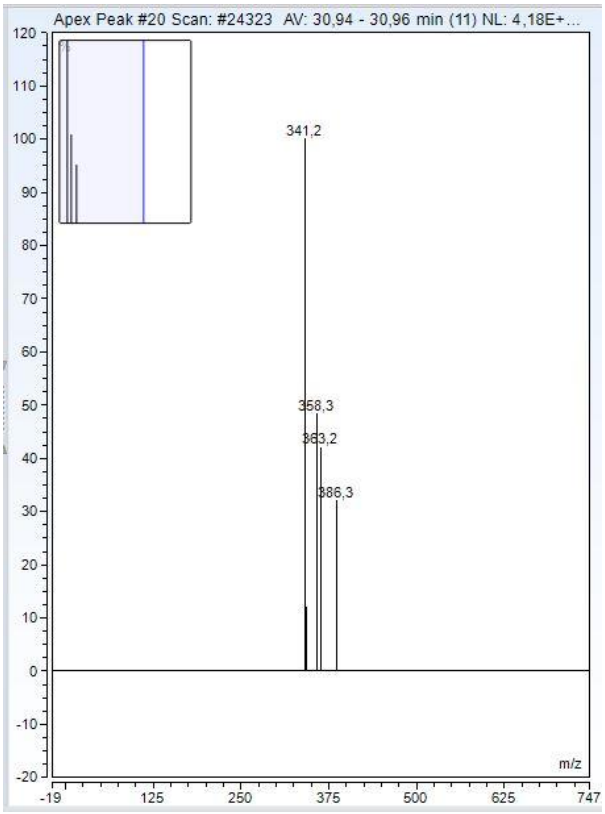

Figure: A_2_43: SP10_peak 19_MS-specter

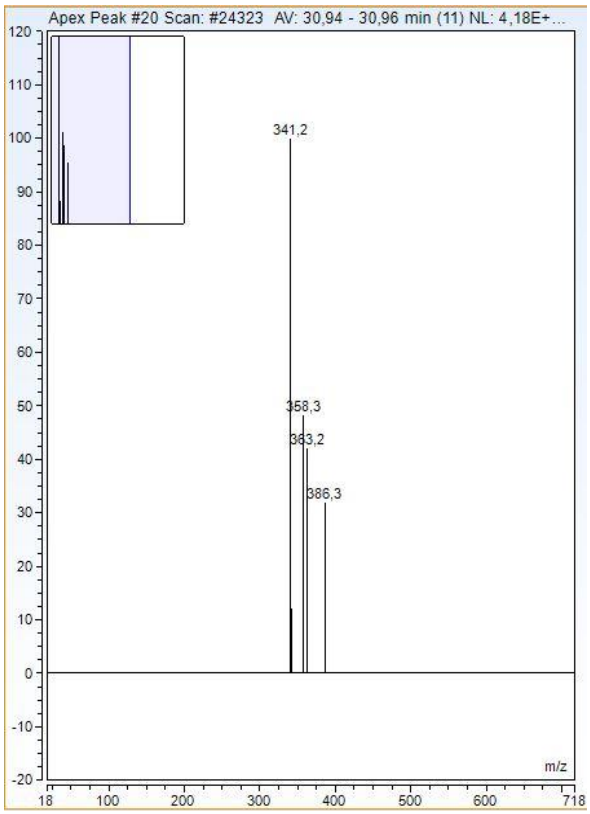

Figure: A_2_44: SP10_peak 20_MS-specter

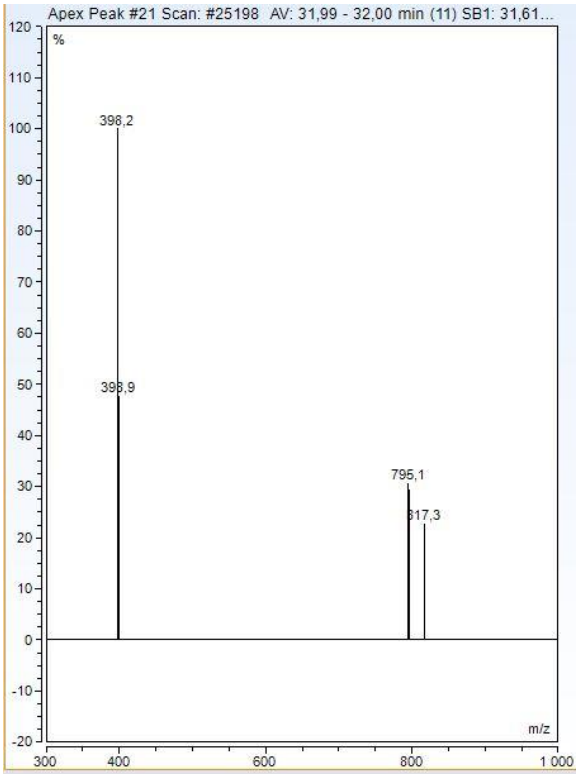

Figure: A_2_45: SP10_peak 21_MS-specter specter

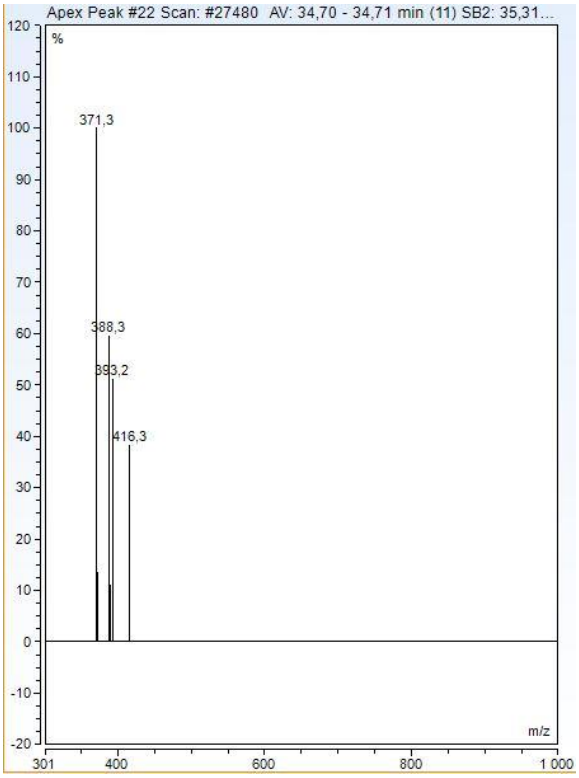

Figure: A_2_46: SP10_peak 22_MS-specter

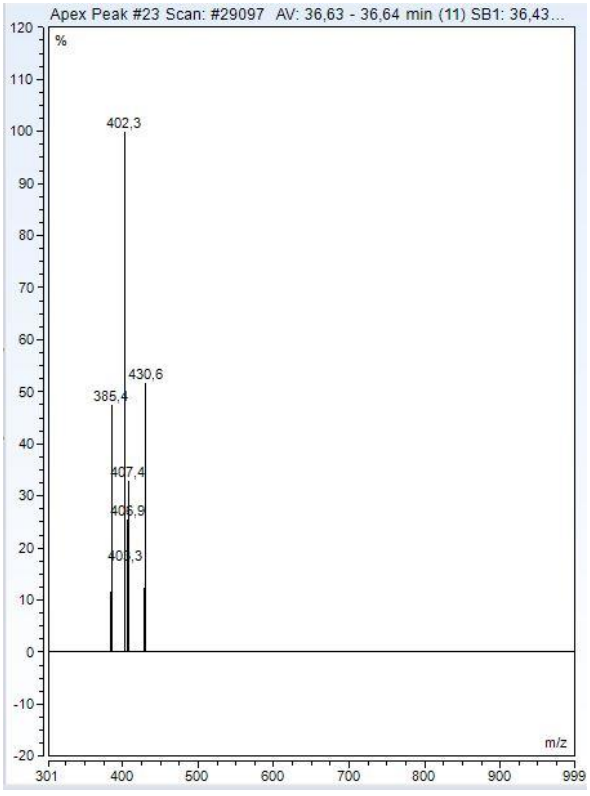

Figure: A_2_46: SP10_peak 23_MS-specter

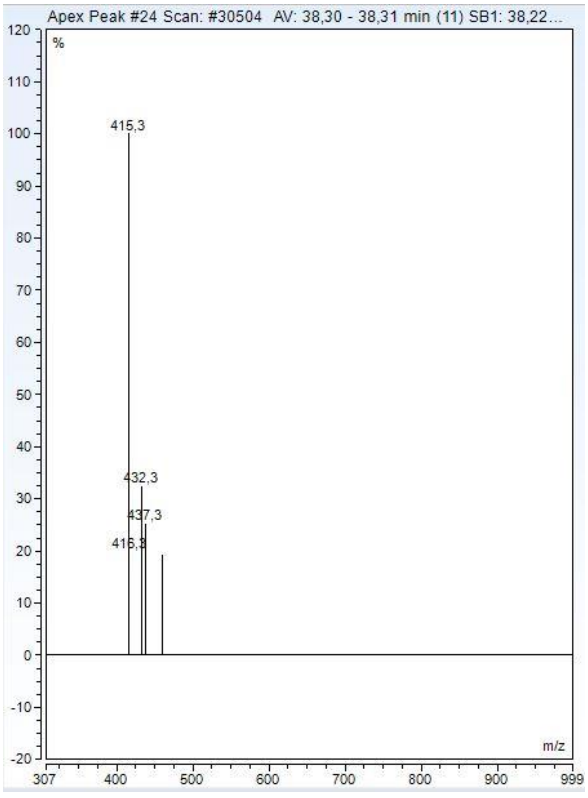

Figure: A_2_47: SP10_peak 24_MS-specter

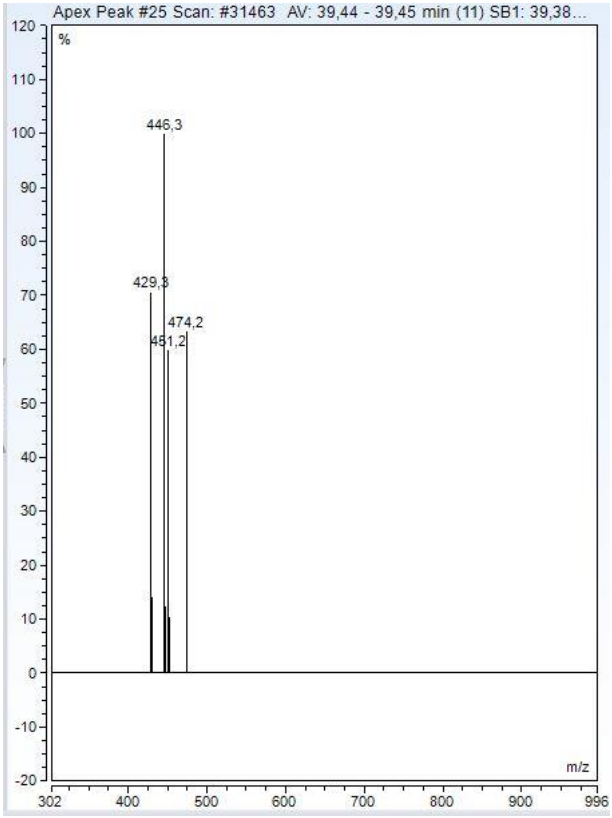

Figure: A_2_46: SP10_peak 25_MS-specter

Peaks TPs SP36 (EGSB 3)

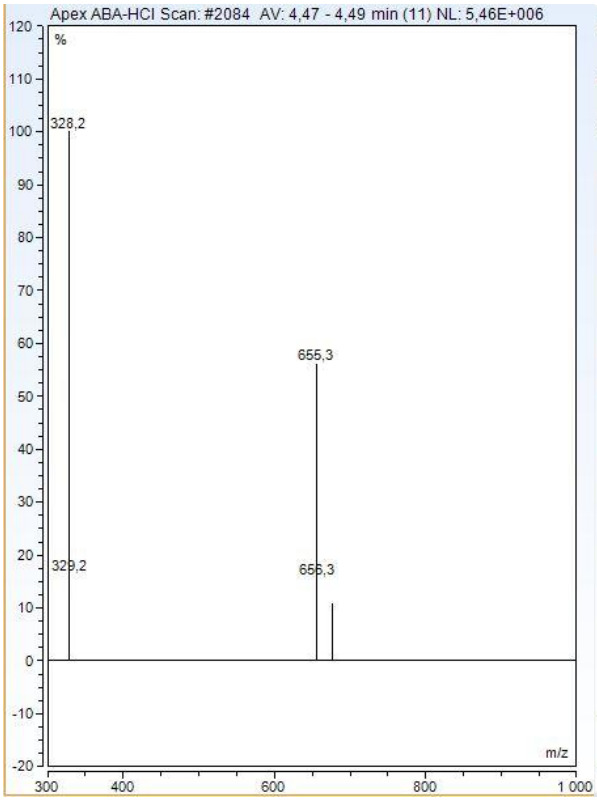

Figure: A_2_47: SP36_peak 1_MS-specter

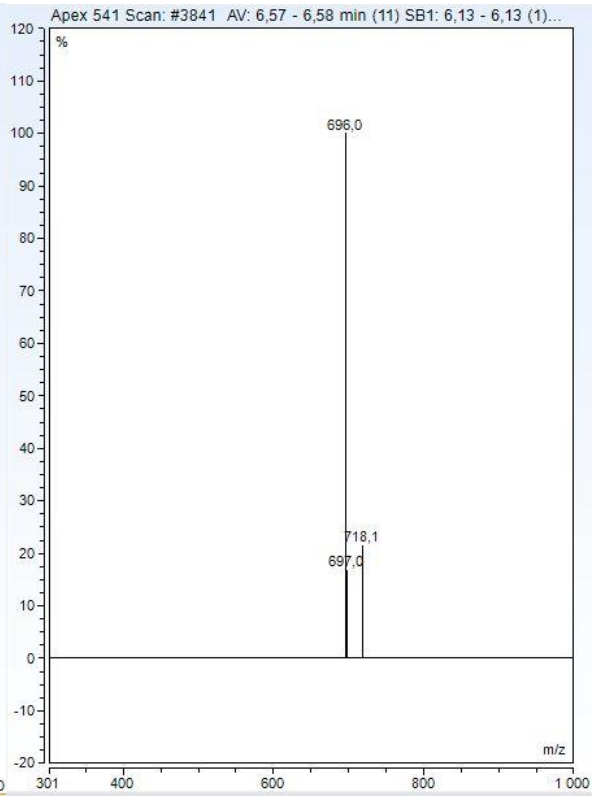

Figure: A_2_48: SP36_peak 2_MS-specter

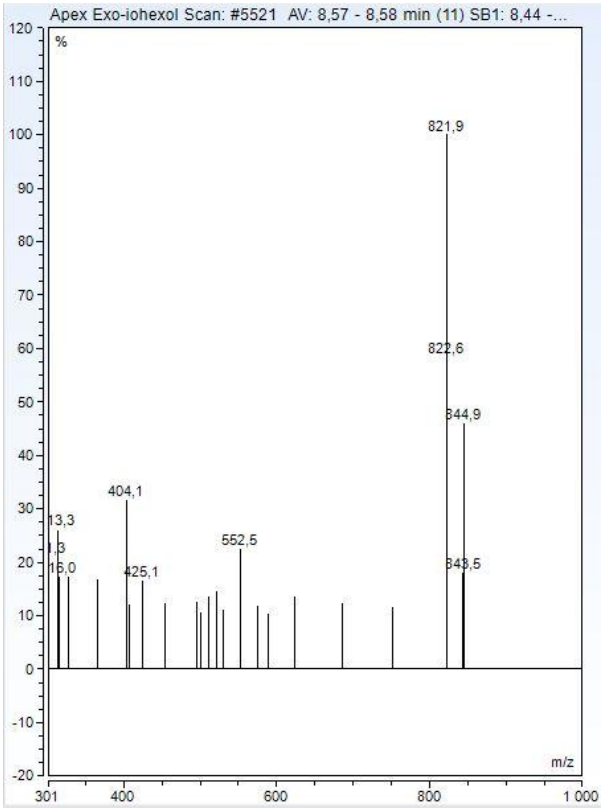

Figure: A_2_49: SP36_peak 3_MS-specter

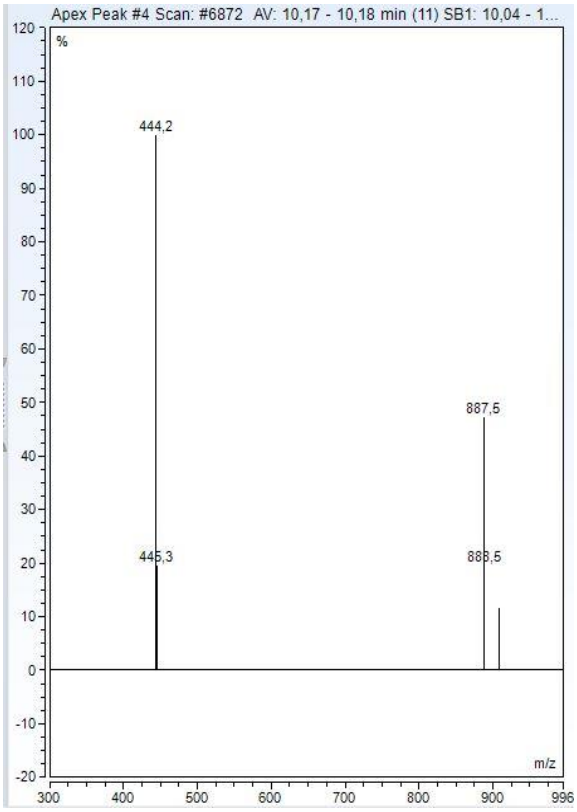

Figure: A_2_50: SP36_peak 4_MS-specter

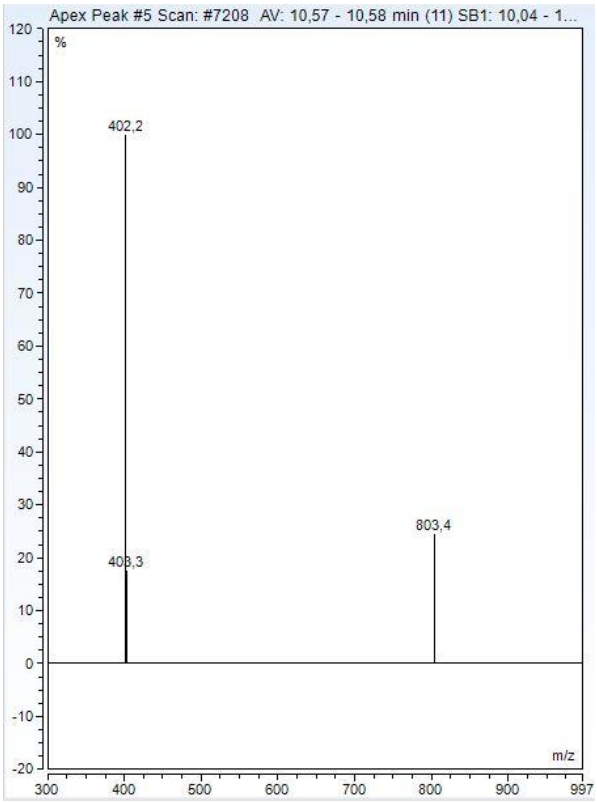

Figure: A_2_51: SP36_peak 5_MS-specter

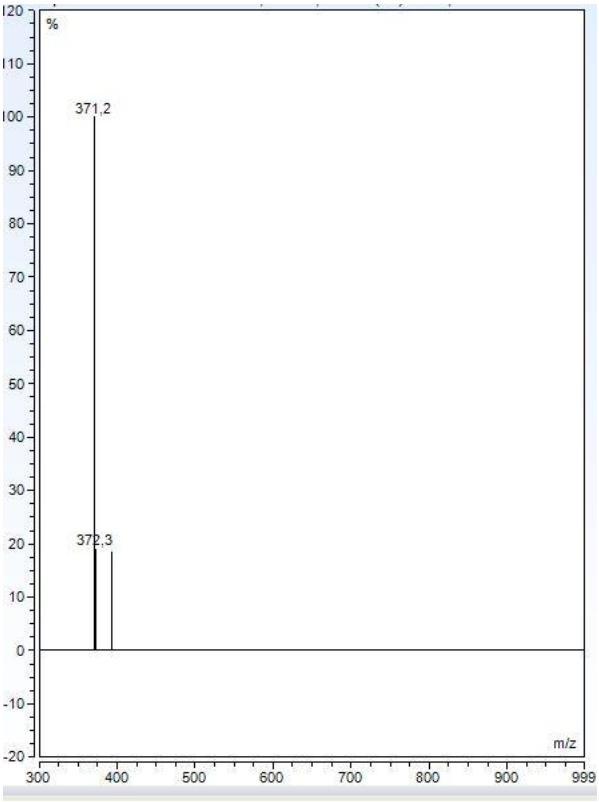

Figure: A_2_52: SP36_peak 6_MS-specter

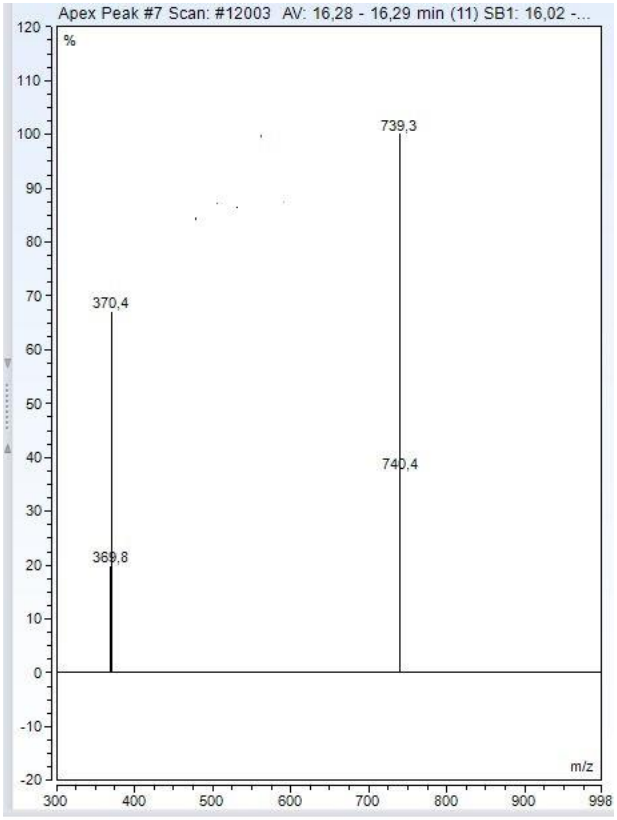

Figure: A_2_53: SP36_peak 6_MS-specter

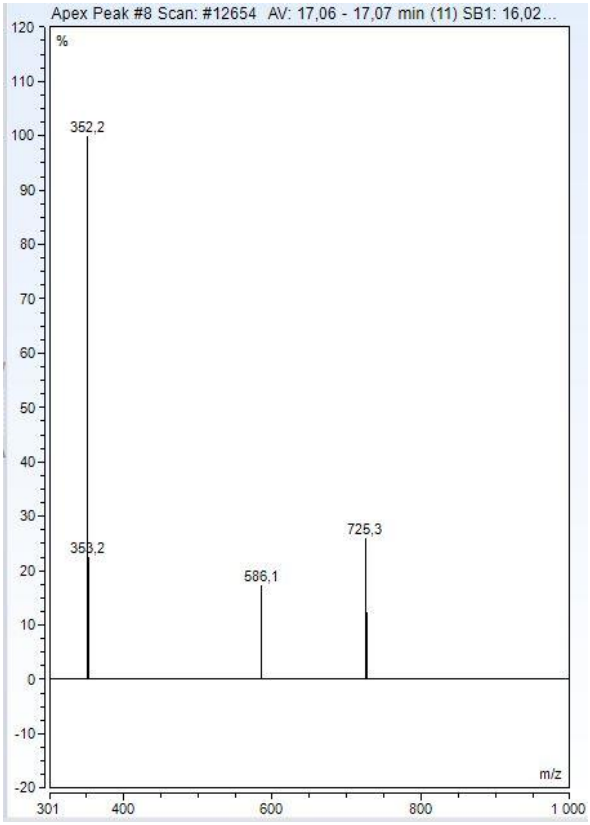

Figure: A_2_54: SP36_peak 7_MS-specter

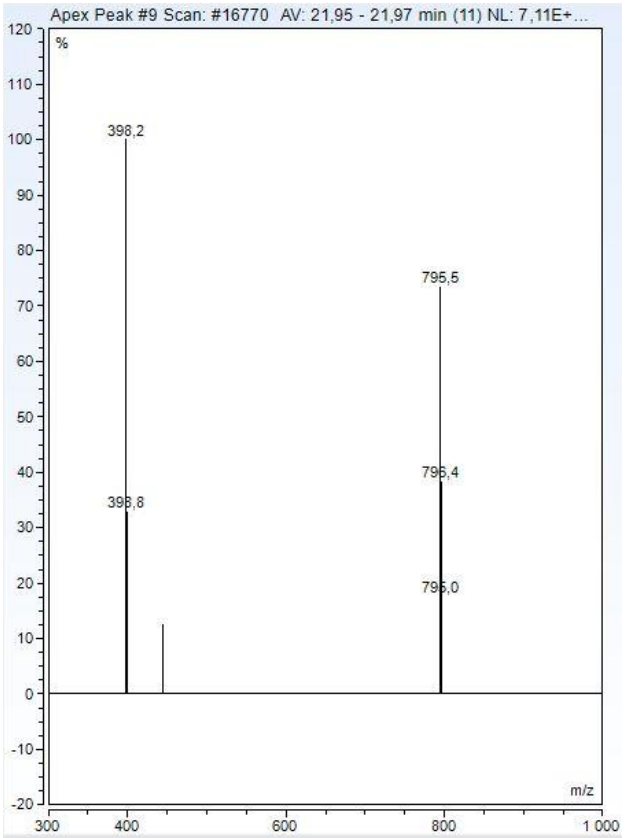

Figure: A_2_55: SP36_peak 8_MS-specter

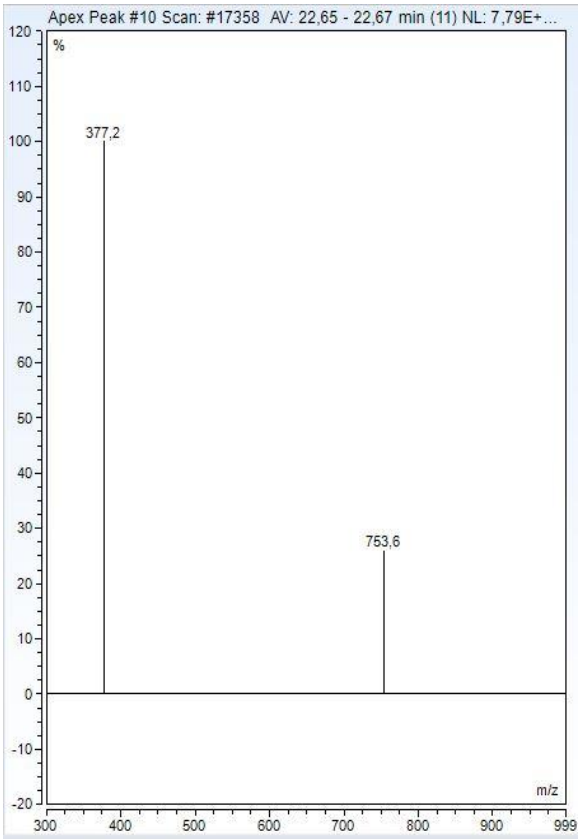

Figure: A_2_56: SP36_peak 9_MS-specter

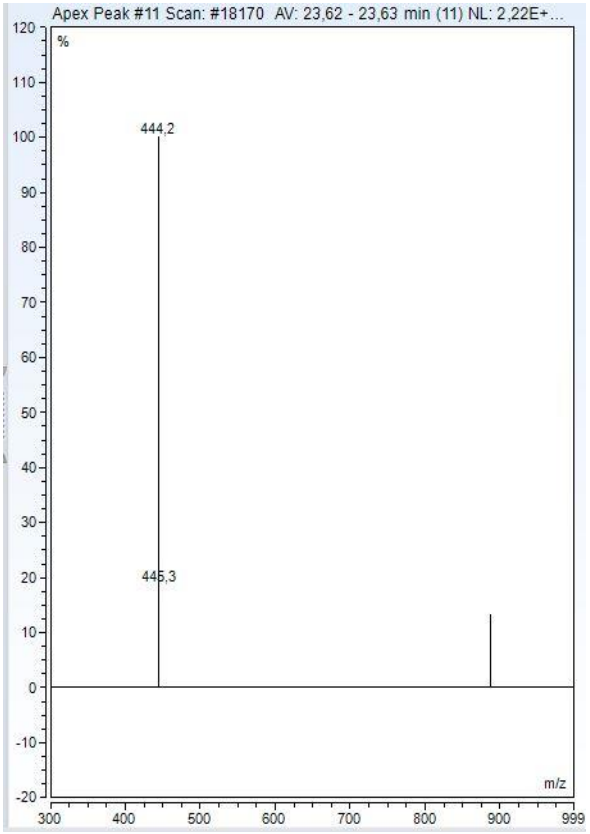

Figure: A_2_57: SP36_peak 10_MS-specter

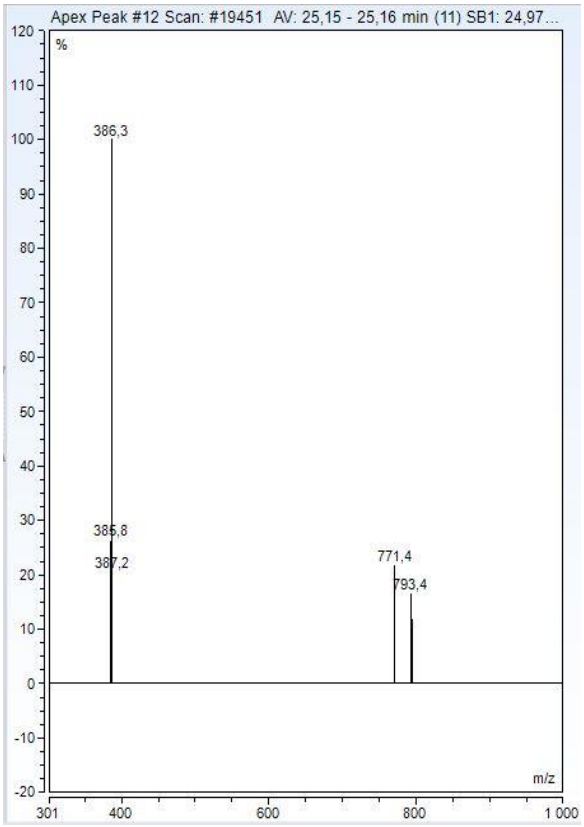

Figure: A_2_58: SP36_peak 11_MS-specter

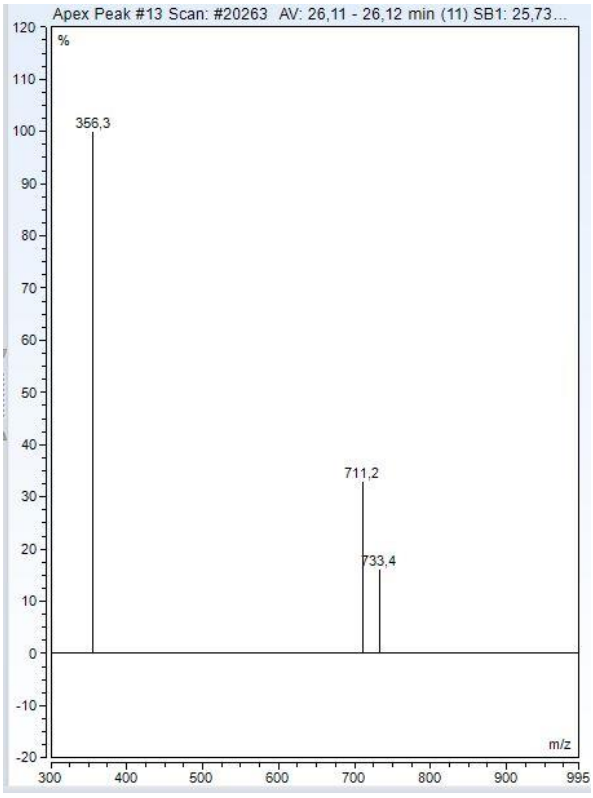

Figure: A_2_59: SP36_peak 12_MS-specter

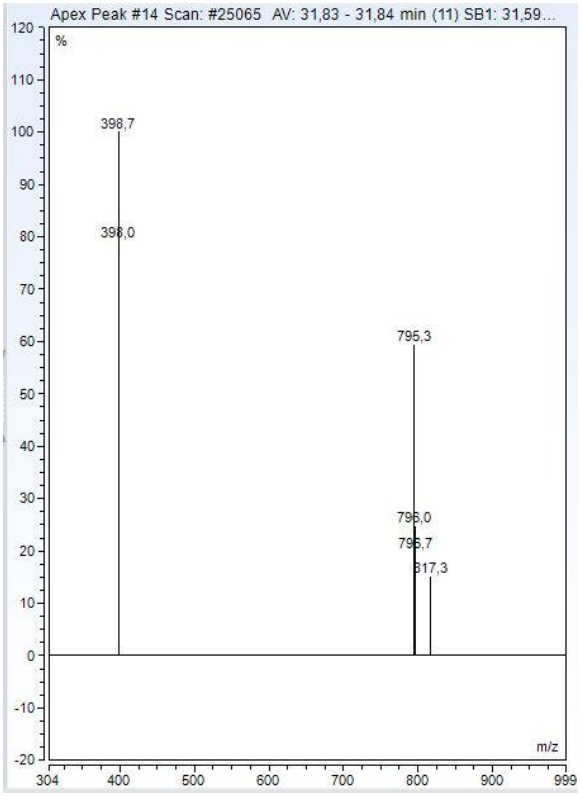

Figure: A_2_60: SP36_peak 13_MS-specter

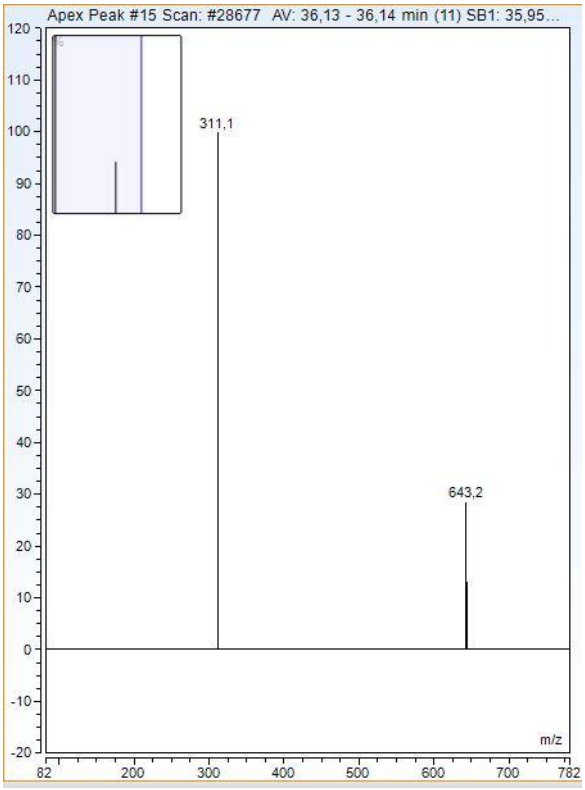

Figure: A_2_61: SP36_peak 14_MS-specter

Peaks TPs SP29

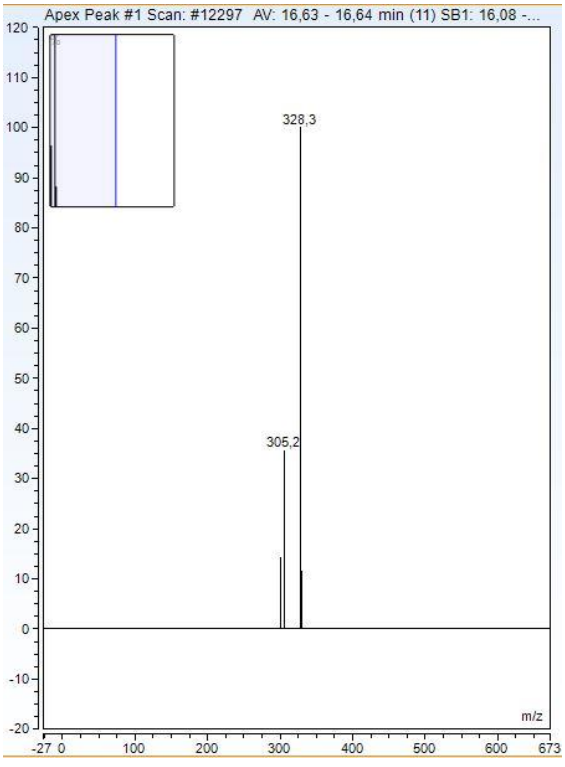

Figure: A_2_62: SP29_peak 1_MS-specter

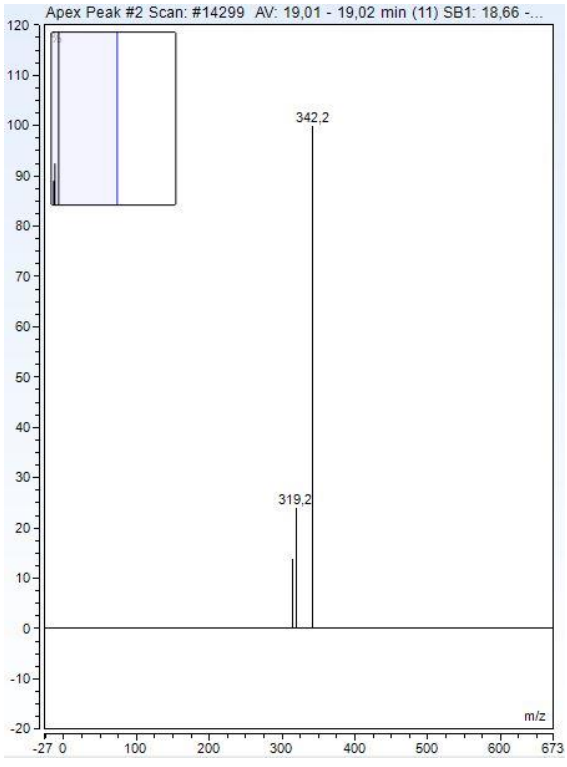

Figure: A_2_63: SP29_peak 2_MS-specter

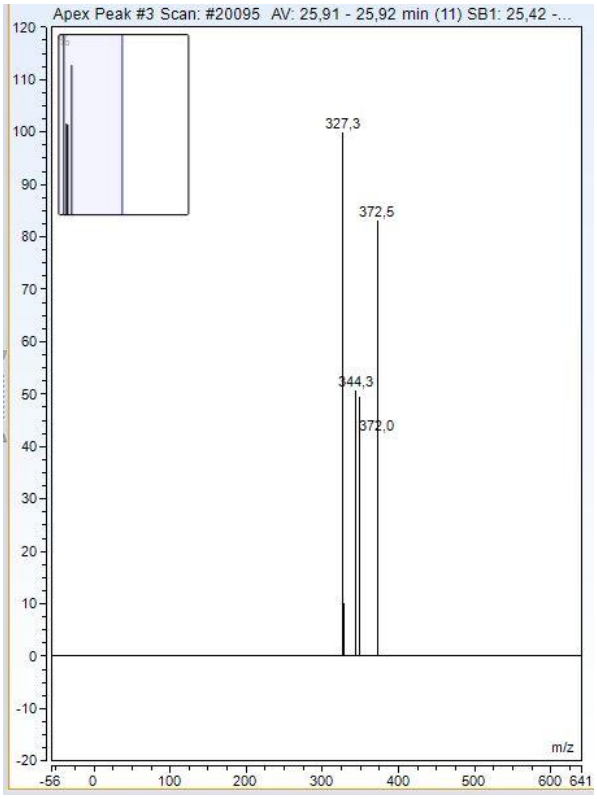

Figure: A_2_64: SP29_peak 3_MS-specter

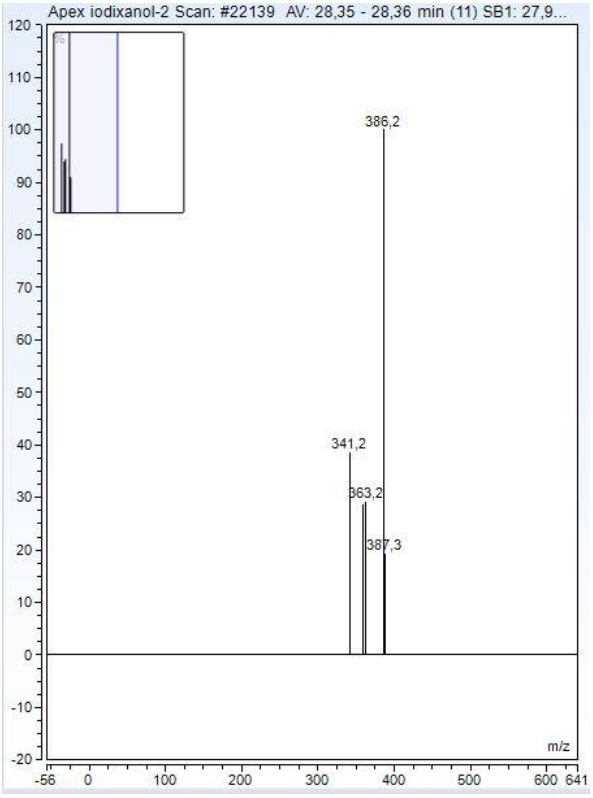

Figure: A_2_65: SP29_peak 4_MS-specter

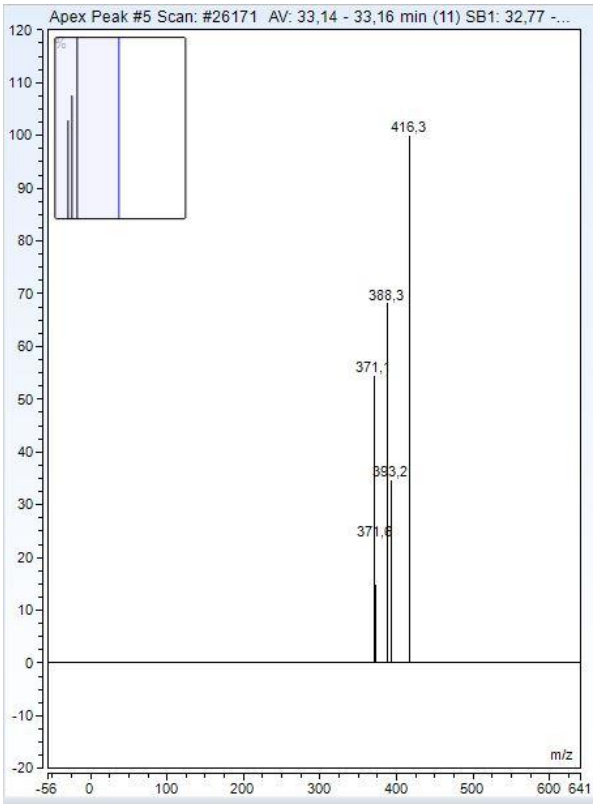

Figure: A_2_65: SP29_peak 5_MS-specter

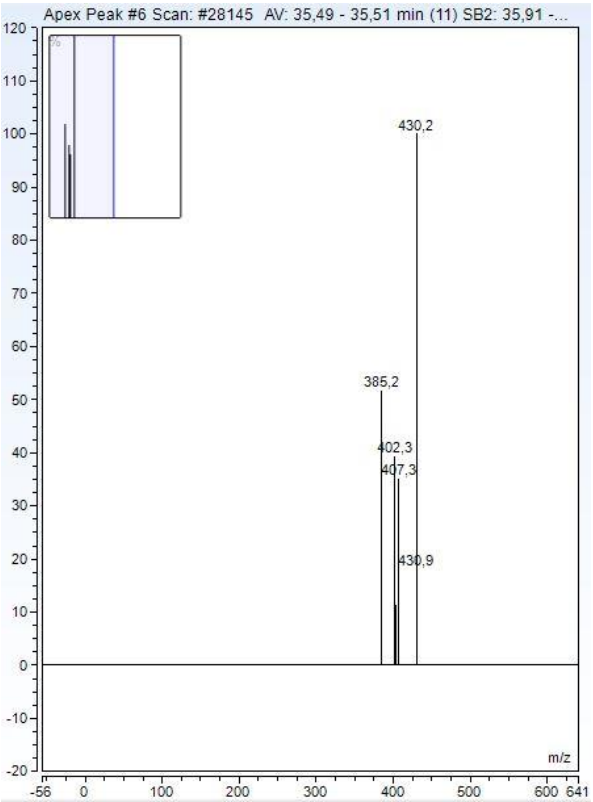

Figure: A_2_66: SP29_peak 6_MS-specter

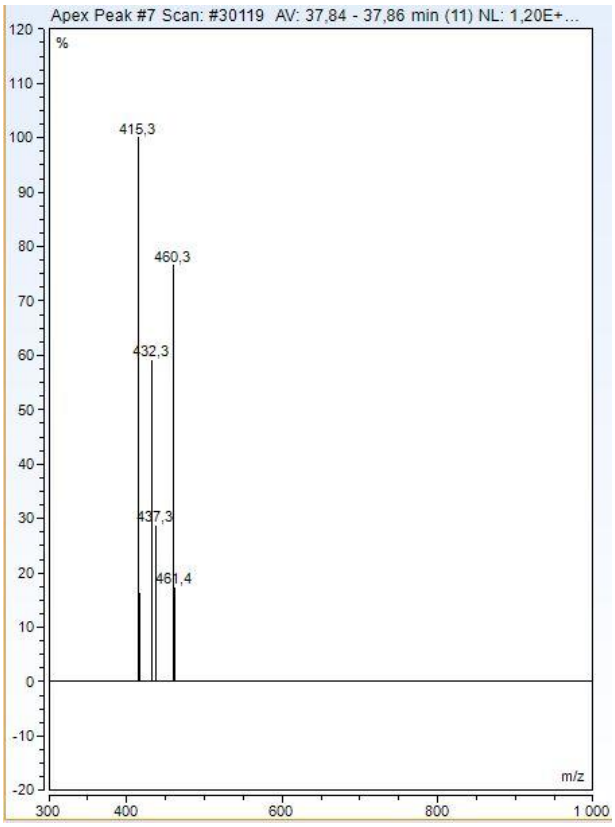

Figure: A_2_67: SP29_peak 7_MS-specter

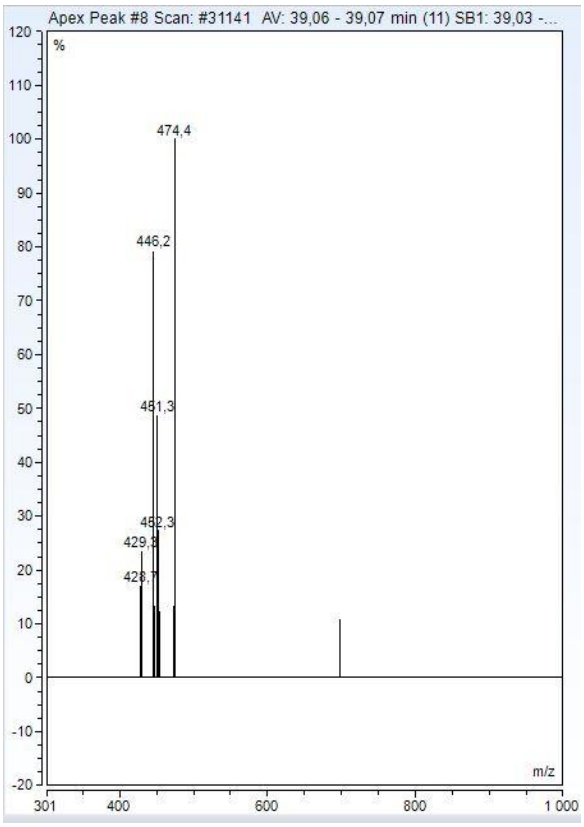

Figure: A_2_68: SP29_peak 8_MS-specter

Peaks TPs SP39 (effluent all EGSBs)

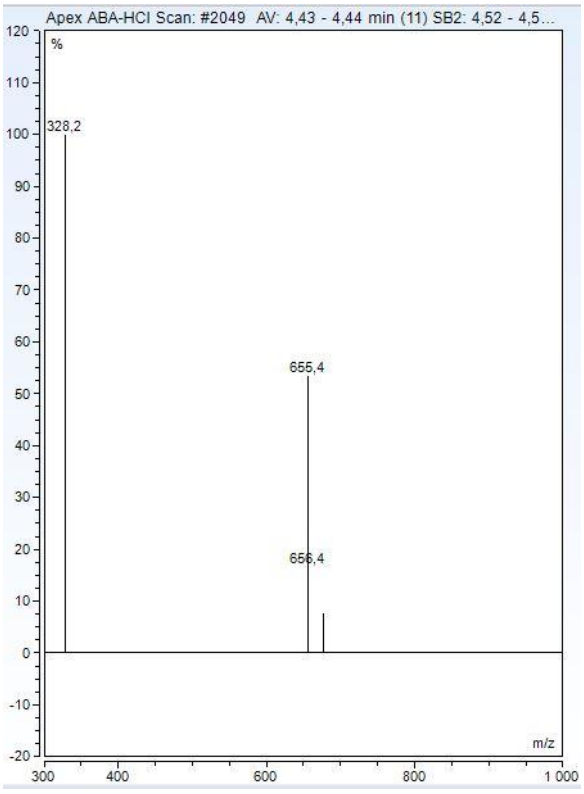

Figure: A_2_69: SP39_peak 1_MS-specter

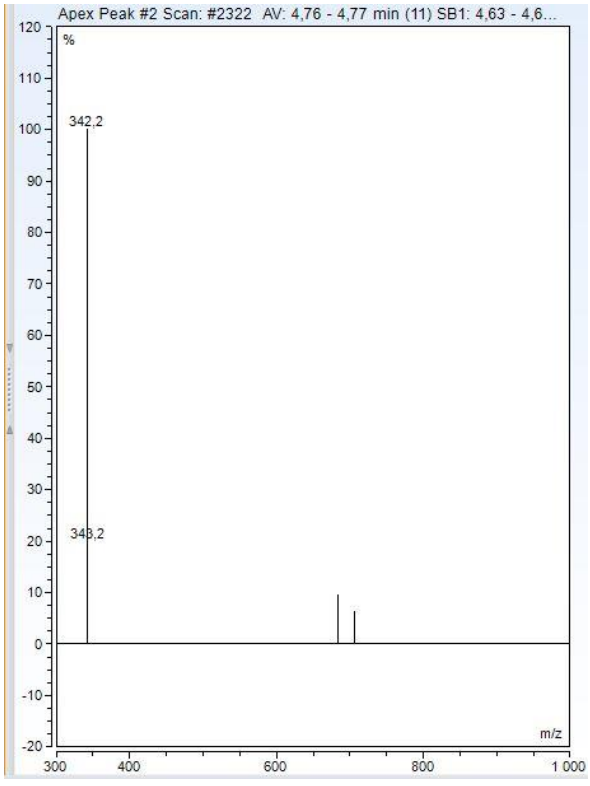

Figure: A_2_70: SP39_peak 2_MS-specter

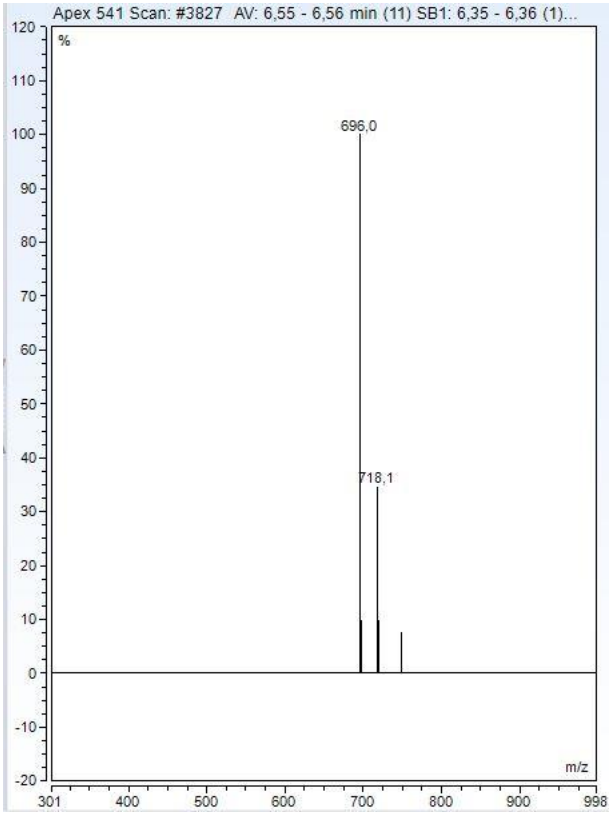

Figure: A_2_71: SP39_peak 3_MS-specter

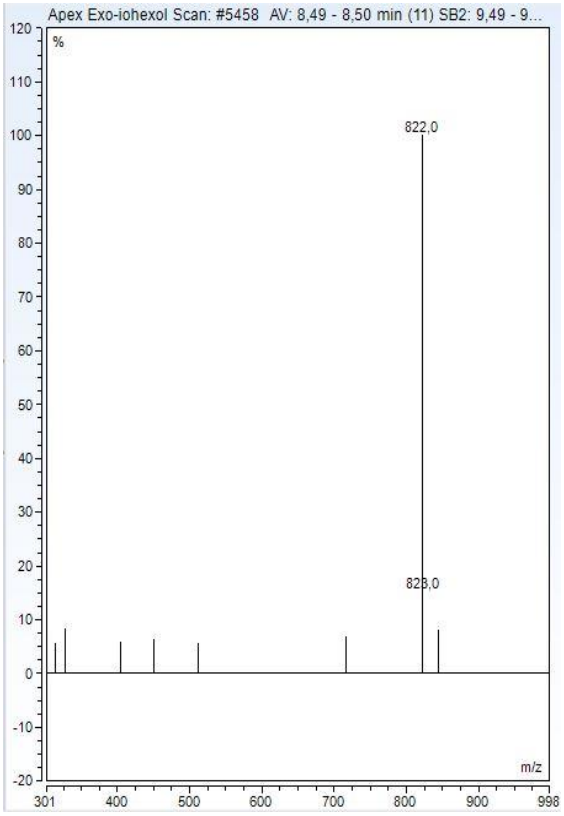

Figure: A_2_72: SP39_peak 4_MS-specter

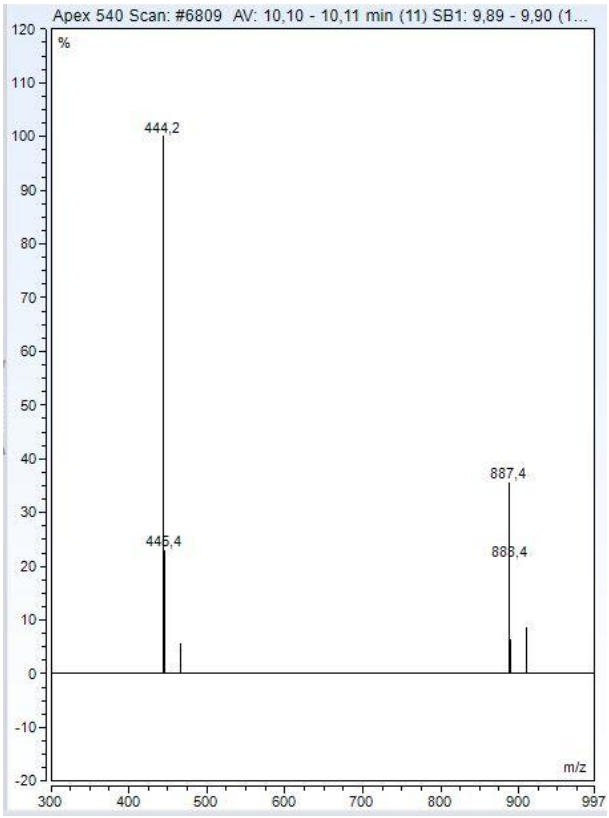

Figure: A_2_73: SP39_peak 5_MS-specter

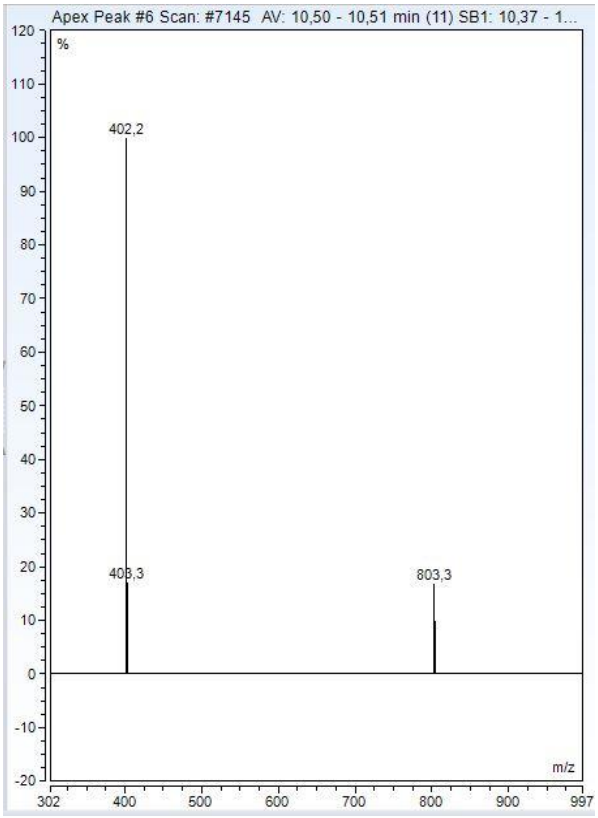

Figure: A_2_74: SP39_peak 6_MS-specter

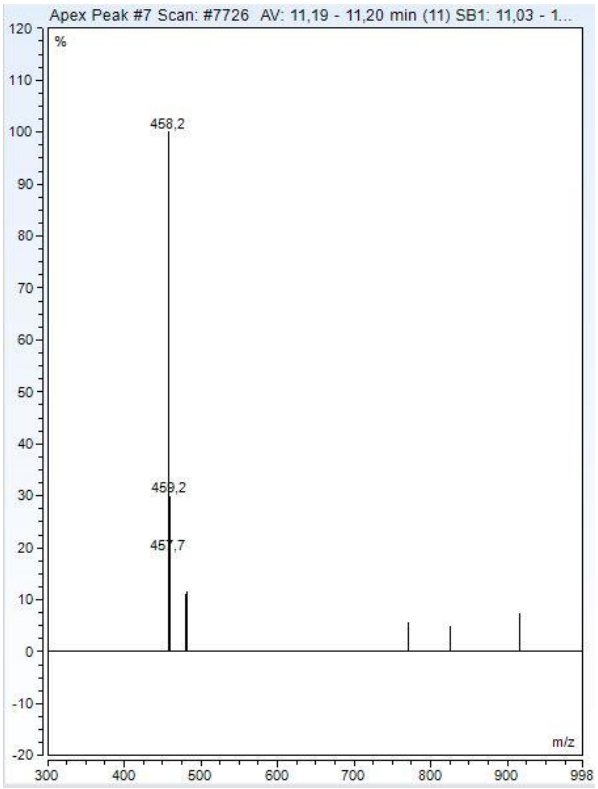

Figure: A_2_75: SP39_peak 7_MS-specter

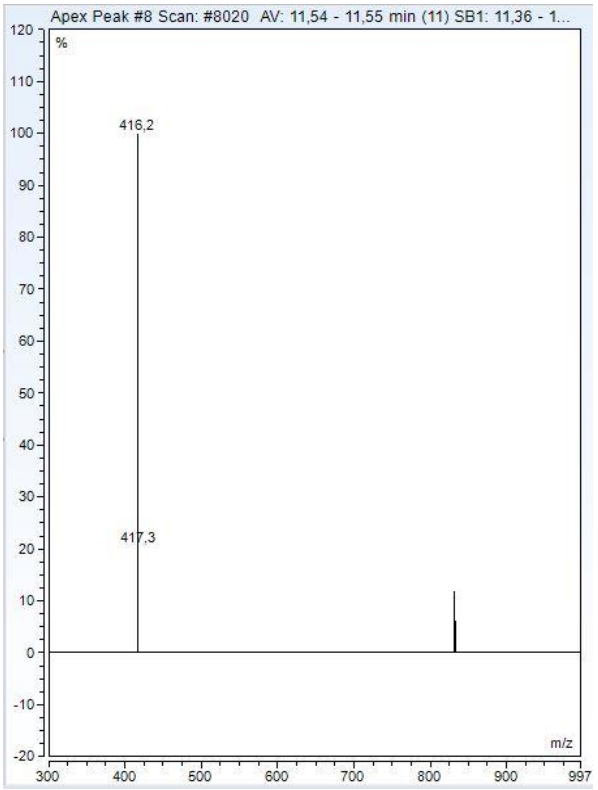

Figure: A_2_76: SP39_peak 8_MS-specter

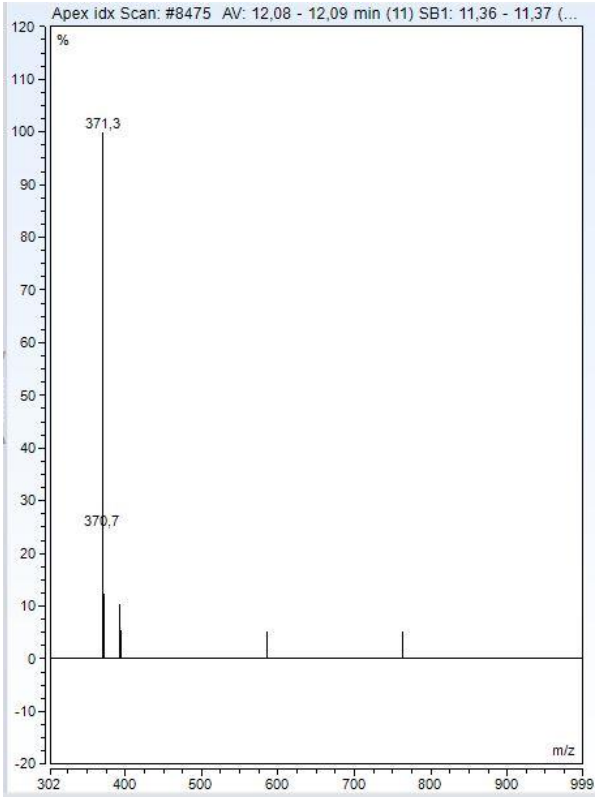

Figure: A_2_77: SP39_peak 9_MS-specter

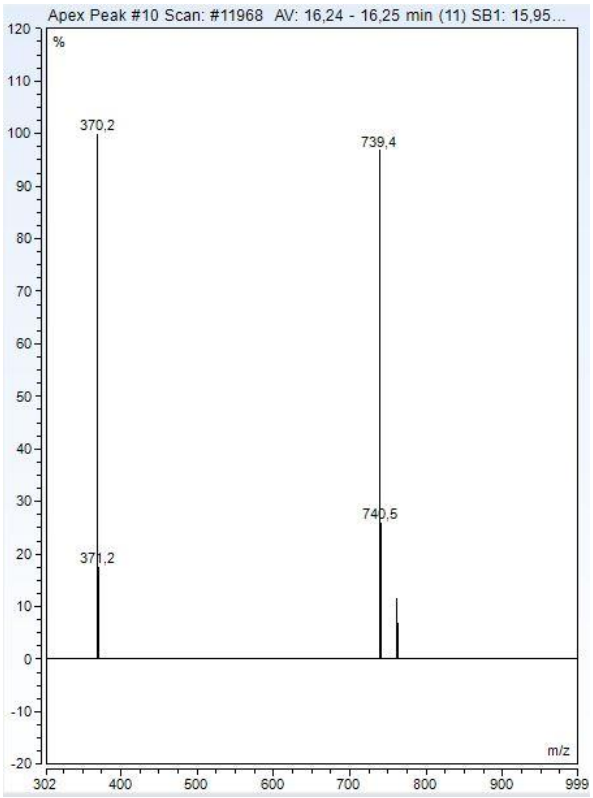

Figure: A_2_78: SP39_peak 10_MS-specter

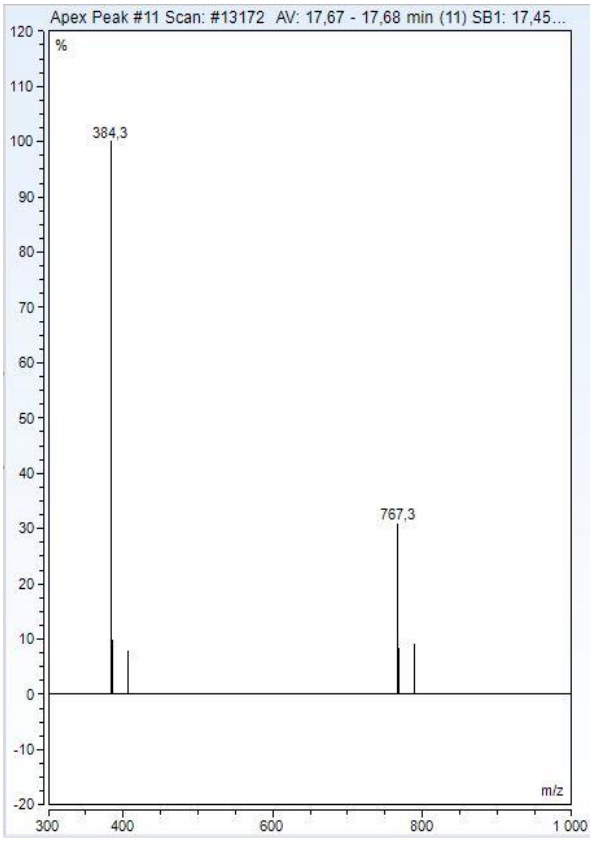

Figure: A_2_79: SP39_peak 11_MS-specter

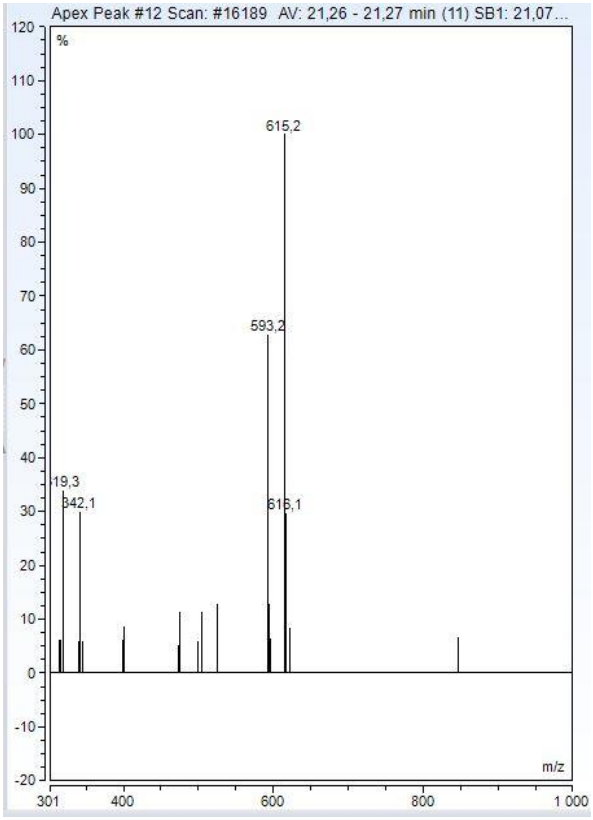

Figure: A_2_80: SP39_peak 12_MS-specter

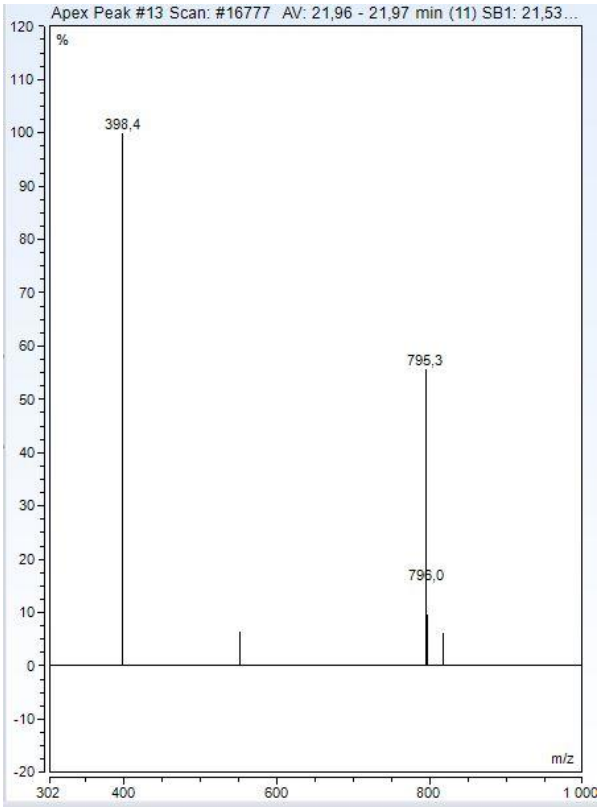

Figure: A_2_81: SP39_peak 13_MS-specter

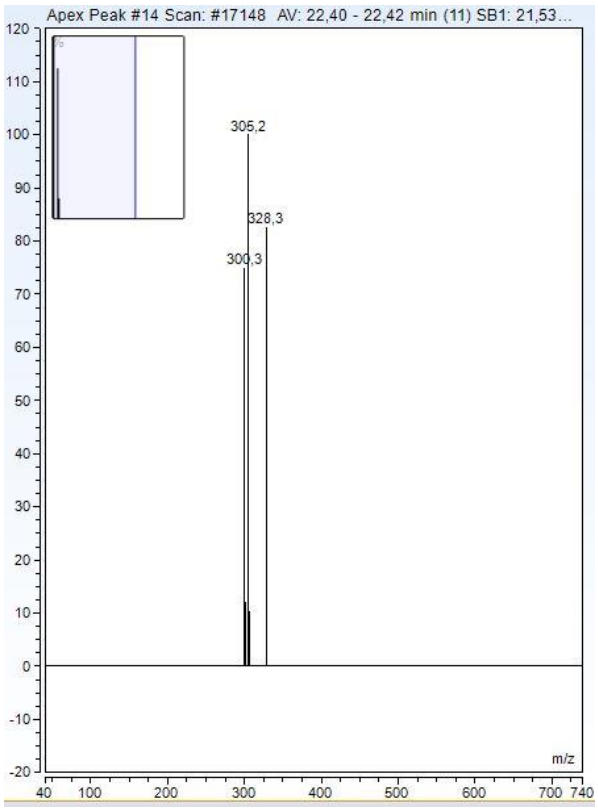

Figure: A_2_82: SP39_peak 14_MS-specter

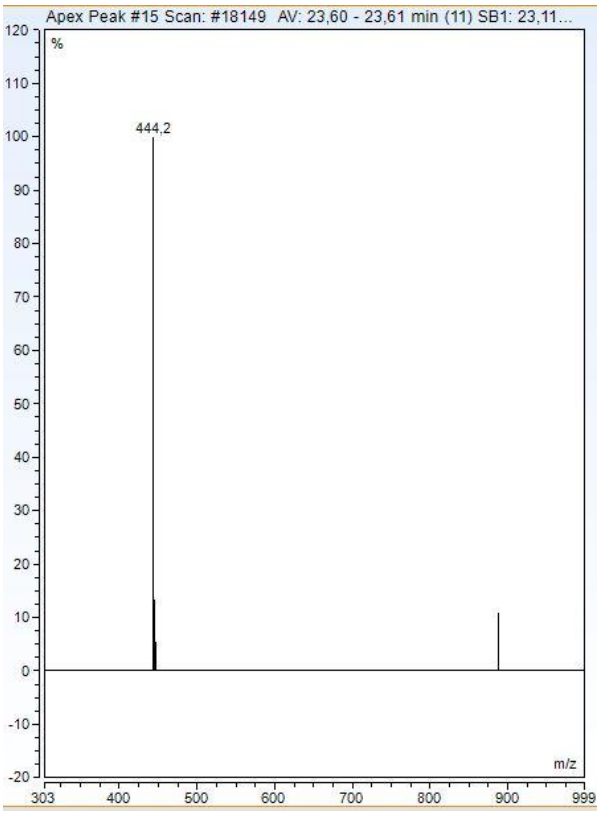

Figure: A_2_83: SP39_peak 15_MS-specter

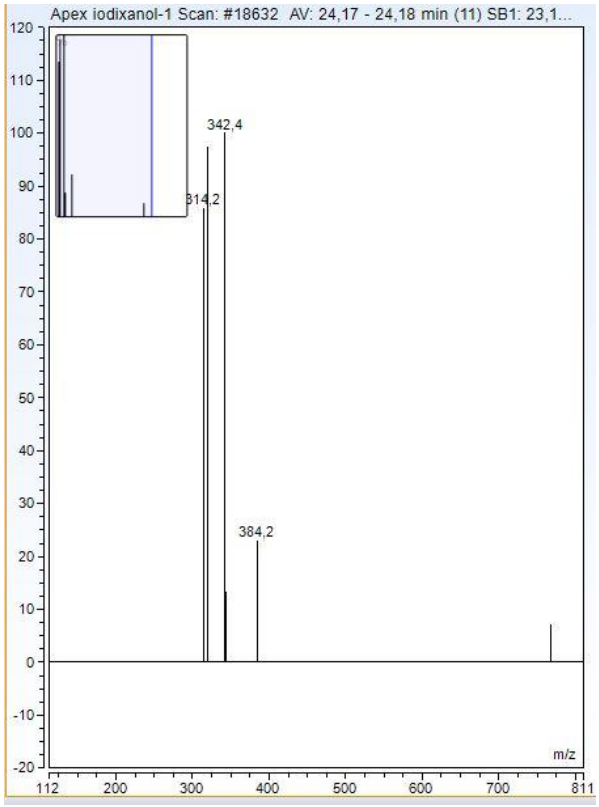

Figure: A_2_84: SP39_peak 16_MS-specter

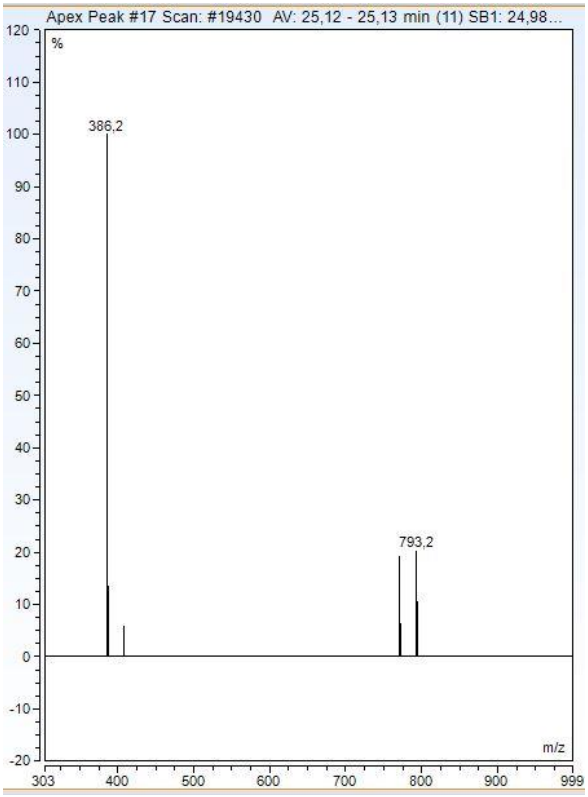

Figure: A_2_85: SP39_peak 17_MS-specter

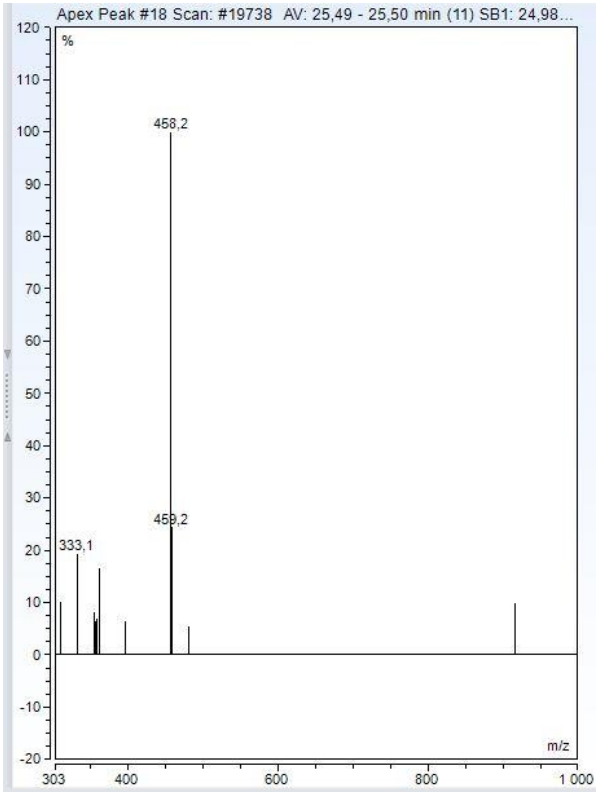

Figure: A_2_86: SP39_peak 18_MS-specter

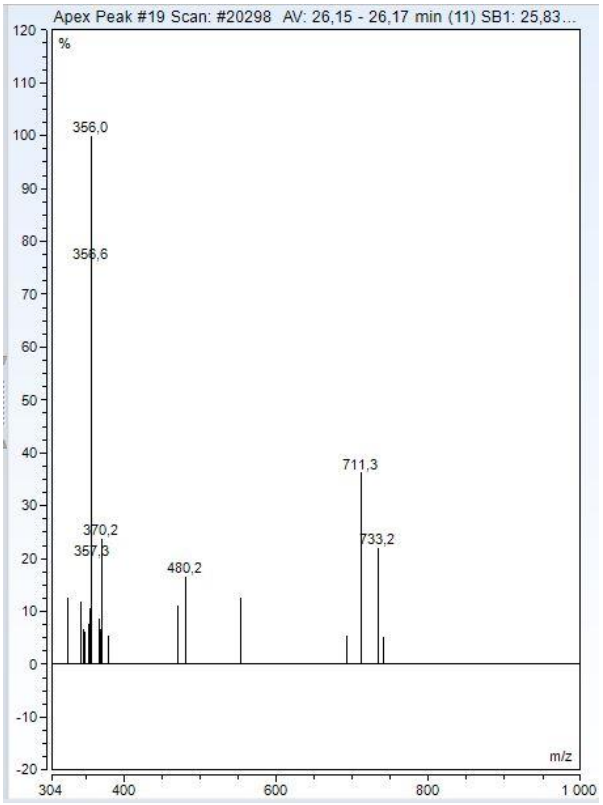

Figure: A_2_87: SP39_peak 19_MS-specter

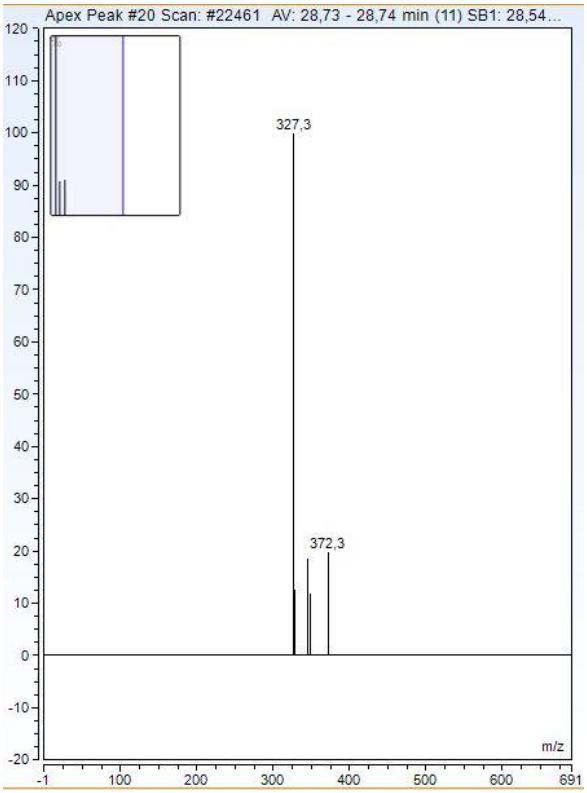

Figure: A_2_88: SP39_peak 20_MS-specter

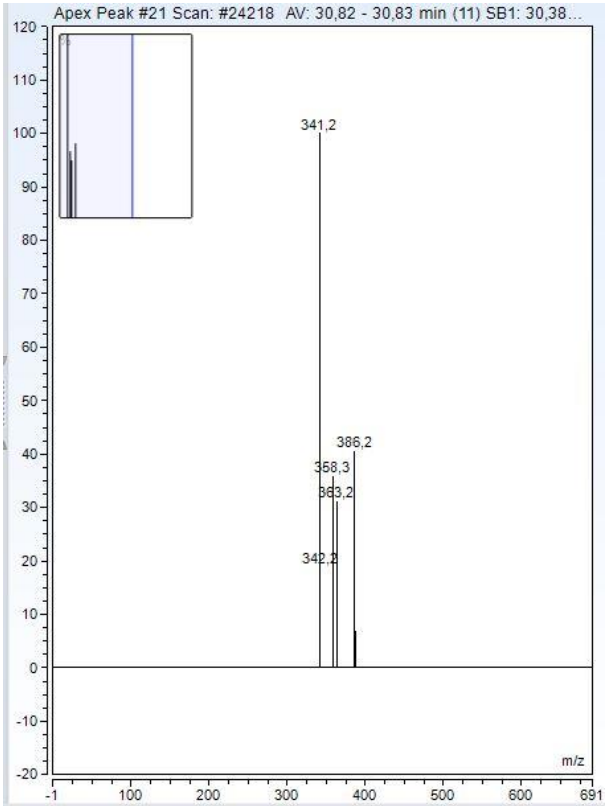

Figure: A_2_89: SP39_peak 21_MS-specter

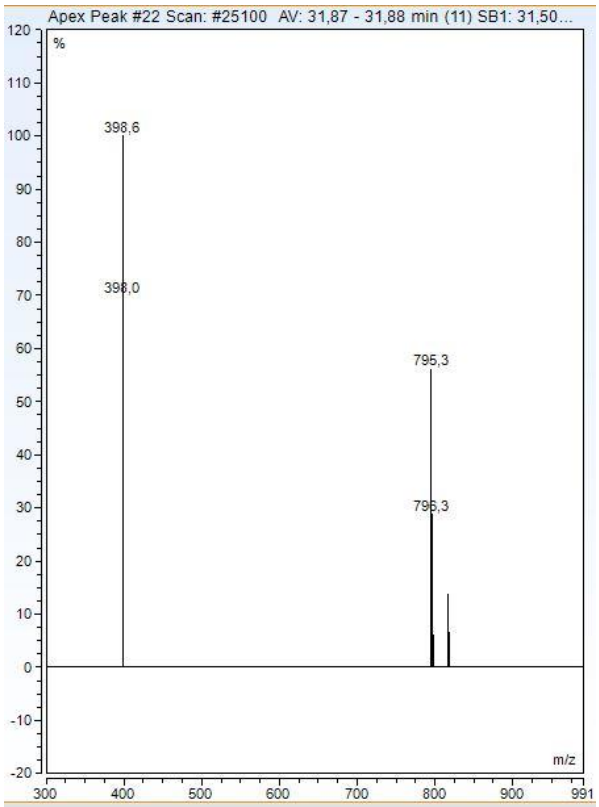

Figure: A_2_90: SP39_peak 22_MS-specter

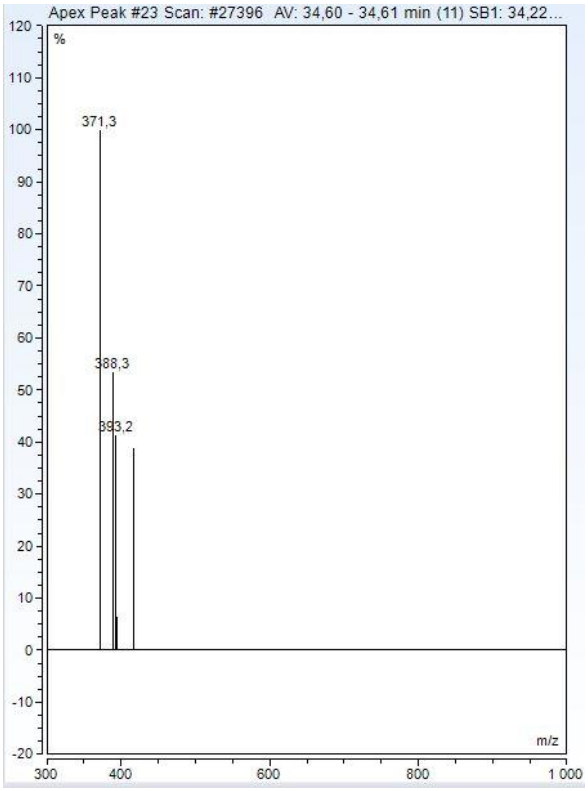

Figure: A_2_91: SP39_peak 23_MS-specter

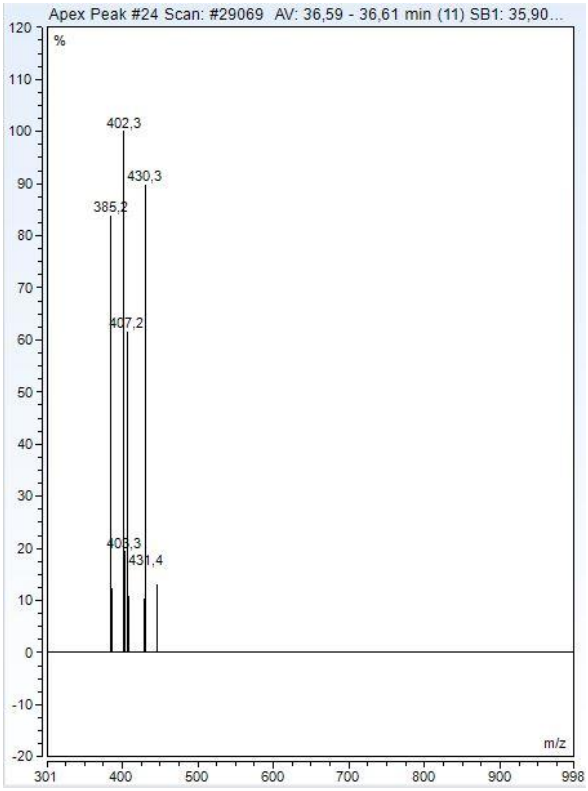

Figure: A_2_92: SP39_peak 24_MS-specter

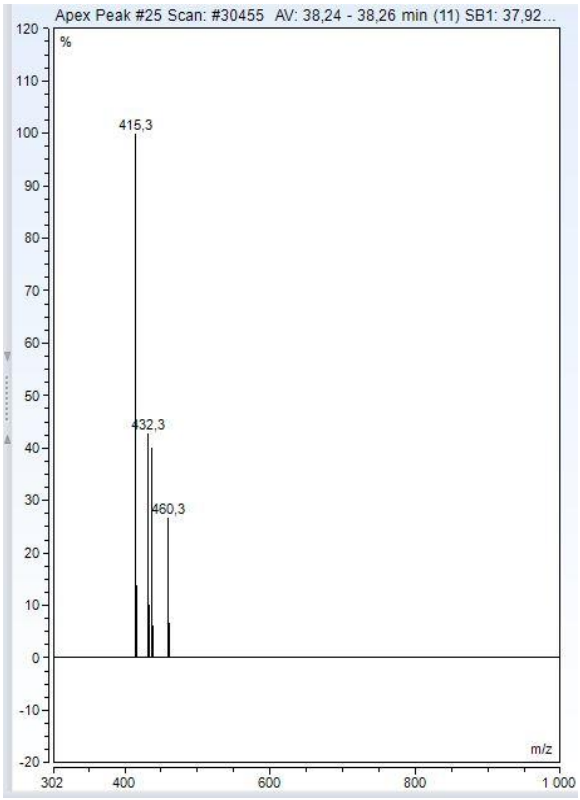

Figure: A_2_93: SP3_peak 25_MS-specter

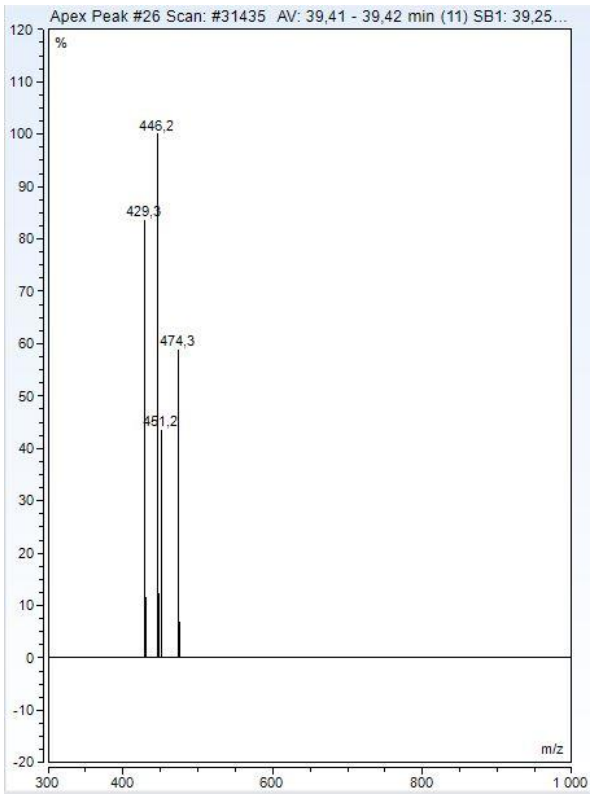

Figure: A_2_94: SP3_peak 26_MS-specter

Peaks TPs in SP3 (BC70/71 feedtank)

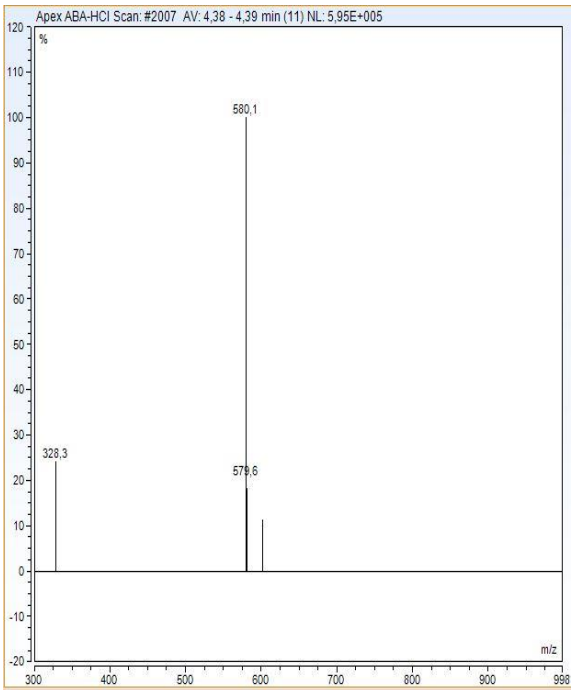

Figure: A_2_96: SP3_peak 1_MS-specter

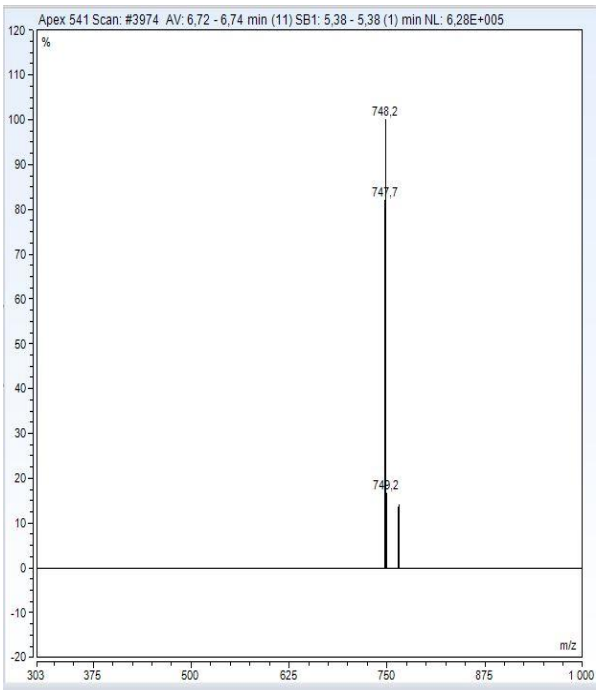

Figure: A_2_97: SP3_peak 2_MS-specter

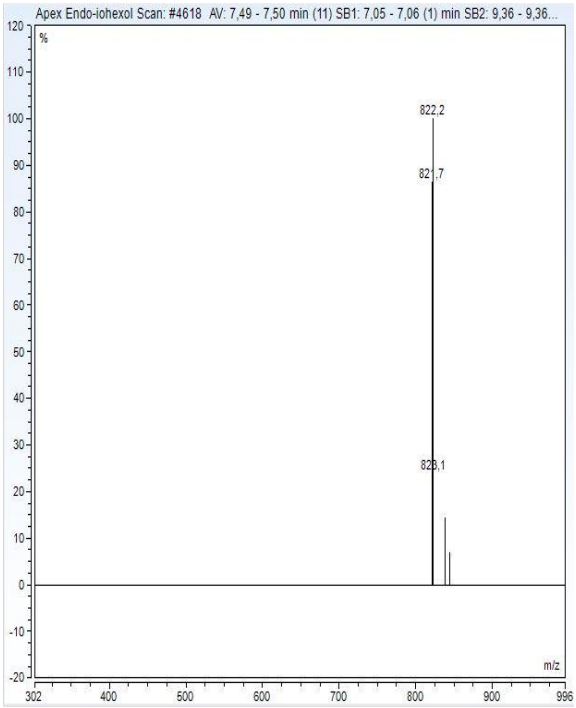

Figure: A_2_98: SP3_peak 3_MS-specter

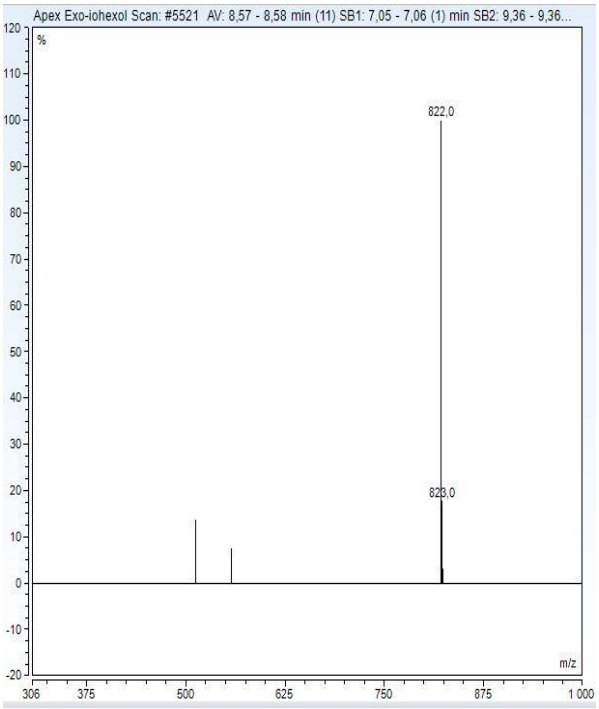

Figure: A_2_99: SP3_peak 4_MS-specter

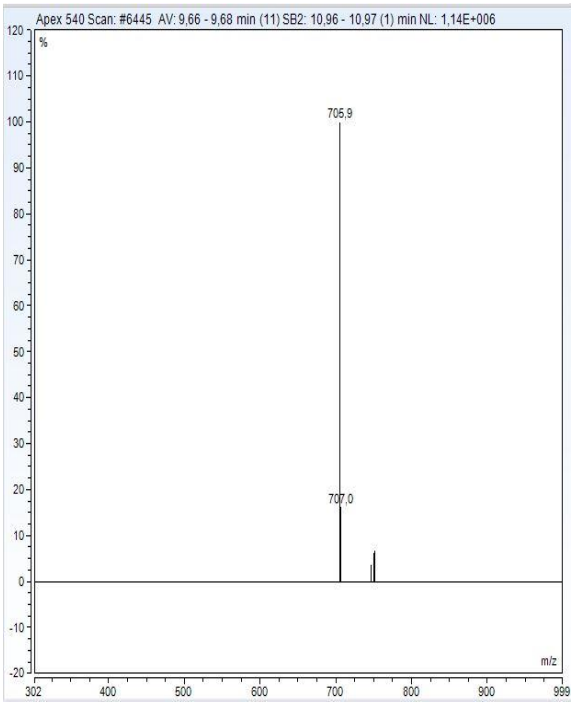

Figure: A_2_100: SP3_peak 5_MS-specter

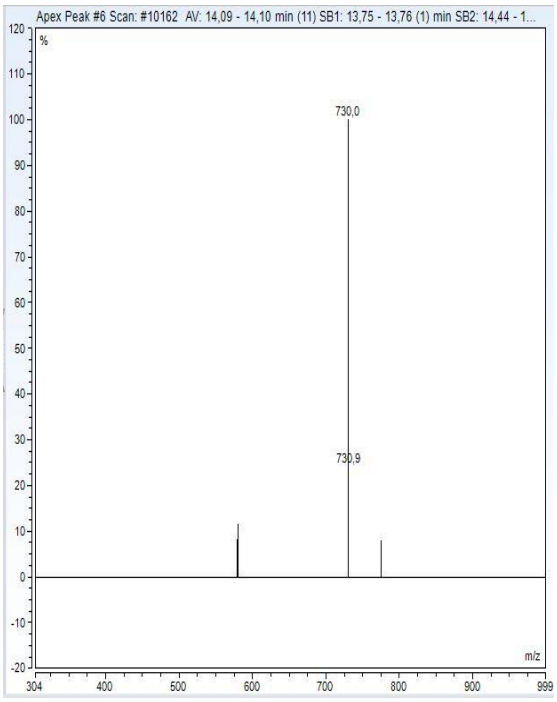

Figure: A_2_101: SP3_peak 6_MS-specter

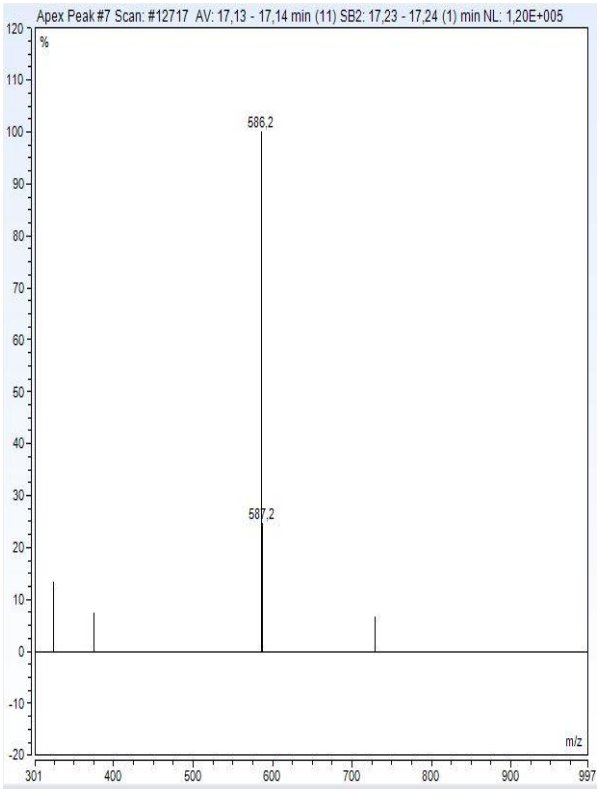

Figure: A_2_102: SP3_peak 7_MS-specter

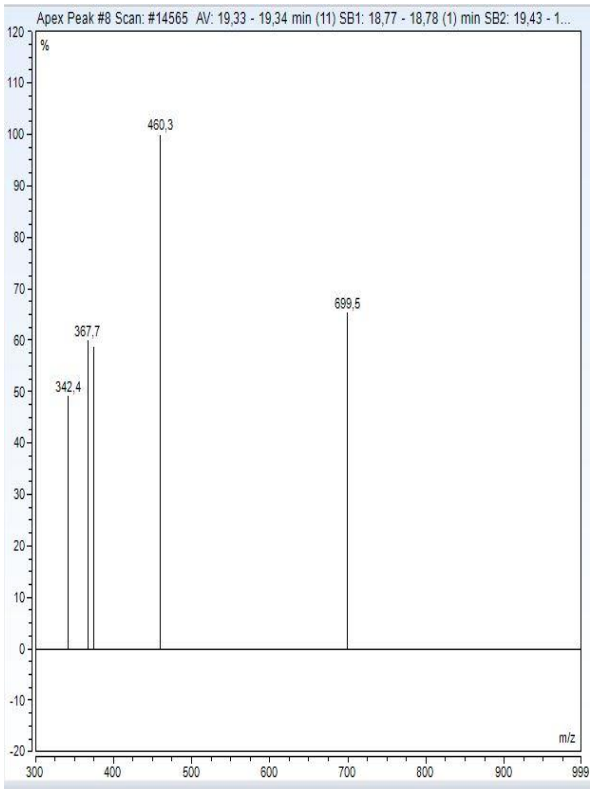

Figure: A_2_103: SP3_peak 8_MS-specter

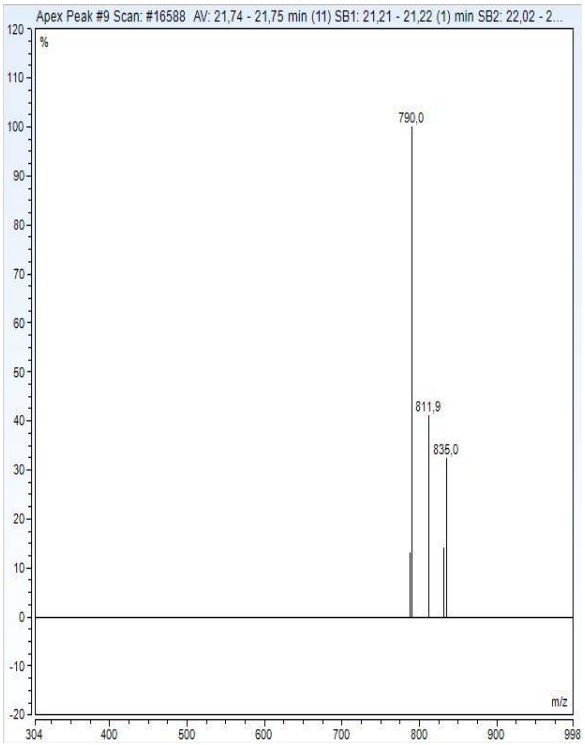

Figure: A_2_104: SP3_peak 9_MS-specter

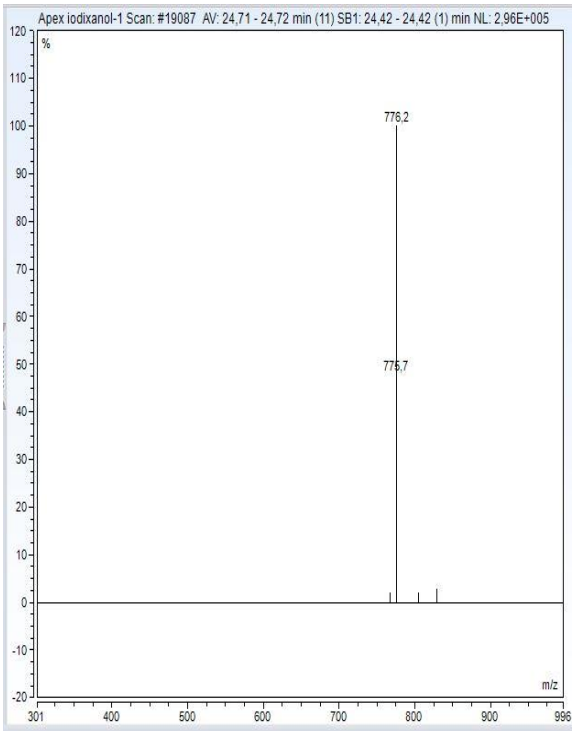

Figure: A_2_105: SP3_peak 10_MS-specter

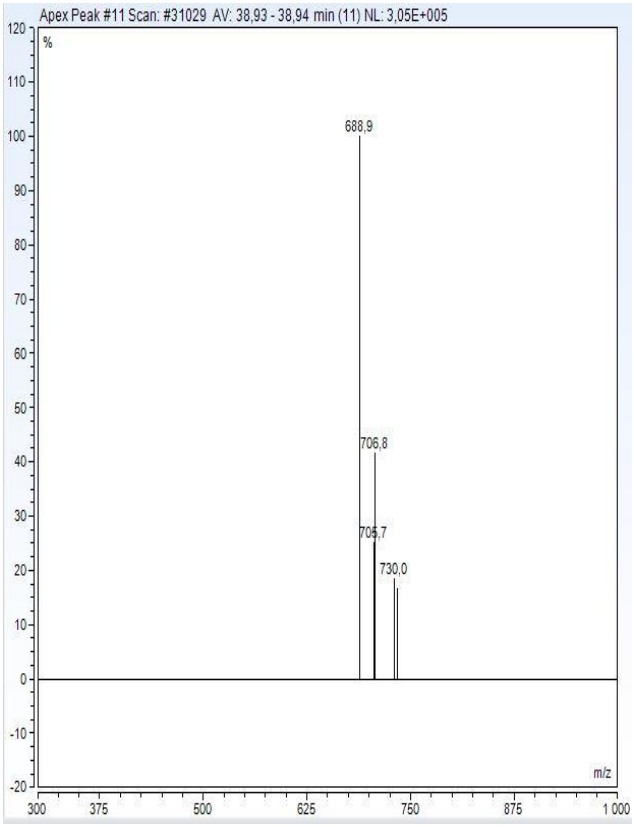

Figure: A_2_9: SP3_peak 11_MS-specter

Appendix 3

Following section is the validation protocol and report that was made in MLJ-690 as a preparation for this thesis. The method principle and evaluation of robustness, QL/DL and repeatability was assumed comparable to the method that after change of column from Altima to YMC. The reason for the change was the need for a smaller diameter column to use with flow rate 0,250 ml/min to the MS-spectrometer. The change in system from Ultimate 3000 to Vanquish Flex (both from Thermo Scientific) did not show changes of consequence under system suitability testing using the same standard solution.

Method validation for detection of X-ray media in wastewater effluent from biological treatment.

Method: **BIO-DET_IOX_541_540_ABA-HCl**

Abstract:
This validation protocol describes the procedure for validation of analytical method used to detect X-ray media and degradation products found in wastewater.

The validation includes the evaluation of accuracy, precision (as repeatability and intermediate precision), linearity, range, detection limit, and robustness against change in pH and salt concentration.

This protocol also describes the acceptance criteria for all parameters and handling of deviations from protocol.

Report of the results, statistical data and verification of method suitability is added to the protocol when finished.

Table of content

1. Aim & objective

This protocol describes the validation of method BIO_IOH_IDX_541_540 to be used in quantification of iodine contrast media in wastewater.

The purpose of the validation is to give validated documentation of the ableness of the method to be used as intended.

The method is to be used to detect the change in contrast media before, during and after biological treatment with anaerobic and aerobic reactors. The method shall be able to detect all parent compounds as-well as detection of intermediates and degradation products.

Quantitative detection for all parent compounds and qualitative detection of degradation products.

1.1 Scope

Parameters that will be evaluated

- Accuracy
- Precision as repeatability
- Linearity I the range 0-0,300 Kg/m^3 contrast media.
- Detection limits (DL)
- Quantification limit (QL)
- Robustness in gradients of salts and variation in pH.

The HPLC- method is to be used in R&D projects concerning optimization and testing of the conditions during biological treatment.

2. Instrument description.

The validation will be performed using a HPLC system referred to as system 183 from now on. The system is a Thermo Scientific model Ultima 3000. The system used a variable-wavelength UV-detector operated at 254 nm. The system uses Chromeleon data management system for integration and reporting.

HPLC column to be used during the validation of the method is an Alltima, C18 Rocket from HICHROM (53x7 mm). Particle size in the stationary phase in the column is 3 µm.

3. Sample description

Method is to be used in analysis of feed and effluent from biological treatment. The method can be used for detection and quantification of contrast media in both bench-top, pilot and full-scale biological treatment tests/evaluations. The range of the test concentrations used represents the normal expected feed and effluent concentration from the facility. Variations is pH, salt is not large in the facility, but is included in the validation for use in R&D testing and purposes. The concentration of contrast media range is normally 0,01-0,02 %, normal salt concentration is from 0,5-1,5 %. Max conductivity at 25 mS/cm. The pH in feed usually ranges from 4,5-5,3 into the anaerobic reactor while the effluent is about 7,5-8,0. The effluent from the aerobic plant usually ranges from 7,9-8,3. The validation accommodates the observed ranges in salts and pH. Testing of the effect of pH and salts will be included, but no higher than necessary due to risk of precipitation in HPLC eluent (Acetonitrile) and damage on the HPLC column.

4.Method description

The analysis is used to quantify contrast media in wastewater. The components that are quantified range from very water soluble to low water solubility. The column C18 is often used to separate hydrophobic compounds. However, the separation on the C18, has been proven stable and less difficult to operate than helix column that often is recommended for separation of hydrophilic compounds. Reversed phase HPLC is used with a gradient using milliQ-water and 50% acetonitrile. He sample is injected and applied on the column. Separation is accomplished by utilizing the difference in interaction between the analyte and the non-polar stationary phase in the column. Water is used initially to carry the components over the column, the acetonitrile increases during the run to slow down the passage of the components enough to insure proper separation. In the end of the run the water is used to elute the component of the substance. The analytes contain double bonds (benzene ring) that absorbs UV-light with a peak at 245 nm. The analytes have a high response, and it is sufficient to use 254 nm as detection wavelength. This is the standard wavelength for mercury-lamp. The response from the detector is proportional with the amount of each analyte. Standards with known concentration are used in each sequence run and is used to accurately quantify the analytes. The amount of each component is reported as areal %, while the standards is used after the analysis to calculate the actual amount of the analyte in the wastewater.

Instrument: **HPLC system 183**

Column	Alltima, C18 Rocket fra HICHROM (53x7 mm)	
Particle size:	3µm	
Mobil phase:	Eluent A: 100 % Milli-Q water	
	Eluent C: 50 % Acetonitrile in Milli-Q water	
Flow:	1,5 mL/min	
Injection volume	10 µL	
Detector:	UV:	254 nm
Methode/Chromeleon	Method, with report format, selected system and gradient check before starting up.	

Gradient program: during all runs on the HPLC system.

Time (min)	*C: 50 % ACN*	*A: Milli-Q*
0	0.5	99.5
13	23	77
20	23	77
22	0.5	99.5

5. Experimental set-up

5.1 Equipment

HPLC system 183 (Thermo scientific Ultimate 3000) with quad-pump, UV/VIS-variable wave-length detector, column-compartment with oven, and autosampler. Method set-up is generated in Chromeleon chromatography system.

5.2 Chemicals and standards

The validation will be using standard solutions of intermediates and parent compound as well as first raw material.

540: 10000 **µg/mL (10 kg/m^3)**
541: 10000 µg/mL (10 kg/m^3)
Iohexol: 15000 µg/mL (15 kg/m^3)

ABA-HCl: 10000 ug/ml (10 Kg/m^3)

The weight of the compounds must be corrected for the water content before calculation and preparation of the standards. Weight corrected for water content shall be:

540: 1,0 g ±0,01 g
541: 1,0 g ±0,01 g
Iohexol: 1,5 g ±0,01 g
ABA-HCl 1,0 g± 0,01 g

Water contents are analyzed by using Carl Fisher titration. Dry powdered standard compounds are added to methanol and hydranal- 5 (titrant) is added, reacting with water until an end point is met.

Samples in the method will be calculated using following formula:

$$\text{Consentration (mg/L)} = \frac{\text{Areal component (sample)}\cdot\text{cons (std)}}{\text{Areal (std)}}$$

5.3 Validation program

Validation program is given in table 5-3-1.

Test set	Instrument	Day	Concentration level (number of samples)						Validation parameter.
			L_0	L_1	L_2	L_3	L_4	L_5	
1	System 183	1	3	6	1	6	1	6	Accuracy Repeatability Linearity DL/QL
2	System 183	2	3	6	1	6	1	6	Replicate
3	System 183	1	-	-	-	3	-	-	Robustness

5.4 Program for testing robustness.

Robustness testing is tested for evaluation the impact of variation in pH and salt content that can be expected in the wastewater. Variation in the validation is set within the realistic values and will quantify the potential impact of these variations on the quantification of analytes (X-ray contrast media).

Salt content: 0%, 3%

pH: 3, 5 and 9.

The robustness will be performed on a single concentration level (L_3). Three parallels will be analyzed.

Table 5-4-1: Program showing the tests of robustness.

Concentration level	Number of parallels	Salt content (%)	pH
R_1	3	0	5
R_2	3	0	3
R_3	3	3	5
R_4	3	3	3
R_5	3	3	9
R_6	3	0	9

5.5 Specificity

Specificity in HPLC analysis is performed by verifying that the peak in the sample is sufficiently separated when together in a matrix. Verification of this will be done by observing chromatograms of all test sets.

5.6 Calculation of results.

Calculation is done manually in Exel by using following formula:

$$\text{Kg/m}^3 = \frac{KOns.Std * areal\ \%\ (sample)}{Areal\ \%\ of\ standard}$$

6. Validation procedure

6.1 Preparation of test samples.

6.1.1 Determination of water content in standards.

Table 5-6-1. Water content registered in standards.

Contrast media	Water content (%)
540 (intermediate 1)	0,17
541 (intermediate 2)	0,90
Iohexol	2,12
ABA-HCl (raw-material)	0,19

Signature (user-ID, date)	16/12-22 [illegible] SUHT

6.1.2 Preparation of stock-solutions.

1,00 ±0,01 g, corrected for water content given in table 5 is added to 100 ml glass measuring flask and diluted by distilled water. Concentration is equal to 100 mg/L.

Table 6-1-1: Amount of contrast media standards in stock solutions.

Contrast media	Weight (g)	Weight, adjusted for water content (g)
540	1,0025	1,000
541	1,0144	1,005
Iohexol	1,0297	1,008
ABA-HCl	1,0144	1,001

Analytical-scale ID: 162

Signature ID/date Susanne Halvorsen 16/12-22

6.1.3 Preparations of test samples.

Test samples is made by diluting stock solutions from table 7. L_0 and L_1 is diluted in a 500 ml measuring flask and L_2-L_5 is diluted in a 100 ml measuring flask using fresh distilled water.

Replicates for each level is given in table 3.

Table 6-1-2: Added contrast media to each concentration level used in the validation.

Concentration level	L_0	L_1	L_2	L_3	L_4	L_5
Theoretical concentration (mg/L)	10	20	50	100	200	300
Amount of stock solution (ml)	0,5	1,0	0,5	1,0	2,0	3,0

Signature ID/date: Susanne Halvorsen 13/12-22

6.1.4 Preparation of samples for robustness testing.

Salt-solution (15%) is made by weighing in 30,0 g ± 0,1 g NaCl in a 200 ml measuring flask in distilled water.

Test samples are made by diluting from stock solutions for the different analytes, adding salt solution and adjusting the pH according with table 8. Each sample level of dilution is made in a 100 ml measuring flask with distilled water.

R_1 is the same level as L_3 described in table 7. pH values are measured by using pH-test strips and is ca values for this reason.

Table 6-1-3: Preparation of samples for robustness testing.

Concentration level	R_1	R_2	R_3	R_4	R_5	R_6
Theoretical concentration (mg/L)	100	100	100	100	100	100
Addition of standards (ml)	1,0	1,0	1,0	1,0	1,0	1,0
Addition of salt solution (ml)	0	0	20	20	0	20
Adjusting pH	-	2 dr 2M HCl	6 dr 0,5 NaOH	2 dr 2M HCl	6 dr 0,5 M NaOH	-
Measured pH (test-strips)	5	3	9	3	9	5

6.2 Test set 1.

- **3 parallels on level L_0**
- **6 parallels on level L_1**
- **1 Parallels on level L_2**
- **6 parallels on level L_3**
- **6 parallel on level L_4**
- **1 Parallels on level L_5**

In addition, a blank sample is made.

Table 6-2-1: Data recording test-set 1.

Level	Parallel	Cons 540	Cons 541	Cons iohexol	Cons ABA-HCl
Blank	1	0	0	0	0
L_0	1	9,95	9,99	10,03	9,39
L_0	2	9,93	10,13	10,05	9,23
L_0	3	9,89	10,09	10,08	9,50
L_1	1	20,78	21,15	21,19	19,76
L_1	2	20,86	21,11	21,27	21,63
L_1	3	20,89	20,86	21,29	19,79
L_1	4	20,90	21,04	21,22	20,09
L_1	5	20,86	21,12	21,24	19,94
L_1	6	20,90	21,13	21,29	19,80
L_2	1	50,69	50,79	51,34	48,37
L_3	1	97,20	97,42	98,79	98,17
L_3	2	97,09	97,58	98,83	96,17
L_3	3	97,80	98,61	98,53	96,59
L_3	4	97,75	98,18	99,12	97,95
L_3	5	97,91	98,25	98,99	97,95
L_3	6	97,50	97,53	99,64	98,96
L_4	1	201,45	197,42	202,79	202,14
L_5	1	304,67	302,92	307,77	302,97
L_5	2	305,37	303,18	309,01	305,06
L_5	3	305,78	301,60	309,04	306,87
L_5	4	305,15	303,44	309,35	304,67
L_5	5	305,59	306,32	309,11	299,19
L_5	6	305,80	302,19	309,05	306,48

Signature ID/date: 13/12-22 Sessinn Yläverstan SUHA

6.3 Test set 2

Table 6-3-1: Robustness testing.

Level	Parallel	Cons 540	Cons 541	Cons iohexol	Cons ABA-HCl
R_1	1	98,51	98,89	99,93	105,18
R_1	2	98,78	98,16	99,90	106,60
R_1	3	98,82	99,19	99,99	96,01
R_2	1	98,14	97,48	99,13	97,41
R_2	2	98,10	96,96	99,12	98,83
R_2	3	98,35	97,96	99,12	96,91
R_3	1	101,59	100,07	102,24	102,88
R_3	2	101,79	100,47	102,49	102,77
R_3	3	101,84	101,46	102,34	103,43
R_4	1	101,24	99,36	102,33	104,12
R_4	2	101,36	100,20	102,14	102,55
R_4	3	101,58	100,41	101,99	101,91
R_5	1	99,18	98,88	99,93	96,71
R_5	2	99,04	98,41	99,98	97,37
R_5	3	98,91	98,53	100,04	97,33
R_6	1	103,74	101,58	104,75	107,30
R_6	2	103,59	101,39	104,63	107,59
R_6	3	104,11	102,62	104,92	105,68

Signature ID/date: 14/12-22 Jesdanne Hellversen JHH

6.4 Test set 3 (replicate day 2)

Table :11

Level	Parallel	Cons 540	Cons 541	Cons iohexol	Cons ABA-HCl
L_3	1	96,19	96,70	97,71	101,25
L_3	2	96,29	95,87	97,36	101,25
L_3	3	96,18	95,58	97,54	102,33

7. Reporting

7.1 Accuracy

Accuracy is calculated by evaluation recovery after 6 measurements at 3 levels (L_1, L_3 and L_5, 3 Parallels at level L_0.

Accuracy (%) = $\frac{Measured\ consentration\ mg/L}{Theoretical\ concentration\ mg/L}$ * 100 %

Parameters reported: Concentrations, average values (every level), 95% confidens interval (each level).

Accept criteria:

Recovery (average at every level): 90%-110%

7.2 Precision

7.2.1 Repeatability

Precision as repeatability Is calculated using 6 parallels at level L_1, L_3 and L_5 in test set 1.

Reported parameters: Single values (concentrations), Average, standard deviation, relative standard deviation on every level and confident interval on each level.

Accept criteria: RSD ≤ 5%

7.3 Linearity

Linearity is calculated using measured concentrations using 6 levels from test set 1.

Presented by:

- A plot of calculated values (X-axis) against measured values (Y-axis)
- Correlation coefficient ®
- 95 % Confidents interval for cross/section.
- Residual plot
- Regression-line

Accept criteria:

- Correlation factor: r ≥ 0,985
- 95 % Confidence interval for intercept.
- Residuals evenly distributed (around 0)

7.4 Detection limit (DL) and quantification limit (QL)

DL and QL is calculated using formula:

DL (mg/L) = $\frac{3{,}3*Sb}{b}$ QL (mg/L) = $\frac{10*Sb}{b}$

Where S_b is the standard deviation for the 3 parallels of L_0 in test set 1 and b is the slope for the regression line.

If the amount that is in the sample is not detectable the L_1 can be used.

DL and QL is reported as mg/L.

Accept criteria:

- DL/QL by similar methods have been determined previously. Expected level is < 5 mg/L.

7.5 Robustness

Robustness against different levels of salt-concentration and pH.

- Single values (concentration)¨
- Average, absolute (SD), and relative standard deviation.

- Total average using all measurements with belonging absolute and relative standard deviation.

Accept criteria:

- RSD of total average ≤ 10 %

8. Deviations

Problems and deviations from this protocol shall be discussed in under the results.

9. Results

9.1 Accuracy

Concentration measurements from 6 replicated from test set 1 at three levels L_1, L_3 and L_5 and 3 replicates from L_0.

Table 9-1-1: Accuracy for 540 test-set 1

Level	Rep	Theoretical concentration mg/l	Measured concentration mg/l	Recovery %	Statistics
L_{0QL}	1	10	9,95	99,5	Average: 99,2 Confidence interval 95%: 99,2±1,1
	2		9,93	99,3	
	3		9,89	98,9	
L_1	1	20	20,78	103,9	Average: 104,3 Confidence interval 95%: 104,3±0,41
	2		20,86	104,3	
	3		20,89	104,5	
	4		20,90	104,5	
	5		20,86	104,3	
	6		20,90	104,5	
L_3	1	100	97,50	97,5	Average: 97,5 Confidence interval 95%: 97,5 ±0,29
	2		97,20	97,2	
	3		97,09	97,1	
	4		97,80	97,8	
	5		97,75	97,8	
	6		97,91	97,9	
L_5	1	300	304,67	101,6	Average: 101,8 Confidence interval 95%: 101,8±0,40
	2		305,37	101,8	
	3		305,78	101,9	
	4		305,80	101,9	
	5		305,15	101,7	
	6		305,59	101,9	

Table 9-1-2: Accuracy for 541 test-set 1

Level	Rep	Theoretical concentration mg/l	Measured concentration mg/l	Recovery %	Statistics
L_{0QL}	1	10	9,99	99,9	Average: 100,7
	2		10,13	101,3	
	3		10,09	100,9	Confidence interval 95%: 100,7±2,6
L_1	1	20	21,15	105,8	Average: 105,3
	2		21,11	105,6	
	3		21,13	105,7	Confidence interval 95%: 105,3±1,9
	4		20,86	104,3	
	5		21.04	105,2	
	6		21,12	105,6	
L_3	1	100	97,42	97,4	Average: 97,9 Confidence interval 95%: 97,9±1,7
	2		97,58	97,6	
	3		98,61	98,6	
	4		98,18	98,2	
	5		98,25	98,3	
	6		97,53	97,5	
L_5	1	300	302,92	101,0	Average: 101,1
	2		303,18	101,1	
	3		301,60	100,5	Confidence interval 95%: 101,1±2,0
	4		303,44	101,1	
	5		306,32	102,1	
	6		302,19	100,7	

Table 9-1-3: Accuracy for iohexol test-set 1

Level	Rep	Theoretical concentration mg/l	Measured concentration mg/l	Recovery %	Statistics
L_{0QL}	1	10	10,03	100,3	Average: 100,5 Confidence interval 95%: 100,5±0,9
	2		10,05	100,5	
	3		10,08	100,8	
L_1	1	20	21,19	106,0	Average: 106,3 Confidence interval 95%: 106,3±0,3
	2		21,27	106,4	
	3		21,29	106,5	
	4		21,22	106,1	
	5		21,24	106,2	
	6		21,29	106,5	
L_3	1	100	98,79	98,8	Average: 99,0 Confidence interval 95%: 99,0±0,5
	2		98,83	98,8	
	3		98,53	98,5	
	4		99,12	99,1	
	5		98,99	99,0	
	6		99,64	99,6	
L_5	1	300	307,77	102,6	Average: 103,0 Confidence interval 95%: 103,0±0,2
	2		309,01	103,0	
	3		309,04	103,0	
	4		309,35	103,1	
	5		309,11	103,0	
	6		309,05	103,0	

Table 9-1-4: Accuracy for ABA-HCl test-set 1

Level	Rep	Theoretical concentration mg/l	Measured concentration mg/l	Recovery %	Statistics
L_{0QL}	1	10	9,39	93,9	Average: 93,7 Confidence interval 95%: 93,7±4,9
	2		9,23	92,3	
	3		9,5	95,0	
L_1	1	20	19,76	98,8	Average: 100,8 Confidence interval 95%: 100,8±4,7
	2		21,63	108,2	
	3		19,79	99,0	
	4		20,09	100,5	
	5		19,94	99,7	
	6		19,8	99,0	
L_3	1	100	98,17	98,2	Average: 97,6 Confidence interval 95%: 97,6±1,4
	2		96,17	96,2	
	3		96,59	96,6	
	4		97,95	98,0	
	5		97,95	98,0	
	6		98,96	99,0	
L_5	1	300	302,97	101,0	Average: 101,4 Confidence interval 95%: 101,4±1,2
	2		306,87	102,3	
	3		304,67	101,6	
	4		299,19	99,7	
	5		306,48	102,2	
	6		305,06	101,7	

9.2 Precision

Precision as repeatability was tested by comparing results of 540, 541, iohexol and ABA-HCl from 6 replicated from test set 1 at three levels L_1, L_3 and L_5 and 3 replicates from L_0. Table 9-1, 9-2, 9-3 and 9-4 shows the results of analysis.

Table: 9-2-1 Precision for 540 test- set 1.

Level	Rep	Measured concentration mg/l	Statistics
L_{0QL}	1	9,95	Average: 9,9 STD: 0,03 RSD: 0,3 % Confidence interval 95%: 9,9±0,10
	2	9,93	
	3	9,89	
L_1	1	20,78	Average: 20,9 STD:0,05 RSD: 0,2 % Confidence interval 95%:
	2	20,86	
	3	20,89	
	4	20,9	
	5	20,86	

	6	20,9	9,9±0,06
L_3	1	97,5	Average: 97,5 STD: 0,33 RSD: 0,3 % Confidence interval 95%: 97,5±0,44
	2	97,2	
	3	97,09	
	4	97,8	
	5	97,75	
	6	97,91	
L_5	1	304,67	Average: 305,4 STD: 0,43 RSD: 0,1 % Confidence interval 95%: 305,4±0,56
	2	305,37	
	3	305,78	
	4	305,8	
	5	305,15	
	6	305,59	

Table: 9-2-2 Precision for 541 test-set 1

Level	Rep	Measured concentration mg/l	Statistics
L_{0QL}	1	9,99	Average: 10,1 STD: 0,07 RSD: 0,7 % Confidence interval 95%: 10,1±0,26
	2	10,13	
	3	10,09	
L_1	1	21,15	Average: 21,1 STA: 0,11 RSD: 0,5% Confidence interval 95%: 21,1±0,14
	2	21,11	
	3	21,13	
	4	20,86	
	5	21,04	
	6	21,12	
L_3	1	97,42	Average: 97,9 STD:0,48 RSD:0,5% Confidence interval 95%: 97,9±0,62
	2	97,58	
	3	98,61	
	4	98,18	
	5	98,25	
	6	97,53	
L_5	1	302,92	Average: 303,3 STD: 1,64 RSD: 0,5% Confidence interval 95%: 303,3±2,12
	2	303,18	
	3	301,6	
	4	303,44	
	5	306,32	
	6	305,59	

Table: 9-2-3 Precision for iohexol test- set 1.

Level	Rep	Measured concentration mg/l	Statistics
L_{0QL}	1	10,03	Average: 10,1 STD: 0,03 RSD: 0,3% Confidence interval 95%: 10,1±0,09
	2	10,05	
	3	10,08	
L_1	1	21,19	Average: 21,3 STD:0,04 RSD: 0,2 % Confidence interval 95%: 21,3±0,05
	2	21,27	
	3	21,29	
	4	21,22	
	5	21,24	
	6	21,29	
L_3	1	98,79	Average: 99,0 STD: 0,38 RSD: 0,4% Confidence interval 95%: 99,0±0,49
	2	98,83	
	3	98,53	
	4	99,12	
	5	98,99	
	6	99,64	
L_5	1	307,77	Average: 308,9 STD: 0,56 RSD: 0,2 % Confidence interval 95%: 308,9±0,72
	2	309,01	
	3	309,04	
	4	309,35	
	5	309,11	
	6	309,05	

Table: 9-2-4 Precision for ABA-HCl test- set 1.

Level	Rep	Measured concentration mg/l	Statistics
L_{0QL}	1	9,39	Average: 9,4 STD:0,14 RSD: 1,4 % Confidence interval 95%: 9,4±0,47
	2	9,23	
	3	9,5	
L_1	1	19,76	Average: 20,2 STD:0,73 RSD: 3,6 % Confidence interval 95%: 20,2±0,94
	2	21,63	
	3	19,79	
	4	20,09	
	5	19,94	
	6	19,8	
L_3	1	98,17	Average: 97,6 STD:1,05 RSD:1,1% Confidence interval 95%: 97,6±1,35
	2	96,17	
	3	96,59	
	4	97,95	
	5	97,95	
	6	98,96	
L_5	1	302,97	Average: 304,2 STD: 2,82 RSD: 0,9% Confidence interval 95%: 304,2±3,65
	2	306,87	
	3	304,67	
	4	299,19	
	5	306,48	
	6	305,06	

9.3 Robustness

Table 9-3-1: Robustness shown for analysis of 540 in different concentrations in salt and pH variations.

Level	Par	Result mg/L	Statistics	Total statistic
Level L3 salt 0% pH 5				
R1	1	98,51	Avg: 98,2 STD 0,13 RSD 0,1%	Avg: 100,3 STD: 0,31
	2	98,78		
	3	98,82		
Level L3 salt: 0% pH 3				
R2	1	98,14	Avg: 97,7 STD: 0,99 RSD %: 1,0	
	2	98,1		
	3	98,35		
Level L3 salt: 3 % pH 9				
R3	1	101,59	Avg: 101,7 STD: 0,13 RSD%: 0,1	
	2	101,71		
	3	101,84		
Level L3 Salt: 3% pH 3				
R4	1	101,24	Avg: 101,4 STD: 0,17 RSD %: 0,2	
	2	101,36		
	3	101,58		
Level L3 Salt 0% pH 9				
R5	1	99,18	Avg: 99,0 STD: 0,14 RSD %: 0,1	
	2	99,04		
	3	98,91		
Level L3 Salt 3% pH 5				
R6	1	103,74	Avg: 103,8 STD: 0,27 RSD %: 0,3	
	2	103,59		
	3	104,11		

Table 9-3-2: Robustness shown for analysis of 541 in different concentrations in salt and pH variations.

Level	Par	Result mg/L	Statistics	Total statistic
Level L3 salt 0% pH 5				Avg: 99,7 STD: 0,43
R1	1	98,51	Avg: 98,7 STD: 0,53 RSD%: 0,5	
	2	98,78		
	3	98,82		
Level L3 salt: 0% pH 3				
R2	1	98,14	Avg:98,2 STD: 0,13 RSD%: 0,5	
	2	98,1		
	3	98,35		
Level L3 salt: 3 % pH 9				
R3	1	100,07	Avg: 100,7 STD: 0,72 RSD %: 0,7	
	2	100,47		
	3	101,46		
Level L3 Salt: 3% pH 3				
R4	1	99,36	Avg: 100,0 STD: 0,56 RSD %: 2,0	
	2	100,2		
	3	100,41		
Level L3 Salt 0% pH 9				
R5	1	98,88	Avg: 98,6 STD: 0,24 RSD%: 0,2	
	2	98,41		
	3	98,53		
Level L3 Salt 3% pH 5				
R6	1	101,58	Avg: 101,9 STD: 0,66 RSD %: 0,7	
	2	101,39		
	3	102,62		

Table 9-3-3: Robustness shown for analysis of iohexol in different concentrations in salt and pH variations.

Level	Par	Result mg/L	Statistics	Total statistic
Level L3 salt 0% pH 5				*Avg:101,4* *STD:0,10*
R1	1	99,93	Avg: 99,9 STD 0,05 RSD %: 0,05	
	2	99,9		
	3	99,99		
Level L3 salt: 0% pH 3				
R2	1	99,13	Avg: 99.1 STD: 0,01 RSD %:0,005	
	2	99,12		
	3	99,12		
Level L3 salt: 3 % pH 9				
R3	1	102,24	Avg: 102,4 STD: 0,13 RSD%: 0,1	
	2	102,49		
	3	102,34		
Level L3 Salt: 3% pH 3				
R4	1	102,33	Avg: 102,2 STD: 0,17 RSD %: 0,2	
	2	102,14		
	3	101,99		
Level L3 Salt 0% pH 9				
R5	1	99,93	Avg: 100,0 STD: 0,06 RSD %: 0,1	
	2	99,98		
	3	100,04		
Level L3 Salt 3% pH 5				
R6	1	104,75	Avg: 104,8 STD: 0,15 RSD %: 0,1	
	2	104,63		
	3	104,92		

Table 9-3-4: Robustness shown for analysis of ABA-HCl in different concentrations in salt and pH variations.

Level	Par	Result mg/L	Statistics	Total statistic
Level L3 salt 0% pH 5				
R1	1	105,175	Avg: 101,6 STD 0,62 RSD %: 0,6	*Avg: 101,4* *STD: 0,78*
	2	106,6		
	3	96,0108		
Level L3 salt: 0% pH 3				
R2	1	97,413	Avg: 97,2 STD: 0,99 RSD %:1,0	
	2	98,8266		
	3	96,9114		
Level L3 salt: 3 % pH 9				
R3	1	102,771	Avg: 102,8 STD: 0,55 RSD%: 0,5	
	2	103,432		
	3	102,338		
Level L3 Salt: 3% pH 3				
R4	1	104,116	Avg: 102,9 STD: 1,14 RSD %: 1,1	
	2	102,554		
	3	101,905		
Level L3 Salt 0% pH 9				
R5	1	96,7176	Avg: 97,1 STD: 0,37 RSD %: 0,4	
	2	97,3674		
	3	97,3332		
Level L3 Salt 3% pH 5				
R6	1	107,297	Avg: 106,9 STD: 1,03 RSD %: 1,0	
	2	107,593		
	3	105,678		

9.4 Repeatability test-set 2 (day 2)

Test set 2: Analysis performed by same analyst, instrument, and stock-solutions. Performed to evaluate repeatability.

Level	Par	541	iohexol	ABA-HCl	540
L3	**1**	96,7	97,71	101,25	96,19
	2	95,87	97,36	101,25	96,29
	3	95,58	97,54	102,33	96,18
		Avg: 96,1 STD: 0,58 RSD %: 0,6	Avg: 97,5 STD: 0,17 RSD %: 0,2	Avg: 101,6 STD: 0,06 RSD %:0,6	Avg: 96,2 STD: 0,06 RSD %: 0,1

9.5 Linearity

Samples of known concentration of the for-contrast media 540, 541, iohexol and the raw-material ABA-HCl was analyzed at 6 different levels. Figure: 9-1,9-2, 9-3 and 9-4 shows the

plots of the measured data against the theoretical value. Regression analysis was done in exel using validated spreadsheet for internal validation at GEhealthcare. Following SOP LKK Instrument qualification.

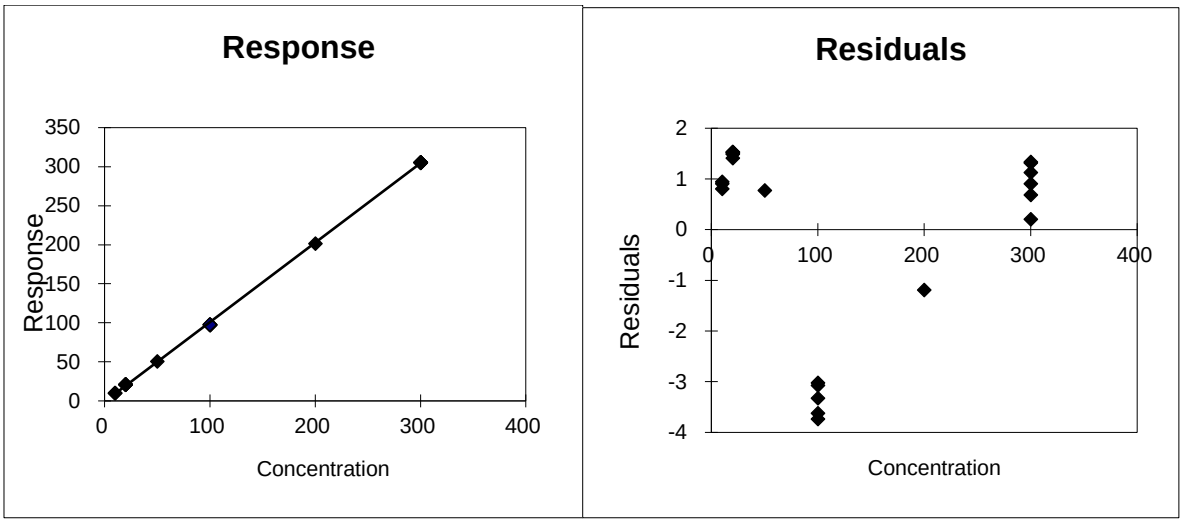

Figure 9-1: Linearity 540 (plot of response and residuals)

Correlation factor= 0,999 (Accept criteria = ≥ 0,985) PASS

Curvation factor = 1,031 (Accept criteria = 0,9-1,1) PASS

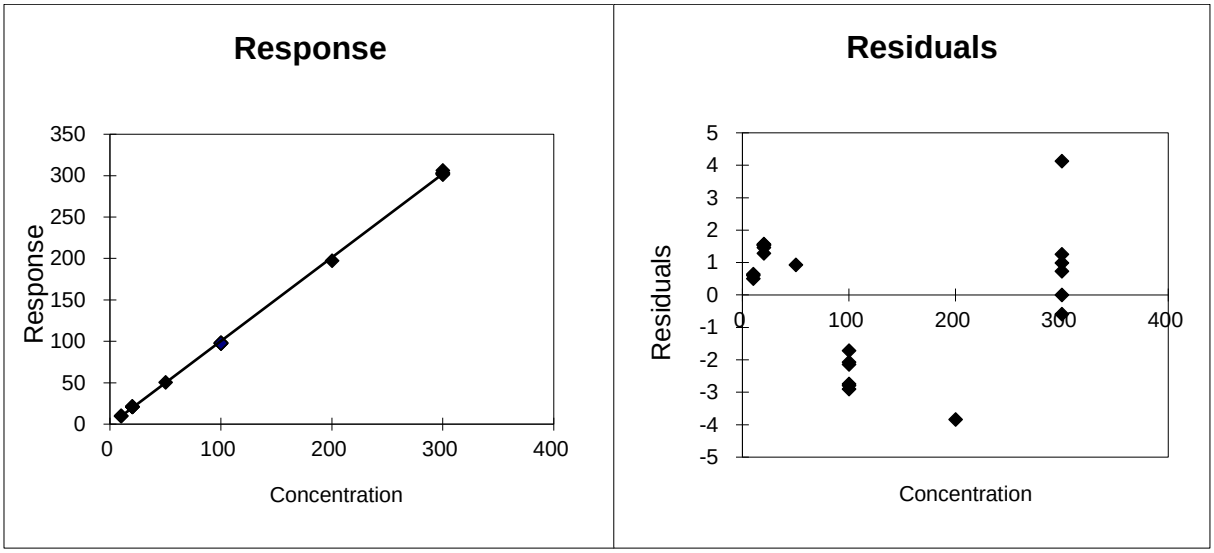

Figure 9-2: Linearity 541 (plot of response and residuals)

Correlation factor= 0,999 (Accept criteria = ≥ 0,985) PASS

Curvation factor = 1,025 (Accept criteria = 0,9-1,1) PASS

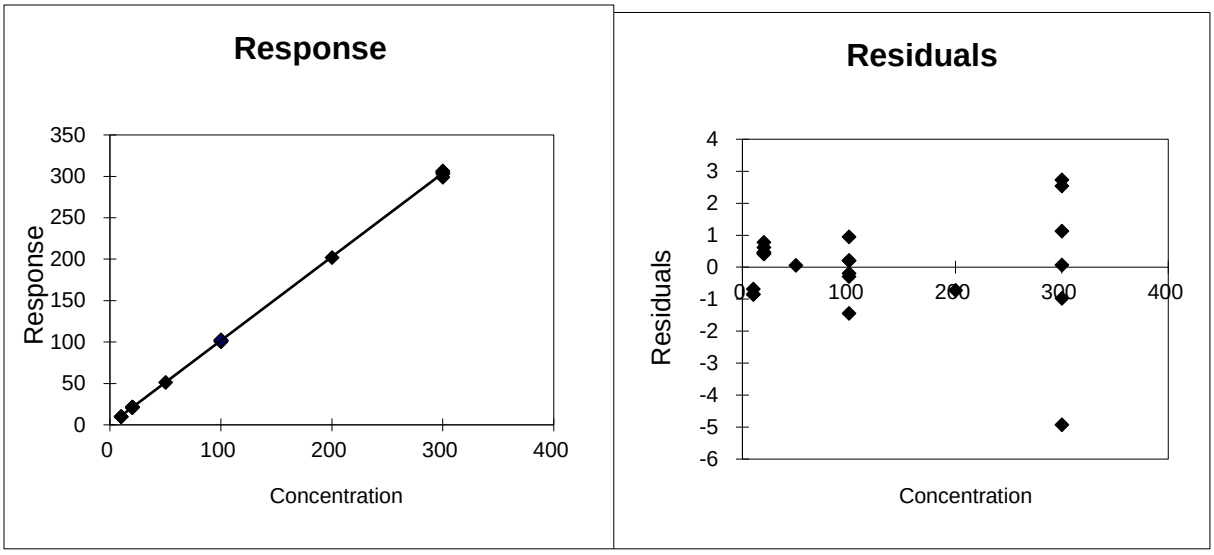

Figure 9-3: Linearity iohexol (plot of response and residuals)

Correlation factor= 0,999 (Accept criteria = ≥ 0,985) PASS

Curvation factor = 1,030 (Accept criteria = 0,9-1,1) PASS

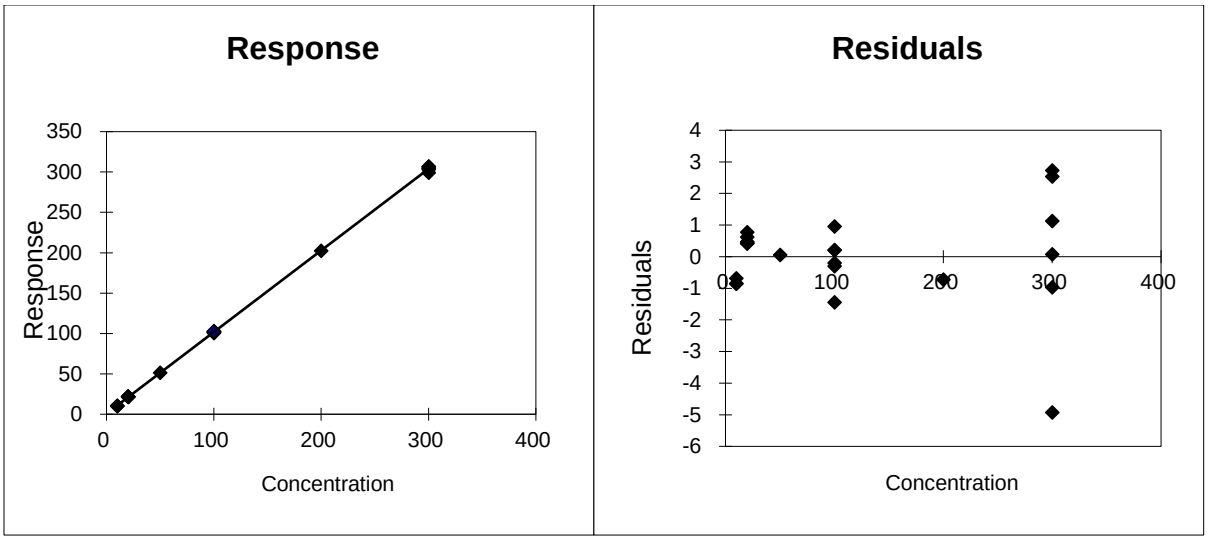

Figure 9-4: Linearity ABA-HCl (plot of response and residuals)

Correlation factor= 0,999 (Accept criteria = ≥ 0,985) PASS

Curvation factor = 0,987 (Accept criteria = 0,9-1,1) PASS

9.6 Quantification (QL) and detection limit (DL)

DL was determined to be: 0,2 mg/L for 540

0,19 mg/L for 541

0,30 mg/L for Iohexol

Not measured for ABA-HCl

QL was determined to be: 0,00059 g/L for 540

0,00059 g/L for Iohexol

0,00118 g/L for 541

Not determined for ABA-HCl

QL and DL had no defined accept criteria in this validation. The levels that will be of interest in bioreactor experiments will be well within the limits seen in QL for main compounds.

10. Discussion/conclusion

All tests were within the accept criteria set in this protocol.

Specificity was not performed as individual test. However, the separation of the compounds was sufficient shown by the recovery data in test-set 1. Base-line separation was not met between 541 and ABA-HCl but is not required at this level. However, some method optimization may improve the separation. ABA-HCl has an acid-group, meaning that it might benefit from addition of an acid to the water eluent.

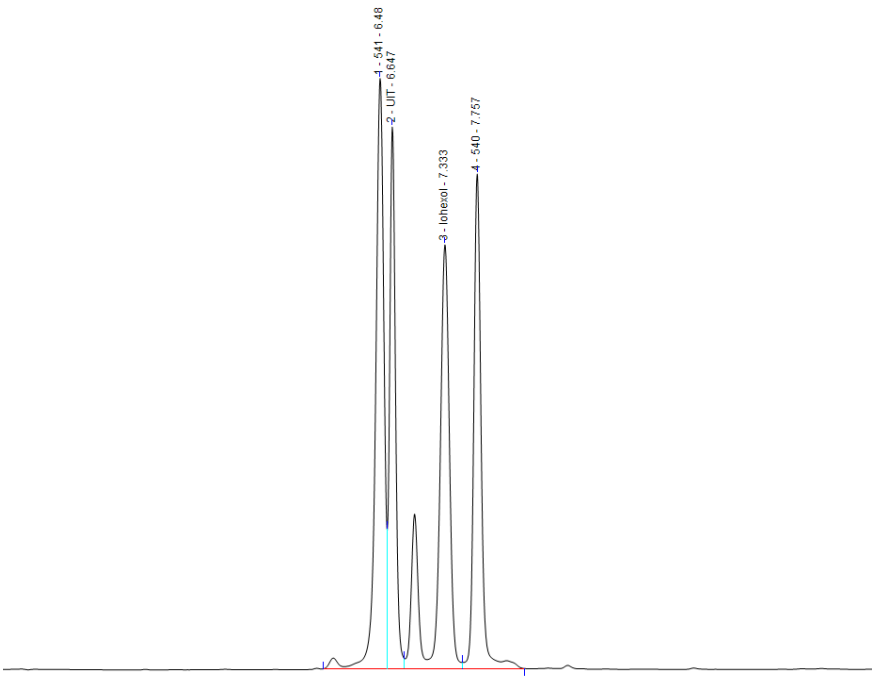

Figure 10-1: Chromatogram from L3-level. Peak 1: 541 peak 2: ABA-HCl, Peak 3: Iohexol and peak 4: 540.

Accuracy: Accept criteria for accuracy was recovery of compound between 90-110 %. All levels in this test proved to be within this range.

Precision and repeatability:

Accept criteria for precision in this test was RSD % ≤ 5 %

All samples presented in table 9-2-1 to 9-2-4 was well within the acceptable range.

Repeatability:

Analysis was performed on one level (L3) by same analyst on day 2.

Accept criterium for RSD% was ≤ 5 %

Observed levels for all compounds ranged from 0,1 to 0,6 %.

Linearity:

Figures 9-1 to 9-4 show a good linearity in the range 10 mg/L to 300 mg/L. Correlation values and curvation factor in the regression analysis was all within the accept criteria

Robustness: Changes in salt content and pH did not cause changes in the values of the compounds in a way that limits the validity of the method. Variations observed is within what is expected in terms of sample preparations and instrument variations.

Accept criteria for the robustness test was RSD % of ≤ 10 %

The method tested in this validation can detect, separate, and quantify the analytes of interest. Specificity, robustness for the intended sample matrix as well as the recovery of the method was well within the determined criteria set in the protocol. The method is suitable for the intended use for detection of contrast-media in wastewater from biological treatment plant and for testing in bio-pilotplant.

11.References

SOP LFK 0222 Instrument qualification

SOP LKK 0059 Use of HPLC thermos instruments at GEhealthcare.

SOP LFK 0371 Validation procedures at QC (GEhealthcare Lindesnes)